Diplomarbeit

Diploma thesis

Rekombinante Expression und biochemische Charakterisierung eines thermostabilen Motorproteins

Recombinant expression and biochemical characterization of a thermostabile motor protein

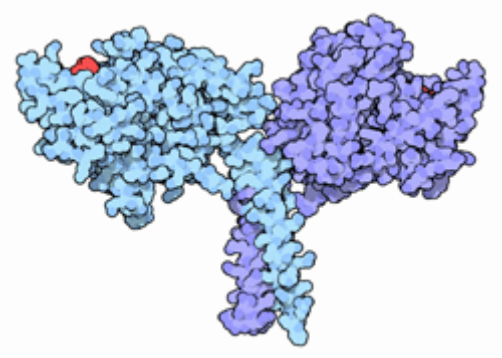

von Dejan Gagoski

Angefertigt am Max-Planck-Institut für molekulare Genetik
Abteilung von Prof. Dr. H. Lehrach, Arbeitsgruppe von Dr. Zoltán Konthur
in Berlin-Dahlem vom August 2009 bis April 2010

UNIKASSEL
VERSITÄT

Eingereicht am Fachbereich Naturwissenschaften, Institut für Biologie,
der Universität Kassel zum Erlangen des Grades „Diplom-Biologe“

Acknowledgements

First off all I want to thank Dr. Zoltán Konthur for giving me the opportunity to do my diploma thesis in his work group. Also I want to thank Dr. Jörn Glökler who together with Dr. Zoltán Konthur provided me with this very interesting project and for the many discussions and advices. Also I want to express my gratitude to Prof. Dr. Reinhard Lipowsky for showing interest about the project and financing me during the work.

Many thanks to Prof. Dr. Firedrich W. Herberg and Prof. Dr. Hans Lehrach for examining my diploma thesis.

The success of many experiments wouldn't be possible without the experience and practical know-how around the laboratory of Carola Stoschek. Also many thanks for the advices, help but also gut company of Yuliya Georgieva, Dr. Volker Sievert, Florian Rubelt, Stephan Klatt and Tonio Schütze.

My sincere thanks also to Dr. David Meierhofer for performing the mass spectrometrical analysis.

I want to express my appreciation to the University of Kassel for granting me a student position and all of the professors and their co-workers from the institute of biology. Especially I want to thank Prof. Dr. Wolfgang Nellen for being my mentor and helping me to work my way through the studies.

I want to thank my colleague Stephan Raphael Starick for the good company and moral support here in Germany and am grateful to all of my numerous friends in Macedonia for continuously giving me moral support throughout the whole studies and diploma thesis.

But most of all I want thank my parents for the maximal moral and financial support during the studies abroad while helping me pursue my wish to get into the world of scientific research.

Contents

1 Introduction

1.1 The advancement of the high throughput screening technologies

Over the years the need of more high throughput investigations in the molecular biology has increased steadily. However, the time needed to produce sufficient amount of results by classical means, preparing and testing sample after sample at a time has risen proportionally with the number of samples. Thus the efficiency of many high-throughput investigations is falling. The first steps in improving the efficiency of high-throughput investigation was small scale parallelization using microtiterplates and multi-channel pipettes. However the larger the number of samples, the higher are the chances of human error in the pipetting process. So for the further improvement of the efficiency the use of robots was introduced. This eliminates the chances of miss-pipetting and increases the rate of parallelization. However, there is the possibility to further increase the number of parallel processed samples by introducing miniaturization. This has been successfully applied in the field of DNA sequencing (next generation sequencing). Another platform for miniaturizing experiments are microfluidic chip systems in a glass slide format (Figure 1-1). This is similar to the advancement in semiconductor technology where it all started with large vacuum tubes and is at the stage of nano-meterscale integrated circuits today.

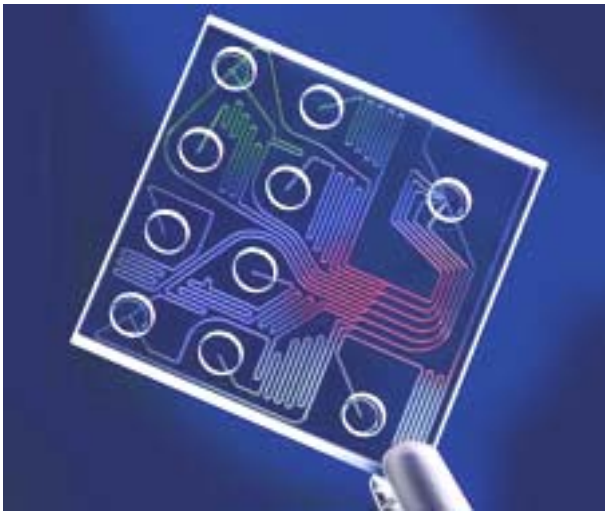

Figure 1-1: An example of a microfluidic lab-on-a-chip system from Agilent Technology. Picture taken from www.agilent.com

In order to be able to analyze or process even more samples, nanofluidic systems should be further adapted to fit scientific needs. For this purpose some technical problems have to be solved. One of those is the transfer of the sample from one chamber to another, since

reduction of the channels size is limited. Even in microfluidic systems the samples can not run under pressure or electrophoretically through channels smaller than 100 µm due to the viscosity. A brief look how nature solves this problem. In neuronal cells vesicles are continuously being actively transported from the soma to the axon terminal through axons of ~1 µm diameter. Hence the transportation system of the axons, where the motor protein kinesin tows cargo along microtubule tracks, can be applied in microfluidic and nanofluidic systems (Hess et al. 2004). Initial investigations exploring this application have already been done (Nitta and Hess 2005). But the use of this transportation system is initially not that flexible in regard of the working conditions since it has evolved under physiological conditions. The microtubules can be easily polymerized *in vitro* (Lee et al. 1974) and kept stable at ambient temperatures using taxol (Wilson et al. 1985). The kinesin on the other hand is more susceptible to different conditions, but it is also very diverse. So, for each application a compatible kinesin has to be chosen from the known different kinesins present in different organisms. To make the process of finding the compatible kinesin easier, it might be possible in the future to apply phage display to produce a kinesin library by *in vitro* evolution and select under the application defined conditions.

1.2 Kinesin

1.2.1 Diversity

Kinesin was first identified as a motor protein moving along microtubules after purification from a giant squid axon (Vale et al. 1985). This specific kinesin is being also referred to as conventional kinesin. Physiologically, it is a tetramer (Figure 1-2, A). A homodimer of two heavy chains which form the mechanochemical unit. To each of the heavy chain's C-terminal domains a single light chain is associated (DeBoer et al. 2008). While the heavy chains possess mechanochemical and dimerization function, the light chains are responsible for recognition of the specific cargo within the cell, such as mitochondria (Khodjakov et al. 1998) or the Golgi apparatus (Gyoeva et al. 2000). Apart from the kinesin I family, other subfamilies of kinesins have been discovered. The kinesin-2 family is for example built either out of heterodimeric heavy chains and a single light chain (Figure 1-2, B) or present only as a heavy chain homodimer. Another kinesin family is the Unc104/KIF1 (kinesin-3) which is found normally in a monomeric state (Figure 1-2, C), but it is able to form dimers (Vale 2003).

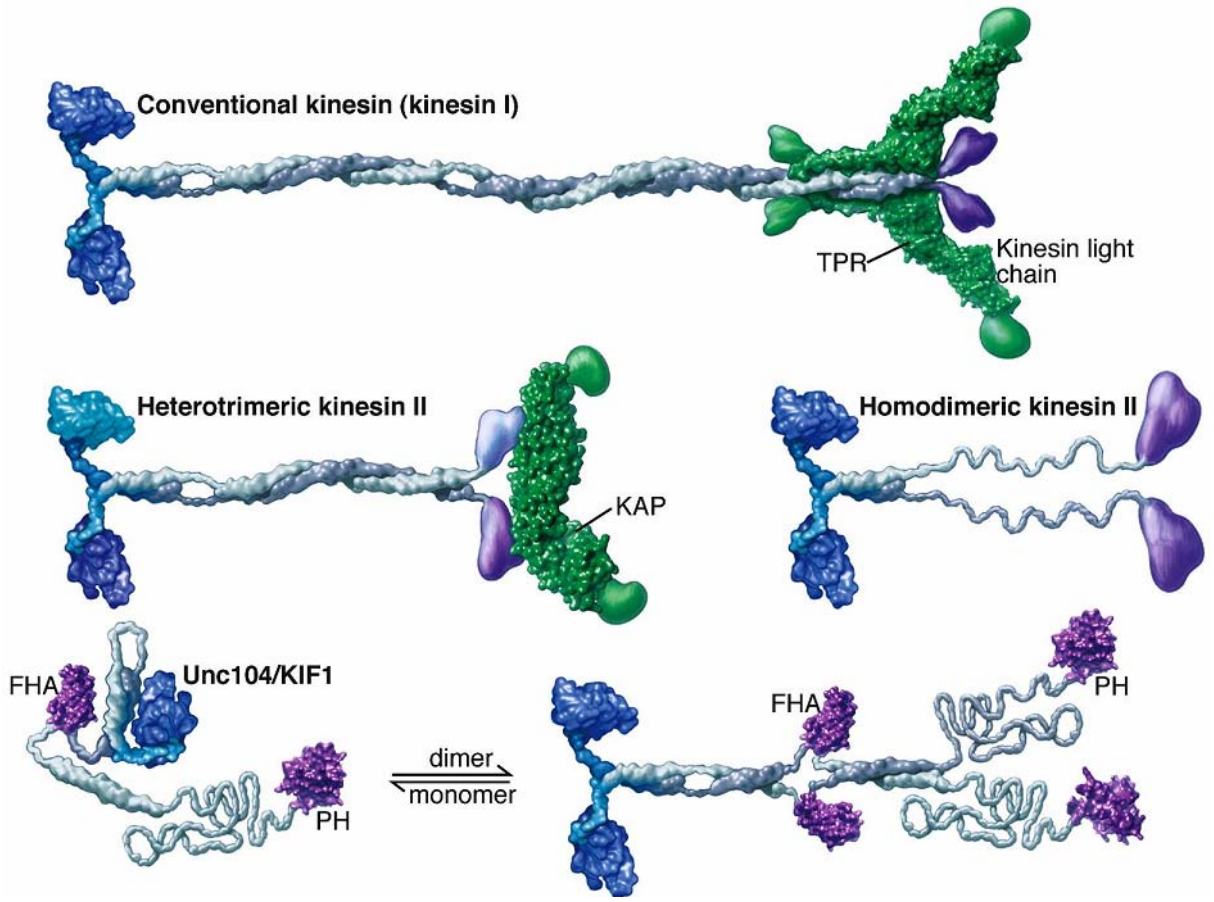

Figure 1-2: Structural depictions of the first three different subfamilies of kinesins. Picture adapted from http:cell.com/cgi/content/full/112/4/467/DC1 (Vale 2003). Gray: stalk, coiled coil; Blue: motor domain; Violet: C-terminal non-motor domains; Green: kinesin light chains.

Structurally, all kinesins have a C-terminal tail responsible for cargo recognition. Different isoforms of the kinesin tail defines its cargo specificity. The repertoire of cargos can be broadened by alternative splicing, where different splice variant bind different cargos. In other kinesin families, such as kinesin-1 and 2, the light chains associated to the heavy chain's C-terminal domains specify the cargo selectivity. This rather variable part of the protein among the kinesin superfamily has also a secondary function, which is the autoinhibition of the motor domain (Verhey and Hammond 2009). Depending on the overall structure variability, currently 14 kinesin subfamilies are known (Figure 1-3). Although most of the subfamilies have different light chain and heavy chain C-terminal domains there are also subfamilies with more radical structural differences. Such is the kinesin-14 subfamily including the *Drosophila* Ncd where the motor domain is on the C-terminus and it moves along microtubules in the opposite direction than most kinesins. Another one is the mitotic spindle associated bimC kinesin from the kinesin-5 subfamily which is a bipolar tetrameric kinesin (Kashina et al. 1997).

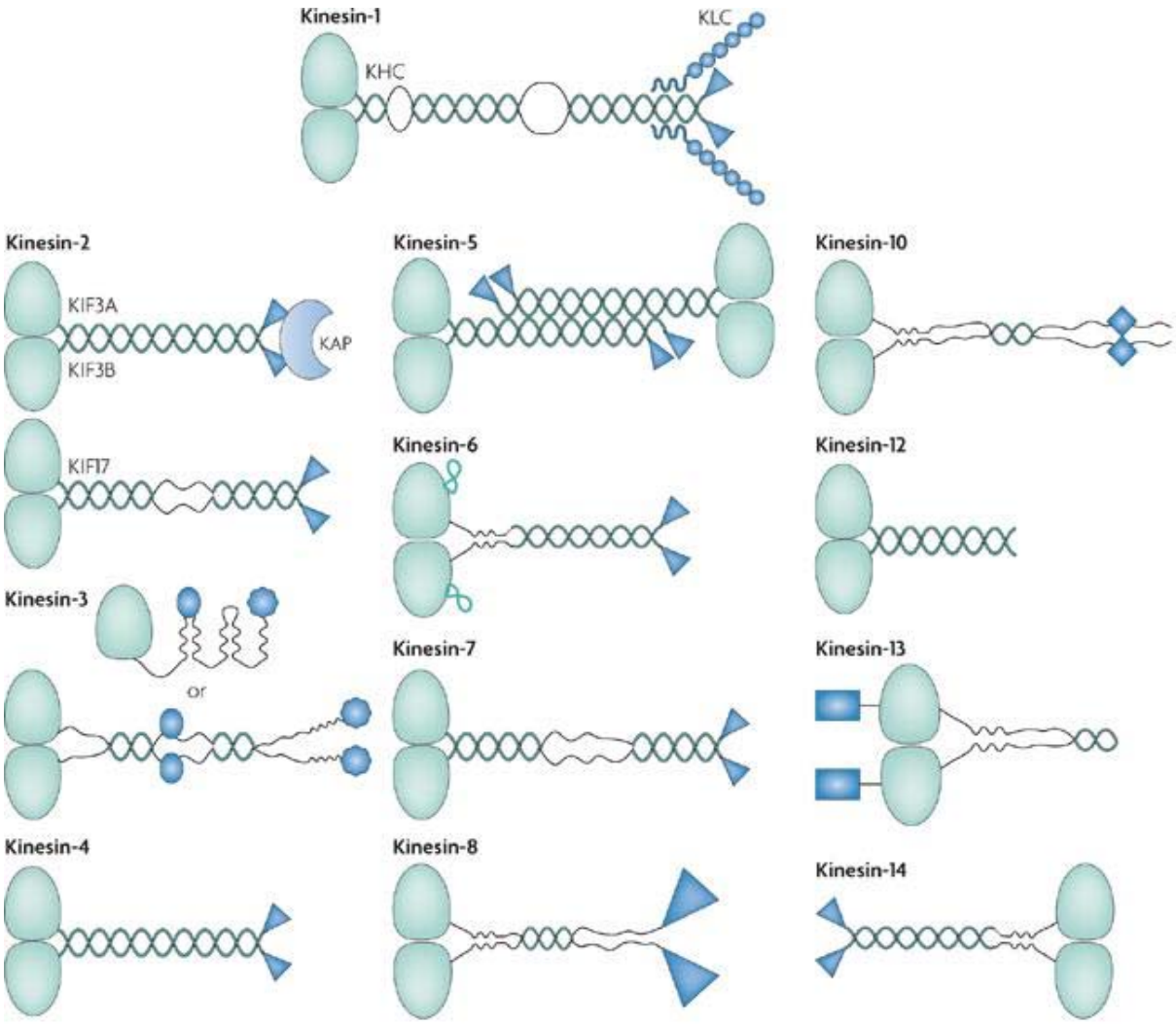

Figure 1-3: Schematic representations of all 14 kinesin subfamilies. Picture taken from http://www.nature.com/nrm/journal/v10/n11/box/nrm2782_BX1.html. The motor domains are in light green, the coiled coils in dark green and the non-motor domains are in blue; KHC: kinesin heavy chain; KLC: kinesin light chain

1.2.2 Heavy chain structure and function

In contrast to the diverse light chains and C-terminal domains of the heavy chains of certain kinesin subfamilies, the principle structure and function of the remainder heavy chain is relatively uniform. Thus the heavy chains contain a globular motor domain most often close to their N-terminus, a ~13-amino acid-long neck linker and a C-terminal stalk (Figure 1-4). The stalk region carries the dimerization function by forming a coiled coil with the stalk of another heavy chain. Heptade amino acid-repeats are crucial for the interaction between the stalks.

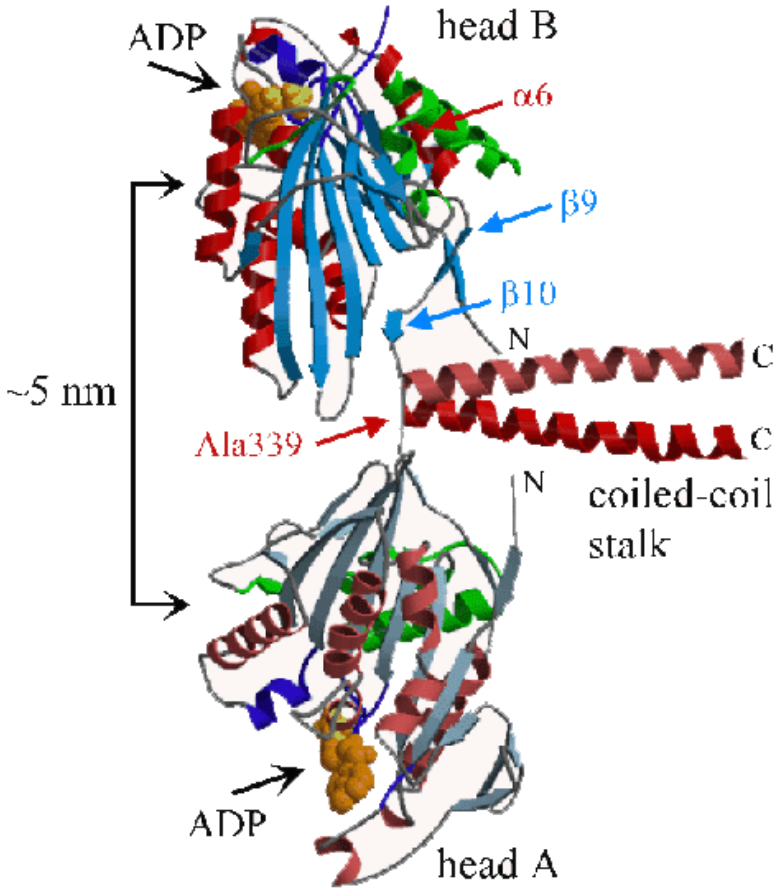

Figure 1-4: A crystal structure of a kinesin-1 heavy chain homodimer. Picture taken from http://www.stanford.edu/group/blocklab/kinesin.html. The different secondary structures are designated with different colours

The stalk is connected to the motor domain through the neck linker. The neck linker does not have a characteristic secondary structure, but it plays a key role in the mechanism of movement. The remainder of the motor domain, contains a P-loop for binding ATP, two switches (I and II) and a large β-sheet near the core of the motor domain where the neck linker is docking (Marx et al. 2008). There are however some loops in the motor domain, which are suggested to be responsible for the specific binding of αβ tubulin heterodimers (Figure 1-5).

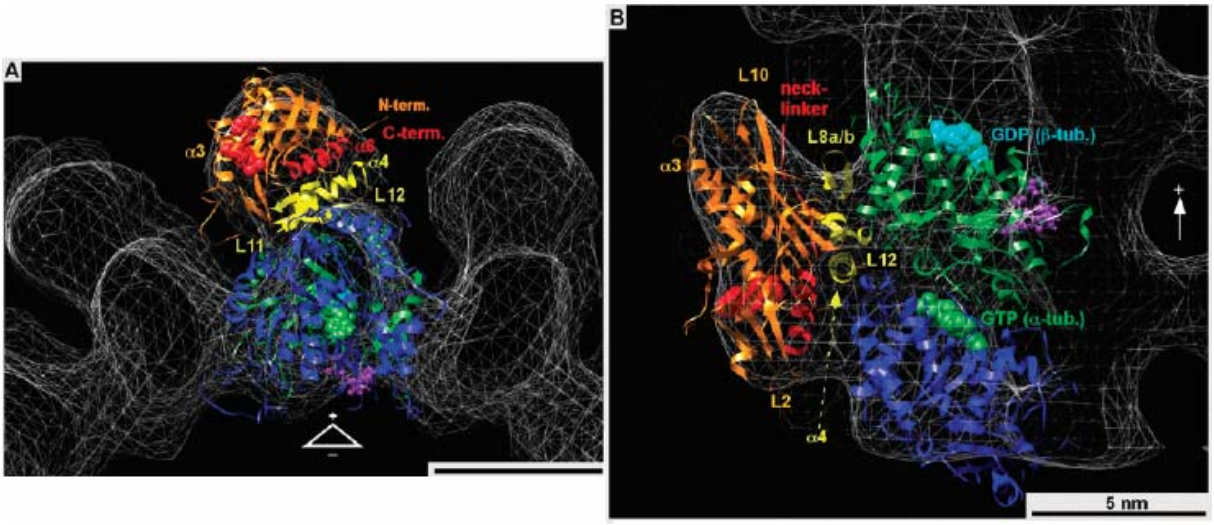

Figure 1-5: An overlay of crystal structures of *Neurospora crassa* kinesin-3 (red-yelow), α (green) and β tubulin (blue) with a cryo-EM image of kinesin decorated microtubule where the kinesins interaction with the microtubule is locked through AMPPNP, a non-hydrolysable ATP analog. Figure taken from Marx et al. 2008 ; A: End-on view of the microtubule-motor complex with the minus end oriented to the observer; B: Slightly tilted sideview of the motor-dimer complex with the microtubule plus end at the top

1.2.3 Mechanism of movement

In general, kinesins are motor proteins which move along microtubules. The microtubules are polar, long, tube-like polymers build out of αβ tubulin heterodimers. Most kinesins move towards the plus- or growing end of the microtubules. There are however, as mentioned above, some kinesins which are minus-end orientated. The energy needed for the movement is gained through the hydrolyzation of ATP to ADP. Depending on the type and structure, kinesins can move processively, when both motor domains from the heavy chain dimer contribute to the movement, or non-processively when the kinesin is either monomeric, or is a heterodimer. In such as case, one of the motor domains does not contribute actively to the movement. The majority of non-processive kinesins move at a slower pace when compared to processive kinesins. Kinesin 3, is mostly found in its monomeric form, but can transform itself in a processive kinesin after dimerization (Hammond et al. 2009). During the process of movement one of the motor domains of processive kinesin strongly interacts with the microtubule and throws the other, trailing motor domain forwards. This motor domain than undergoes a stronger bond with the microtubule and takes its turn to throws the now loosely bound motor domain forwards. Since each motor domain can only interact at a specific site of a single αβ tubulin heterodimer, one step of a kinesin is exactly as

long as the length of the αβ tubulin heterodimer, that is 8 nm. However, the most interesting characteristic about the movement of kinesins is that they always move in one direction, implying the presence of a gating mechanism. In a recent single molecule study this mechanochemical gating mechanism was well described (Guydosh and Block 2009). It was shown that in the absence of a nucleotide in the ATP binding pocket of the leading motor domain, it binds intermediately tight to the microtubule, whereas the trailing motor domain containing ADP is just loosely bound. Upon entrance of ATP in the binding pocket the leading motor binds tightly and the trailing motor domain is being thrown to the front. During this movement the ATP in the now trailing motor domain is being hydrolyzed. At the same time in the now leading motor domain the ATP binding pocket releases the ADP and is ready to accept ATP. With this, the cycle is closed and can be repeated (Figure 1-6). During its microtubule-bound state, the ATP-binding domains of the kinesin heads can only be fitted with the described combination of ADP or ATP due to mechanistic reasons. This gating mechanism confirms the one-head-bound mode of movement.

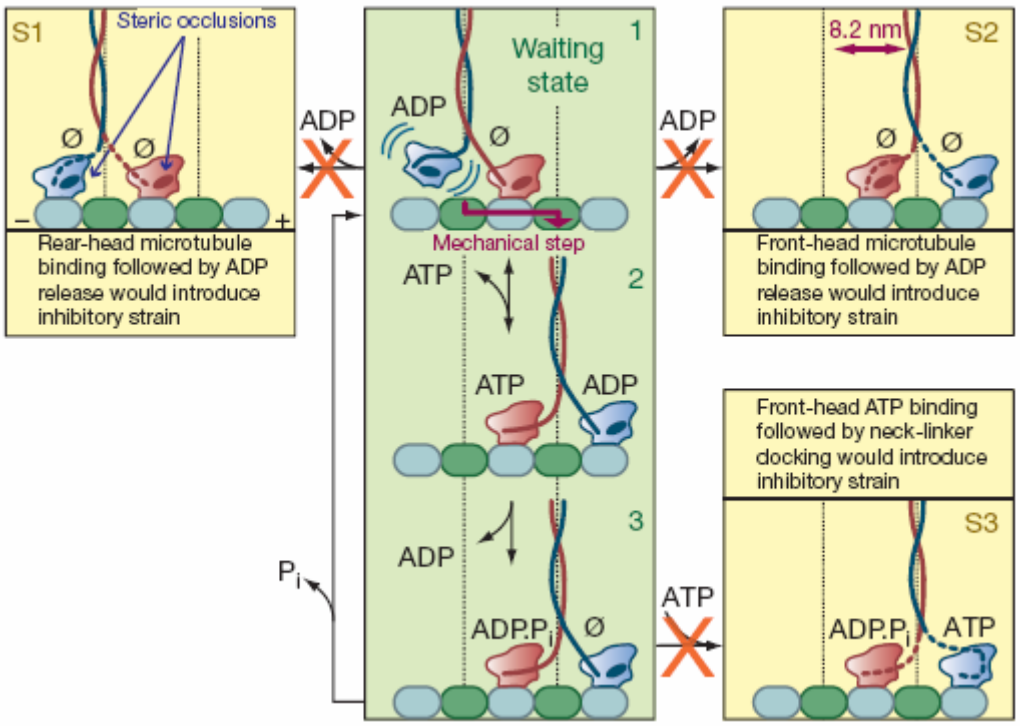

Figure 1-6: A schematic model of the mechanochemical gating mechanism of the processive kinesin movement along microtubules. Firgure taken form: Guydosh and Block 2009; S1-S3 are the hypothetical states at which the kinesin can not be found in, which contributes to the rigid gating of the state conversionts

The unique processive movement mechanism of dimeric kinesins is not defined only by the mechanochemical gating system, but also by other mechanistic properties. Recently, it has been additionally shown that the length of the neck linkers as well as their attachment points are crucial for the processive movement (Miyazono et al. 2009). The neck linker is the part of

the motor domain which changes position upon ATP induced conformational change. In this process, the neck linker moves from the undocked position towards the motor domain core-β-sheet where it docks, thus producing a power-stroke (A, Figure 1-7). Since the neck linker acts as a lever, its full length is vital for the movement (B, Figure 1-7). The length of the neck linkers is equally adapted to the length of a single kinesin step. This way the forward thrown motor domain falls as close as possible to the binding site, and needs less time to find its position by diffusion. An engineered alternative binding of the neck linker from the one monomer to the N-terminus of the other monomer shows processive movement but not comparable with natural one. This suggests that the N-terminus might be involved in the conformational changes associated with the powerstroke.

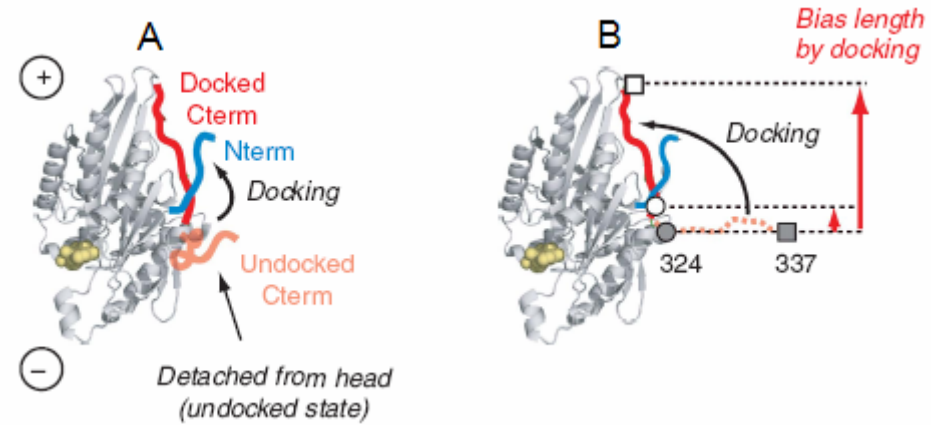

Figure 1-7: **A: Relative position of the neck linker to the whole motor domain in a docked and undocked state; B: hypothetical difference in the bias depending from the neck linkers length; The + and the – represent the relative orientation of the motor domains to the orientation of the microtubule. Figure taken from Miyazono et al. 2009**

1.3 *in vitro* application of the kinesin-microtubule system

Ever since it is possible to polymerize microtubules *in vitro,* it has also been possible to observe the movement of kinesin along these microtubules. In this process the presence of taxol is important as it stabilizes microtubules and preserves ATP for the kinesin to utilize as a source of energy. A number of different set-ups exist to visualize kinesis moving along microtubules. One of the simplest ways is to functionalize a glass slide or a coverslip with kinesins and to add microtubules (B, Figure 1-8). this case the kinesins are moving the microtubules, and this process can be visualized using video enhanced differential interference contrast microscopy (Schnapp et al. 1988), (Schnapp et al. 1988), or using a fluorescence microscope in case the microtubules are fluorescently labeled. This way of observing the movement of the kinesin along microtubules is better known as gliding assay, since the microtubules look like they are gliding over the surface. In this mode of the kinesin-

microtubule transportation systems different microtubules move in different directions. Alternatively, the gliding movement of the microtubules can be used in a micro or nanofluidic system, where the channels are wide enough for a microtubule to enter, but narrow enough so that it can not turn around or get stuck in a perpendicular orientation. Under these conditions the microtubules can be transported along kinesin coated channels. Once they enter the channel they can move only in one direction and act as a shuttle (Carroll-Portillo et al. 2009). Another possibility to observe the kinesin movement is where microtubules are immobilized onto a surface and the kinesin moves along the microtubules, just as it occurs in the nature (A, Figure 1-8). For the observation of a single molecule, kinesins are either fluorescently labeled or they can be conjugated to small beads (bead assay). In this case the transportation system can be more precisely engineered than in the first case. Carefully adjusting the orientation of microtubules, kinesins can move in a given direction. This way the cargo is transported much faster than by a microtubule shuttle which depends on the diffused motion of the microtubules on the kinesin coated surface.

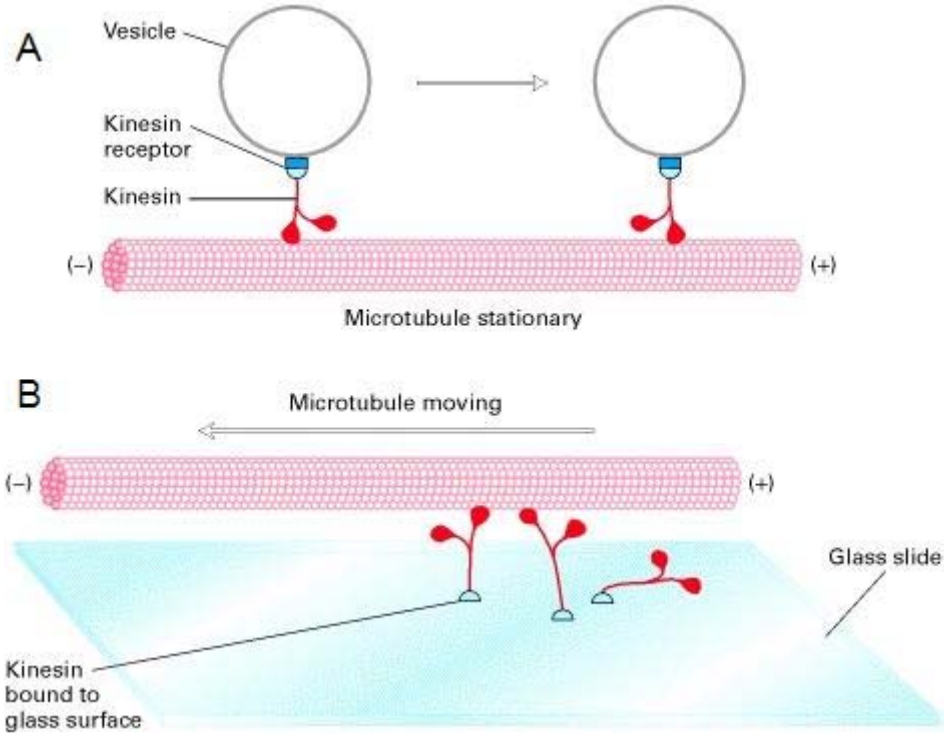

Figure 1-8: Cartoons which shows the concept of a bead assay (A) and a gliding assay (B). Picture taken from http://www.ncbi.nlm.nih.gov/bookshelf/br.fcgi?book=mcb&part=A5452

1.4 Phage display

One Among others, phage display is a very interesting tool used in molecular biology to mimic evolutionary processes. The method is based on presenting proteins or peptides of

interest on the surface of filamentous bacteriophages by genetically fusing the gene of interest to a gene encoding one of the coat proteins of the phage (Smith 1985). Once phage particles are produced by an infected host, the recombinant fusion protein is expressed from the phage genome and integrated into the phage virion during the assembly process of the particle, which harbors' the DNA. Thereby the phenotype is directly coupled with its genotype. The most common phage display system is base on the bacteriophage M13, which is filamenous, non-lytic and contains a circular ssDNA. The DNA is enclosed by a rod shape cylinder assembled from ~2700 copies of protein pVIII. At the proximal, or infectious tip of the phage five copies each of protein pIII and pVI are presented. On the other end, the so-called remote tip, five copies each of proteins pVII and pIX are present (Figure 1-9). Although there are cases where the phage coat protein pIX was fused with peptides, the most successful presentation on the phage is done by fusing the protein of interest to the N-terminus of the phage coat protein pIII.

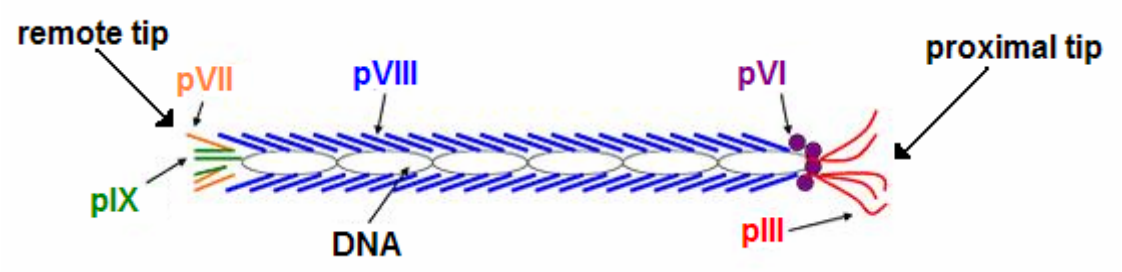

Figure 1-9: Schematic presentation of the M13 filamentous phage; pIII, pVI, pVII, pVIII and pIX are the different proteins found on the phage

For production of protein-presenting phages, an *E. coli* strain containing the F-episome is transformed with an engineered phagemid – essentially a plasmid containing the gene of interest fused to gIII, the M13 origin of replication and packaging signal and a selective marker gene. Next, the bacterial cells are infected with a M13 helper phages. Helper phages contain all genes necessary for the assembly of fully infectious bacteriophage particles, but have an impaired packaging signal. During the assembly process all proteins necessary for the capsid formation are expressed and phage particles start assembling at specifically organized pore complexes at the inner membrane of *E. coli*. Proliferation of a single phage begins with the remote tip and as the capsid is elongated to cover the DNA, it protrudes through the outer membrane into the surrounding milieu. Finally the proximal tip is assembled and the phage is released (Figure 1-10). For efficient incorporation of the pIII protein into the capsid, it has to be transported to the periplasm of the bacteria where it awaits to be recruited by the phage assembly machinery.

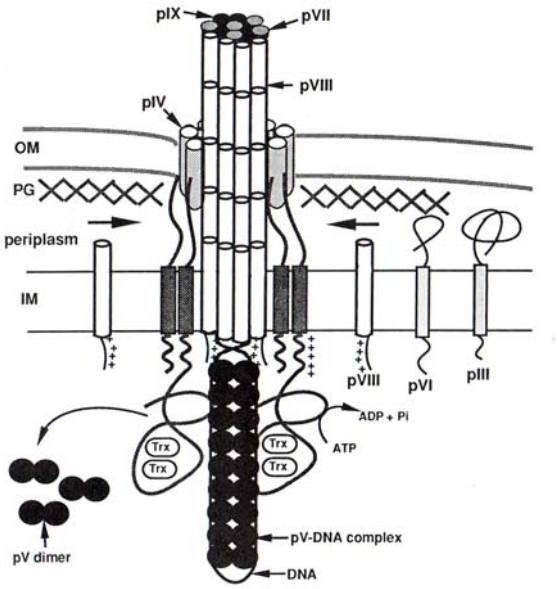

Figure 1-10: Schematic representation of a M13 bacteriophage assembly. Image taken from B. K. Kay, J. Winter, J. McCafferty; "Phage Display of Peptides and Proteins"; Academic press, Harcourt Brace & Co.; OM: outer membrane; IM: inner membrane. pIII-pIX: M13 bacteriophage associated proteins; trx: thioredoxin

Transportation of pIII into the periplasm depends on the leader sequence. Most commonly used leader sequence for phage display is pelB, which is recognized in the Sec-dependent pathway. In this secretory pathway the proteins are being translocated post-translationally through the cytoplasmic membrane in the periplasm in an unfolded state (Nilsson et al. 1991). It has been shown however that pIII fusion proteins can be successfully translocated to the periplasm and incorporated into phages using another, so-called signal recognition particle (SRP) pathway (Thie et al. 2008). This translocation pathway uses different leader sequences and the translocation of the polypeptide is being performed co-translationally (Valent 2001). Additionally, the twin arginine translocation (Tat)-mediated pathway is also present in *E. coli,* whereby proteins are translocated across the cytoplasmic membrane in an already folded fashion. Since pIII can only fold properly in the periplasm and not in the cytoplasm, this translocation pathway is not applicable for its transport to the periplasm. This excludes the possibility to present proteins which need to be folded in the cytoplasm to function properly, for example GFP (Feilmeier et al. 2000). from being presented on the phage surface as a pIII fusion protein. Short peptides where first to be presented on the phage surface using this method (Devlin et al. 1990) in the hope to produce combinatorial library for selection of specific binder peptides. Shortly after that, the first antibody fragment libraries utilizing phage display were generated (Clackson et al. 1991; McCafferty et al. 1991). Notably, for ~10 years, phage display was the only way of selecting fully human antibodies breaking ground for the development of human therapeutic antibodies. Apart from producing

specific binders, functionally active enzymes have also been successfully presented on M13 phage particles (Corey et al. 1993; McCafferty et al. 1991).

1.5 Protein engineering and goal

the development of nanobiotechnology and lab-on-a-chip technologies there is growing need not only for simple tools, but rather for tunable tools. In this respect, a more robust and tunable kinesin-microtubule transportation system would be of great interest and would surely find a much broader use in future lab-on-a-chip applications than the natural systems currently under investigation. Bearing said in mind, the most important criteria for selecting a kinesin molecule to investigate, is its robustness and thermostability. There are many eukaryotic organisms whose optimal living temperature is higher than usual ambient temperatures. These are good candidates for obtaining a kinesin that is stable at higher temperatures. In this respect the fungus *Thermomyces lanuginosus* whose growth optimum is at 50° was the organism of choice for fulfilling the first criteria. Other enzymes form *T. lanuginosus* have already been used before, explicitly due to their thermostable property (Basaveswara Rao et al. 1981; Damaso et al. 2003; Guo et al. 2005; Li et al. 2005; Rezessy-Szabo et al. 2007). Two ortholog of the kinesin-3 family from *T. lanuginosus,* the TLKIF1 and TKIN had been previously cloned, expressed in *E. coli* and functionally characterised (Rivera et al. 2007; Sakowicz et al. 1999) Since TKIN was characterized more recently and in greater detail, TKIN was taken as the basis for this investigation, The speed of this kinesin in a microtubule gliding motility assay has been reported to be up to 5,5 µm/s, which is considerably faster than the conventional kinesin-1 family representatives from the animal kingdom. The basic sequence of TKIN has been modified to match further criteria. First the coiled coil 2 (CC2) domain and the forkhead associated (FHA) domain (Figure 1-2) have been removed. The coiled coil 1 (CC1) domain has been kept in order to test if the normally monomeric TKIN can form dimers using only the CC1 domain, thus producing processive movement after dimerization. In a second step all cysteins and a serine residue were exchanged with other amino acids. This was necessary as free cysteins can be crosslinked in an oxidative environment, such as the periplasm or simply atmospheric conditions. Next, the sequence was optimization for prokaryotic expression by exchanging base triplets with analogous triplets encoding the same amino acid, but corresponding to a more abundant tRNA in *E. coli*. Codon optimization shall allow higher yield of the recombinant proteins as no limitations of tRNAs should be encountered. Thanks to technological progress, the modifications described above were not needed to be introduced one by one. The whole coding sequence of the modified TKIN (mTKIN) including respective cloning site added to each end of the sequence was synthetically ordered from the gene synthesis company

Sloning BioTechnology (Puchheim). Once the construct has arrived, it was cloned behind a lac promotor sequence of the pQDKG2 vector (AG Konthur, MPI for Molecular Genetics, Berlin) which is a pQE30 derivative (QIAGEN). This enables the controlled expression of the protein by adding IPTG to the medium to induce protein expression. Additional features of this vector includes a C_terminal Avi-His6-tag. This is a bi-functional tag where the first part consists of a synthetic minimal recognition motif (Figure 1-11) This motif is recognized in *E. coli* by the endogenous enzyme biotin ligase (birA) which post-translationally modifies the lysine residue of the tag by addition of a biotin. The second part of the tag contains six histidines. Once expressed, the recombinant protein is automatically biotinylated and can be easily immobilized onto streptavidin coated surfaces by exploiting the specific and highly stable biotin-streptavidin interaction. The His_6-tag is important for Ni-NTA affinity purification purposes since this purification method is relatively inexpensive and common for recombinant protein purification.

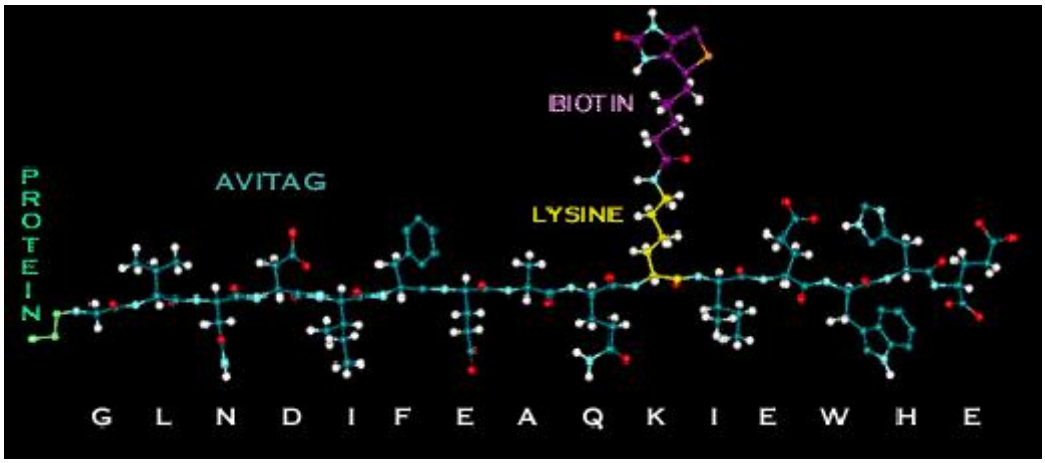

Figure 1-11: structural representation of the Avi-tag amino acid sequence which has been biotinylated. Image taken from http://www.fulengen.com/images/AviTag.gif

For the periplasmic expression and phage display the mTKIN sequence was cloned into the phagemid vector pIT2. mTKIN is introduced in between the pelB leader sequence for translocation into the periplasm and the M13 gene III. The resulting construct expresses mTKIN either with a C-terminal His6-tag only, or as a fusion-protein to pIII, depending on the host strain used. The project pursues three main goal. Primarily, the best expression conditions for mTKIN using the pQDKG2 vector shall be establishing and an affinity chromatography based purification scheme shall be developed. Second goal was to assess the periplasmic expression and presentation efficiency of mTKIN on filamentous M13 bacteriophages using the pIT2 vector. Last, the biochemical and mechanochemical properties of mTKIN expressed in *E. coli* and presented on M13 phages shall be investigated. The project pursues three main goal. Primarily, the best expression conditions for mTKIN using the pQDKG2 vector shall be establishing and an affinity chromatography based

purification scheme shall be developed. Second goal was to assess the periplasmic expression and presentation efficiency of mTKIN on filamentous M13 bacteriophages using the pIT2 vector. Last, the biochemical and mechanochemical properties of mTKIN expressed in *E. coli* and presented on M13 phages shall be investigated.

2 Materials and Methods

2.1 Materials for *E. coli* and phage work

2.1.1 *E. coli* strains

Strain name	Genotype	Source
DH10 B	F- *mcr*A Δ(*mrr-hsd* RMS-*mcr*BC) Φ80d*lac*ZΔM15 Δ*lac*X74 *end*A1 *rec*A1 *deo*R Δ(*ara*, *leu*)7697 *ara*D139 *gal*U *gal*K *nup*G *rps*L λ-	Invitrogen, Carlsbad, USA
BL21 (DE3) star pRARE3	F- *omp*T *hsd*S_B (r_B- m_B-) *gal dcm rne*131 (DE3) [pRARE3, *lac*I^q, *bir*A, Cm^r]	MPI for Molecular Genetics
BL21 (DE3) pLysS	F–, *omp*T, *hsd*S_B (r_B–, m_B–), *dcm*, *gal*, λ(DE3), [pLysS, Cm^r]	Promega, Mannheim
BL21 CodonPlus (DE3)-RIL	F– *ompT hsdS* (r_B– m_B–) *dcm*+ Tet^r *gal* λ(DE3) *endA* Hte [*argU ileY leuW* Cam^r]	Stratagene, La Jolla, USA
Origami™ B (DE3) pLacI	F– *omp*T *hsd*S_B (r_B– m_B–) *gal dcm lac*Y1 *ahp*C (DE3) *gor*522::Tn10 *trx*B [pLacI (Cam^R, Kan^R, Tet^R)]	Merck, Darmstadt
TG 1	*sup*E *thi*-1 Δ(*lac-pro*AB) Δ(*mcr*B-*hsd*SM)5(r_K– m_K–) [F' *tra*D36 *pro*AB *lac*I^qZΔM15]	Stratagene, La Jolla, USA
XL-1 Blue	*rec*A1 *end*A1 *gyr*A96 *thi*-1 *hsd*R17 *sup*E44 *rel*A1 *lac* [F' *pro*AB *lac*I^qZΔM15 Tn10 (Tet^r)]	Stratagene, La Jolla, USA
HB2151	nal^r thi-1ara ∆(lac-proAB) thi [F' pro A+B $lacI^q$ lacZ∆M15]	Clontech, Mountain View USA

2.1.2 Bacteriophage

Bacteriophage	Manufacturer
M13KO7 Helper Phage (N0315S)	New England Biolabs, Frankfurt am Main
Hyperphage (PRHYPE)	Progen, Heidelberg

2.1.3 Culture medium

Liquid	
2xYT (per 1 L):	LB (per 1 L)
16 g Bacto Tryptone	10 g Bacto Tryptone
10 g Bacto Yeast Extract	5 g Bacto Yeast Extract
5 g NaCl	10 g NaCl
pH 7,2 with NaOH	pH 7,5 with NaOH
ad H_2O up to 1 L	ad H_2O up to 1 L
autoclaved	autoclaved
Agar medium	
2xYT Agar (per 1 L)	LB Agar (per 1L)
16 g Bacto Tryptone	10 g Bacto Tryptone
10 g Bacto Yeast Extract	5 g Bacto Yeast Extract
5 g NaCl	10 g NaCl
pH 7,2 with NaOH	pH 7,5 with NaOH
15 g agarose	15 g agarose
ad H_2O up to 1 L	ad H_2O up to 1 L
autoclaved	autoclaved
Top-agar (per 1 L)	M9 Minimal agar medium (per 1 L)
7 g agarose	200 mL 5x M9 salts
in H_2O	2 mL 1M $MgSO_4$
	20 mL 20% Glucose
	0.1 mL $CaCl_2$
	15 g agarose
	in H_2O

Glucose was usually added to the medium to a total concentration of 2%except otherwise designated. For selective growth purposes the following antibiotics were added to the final concentrations of:

Antibiotic (final work concentration in meduim)	Manufacturer
Ampicillin (100 μg/mL)	Carl Roth, Karlsruhe
Kanamycin (60 μg/mL)	Roche, Basel
Chloramphenicol (17 μg/mL)	Roche, Basel
Tetracyclin (10 μg/mL)	Roche, Basel

2.2 Prefabricated materials

2.2.1 Kits

Product	Manufacturer
peqGOLD Plasmid Miniprep Kit I (12-6942-02)	peqlab Biotechnologie, Erlangen
QIAGEN® Plasmid Maxi Kit (12163)	Qiagen, Hilden
ATP Affinity Test Kit (AK-102)	Jena Bioscience, Jena
CN/DAB Substrate Kit (34000)	Thermo Scientific, Bonn
EasyXpress Insect Kit II (32561)	Qiagen, Hilden
RNeasy MinElute Cleanup Kit (74204)	Qiagen, Hilden

2.2.2 Other prefabricated materials

Product	Manufacturer
10X NEB buffer EcoRI (B0101S)	New England BioLabs, Frankfurt am Main
10x HF PCR buffer (K0192)	Fermentas, St. Leon-Rot
GeneRuler™ 100 bp Plus DNA Ladder (SM0321)	Fermentas, St. Leon-Rot
GeneRuler™ 1 kb DNA Ladder (SM0311)	Fermentas, St. Leon-Rot
6x Loading dye (R6011)	Fermentas, St. Leon-Rot
Complete protease inhibitor cocktail (04 693 124 001)	Roche, Basel
Ni-NTA Agarose (30230)	Qiagen, Hilden
Ni-NTA Magnetic Agarose Beads (36113)	Qiagen, Hilden
Ni-NTA SuperFlow Cartridges 1 mL (1034559)	Qiagen, Hilden

Product	Manufacturer
NuPAGE® 4-12% Bis-Tris Gel (NP0329BOX)	Invitrogen, Carlsbad
NuPAGE® Novex® 4-12% Bis-Tris Midi-Gel (WG1403BOX)	Invitrogen, Carlsbad

2.3 Materials for molecular biology work

2.3.1 Enzymes

Enzyme	Manufacturer
EcoRI (R0101S)	New England BioLabs, Frankfurt am Main
HindIII (R0104S)	New England BioLabs, Frankfurt am Main
HF PCR enzyme mix (K0191)	Fermentas, St. Leon-Rot
Lysozime (L 6876)	Sigma, Steinheim
Pyruvate kinase/Lactic dehydrogenase from rabbit muscle (P0294)	Sigma, Steinheim

2.3.2 Oligonucleotides, Plasmids

Oligonucleotide/Plasmid	Producer
pQE276 (GGCAACCGAGCGTTCTGAAC)	Eurofins MWG Operon
JD5' (CCCGAAAAGTGCCACCTGAC)	Eurofins MWG Operon
pUC18	Stratagene, La Jola (CA)
Synthetic mTKIN sequence	Sloning BioTechnology, Puchheim
pQDKG2/mTKIN (Figure 2-1)	MPI for Molecular Genetics, cloned by Dr. Volker Sievert
pIT2/mTKIN (Figure 2-2)	MPI for Molecular Genetics, cloned by Dr. Volker Sievert

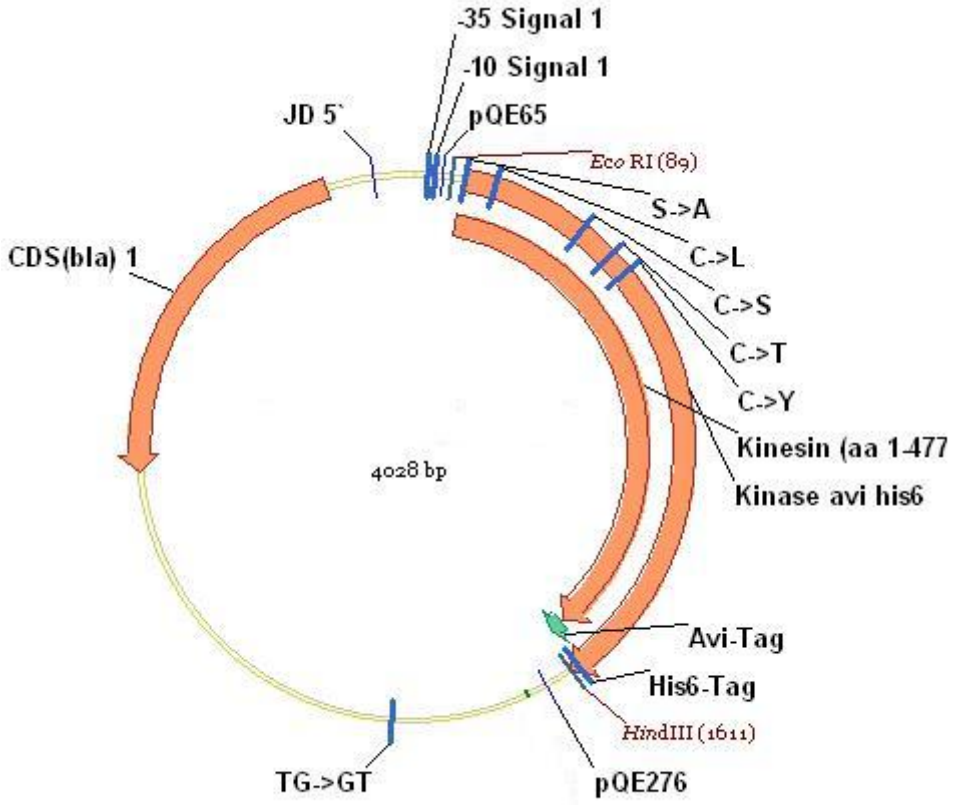

Figure 2-1: pQDKG2/mTKIN plasmid map generated with Vector NTI

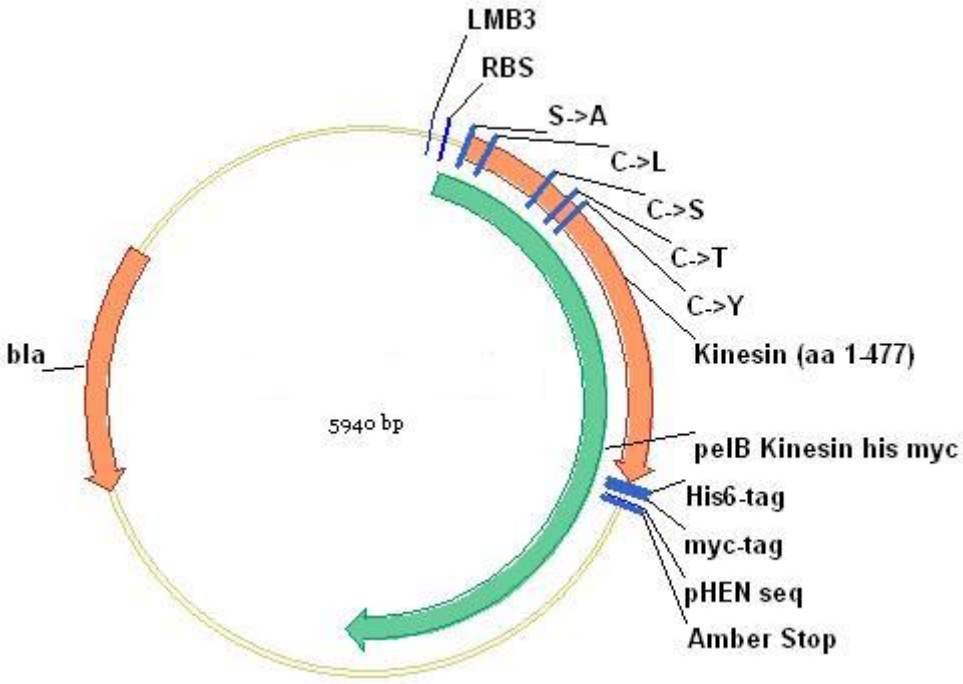

Figure 2-2: pIT2/mTKIN plasmid map generated with Vector NTI

2.3.3 Antibodies, detection protein conjugates and other proteins

Proteins	Manufacturer
Streptavidin-HRP	Thermo Scientific, Bonn
Anti-His (mouse)	Trend Pharma & Tech, Surrey, BC, Canada
Anti-PIII (mouse)	MoBiTec, Göttingen
Anti-mouse-HRP (rabbit)	Sigma, Steinheim
Tubulin from bovine brain (TL238)	Cytoskeleton Inc., Denver
Tubulin X-rhodamine labeled from bovine brain (TL620M)	Cytoskeleton Inc., Denver
Recombinant KIF1A-GFP (kinesin-3, *R. norvegicus*)	MPI for Colloids and Interfaces, Potsdam-Golm

2.3.4 Gel compositions

SDS-PAA stacking gel (per 80 mL):	SDS-PAA separating gel (per 40 mL):
10.4 mL H_2O	23.8 mL H_2O
0.8 mL 10% SDS	0.4 mL 10% SDS
20 mL 1.5 M Tris-HCl pH 8.8	10 mL 0.5 M Tris-HCl pH 6.8
48 mL 29% Acrylamid, 0.8% bisacrylamid	5.3 mL 29% Acrylamid, 0.8% bisacrylamid
Activation of polymerization:	Activation of polymerization:
800 µL 10% Ammonium persulfate	400 µL 10% Ammonium persulfate
25 µL TEMED	40 µL TEMED

2.4 Other compounds and solutions

2.4.1 Compounds

Product	Manufacturer
UltraPure™ agarose (15510-019)	Invitrogen, Carlsbad
IPTG	Fermentas, St. Leon-Rot
Phenylmethanesulfonyl fluorid –PMSF (P7626)	Sigma, Steinheim

Product	Manufacturer
Ethidium bromide	Merck, Darmstadt
Urea (A1361)	AppliChem, Darmstadt
Polyethylene glycol 6000	Merck, Darmstadt
dNTP's	Invitrogen, Carlsbad, USA
D(+)-Glucose monohydrate	Merck, Darmstadt
GTP (G8877)	Sigma, Steinheim
ATP (A3377)	Sigma, Steinheim
PEP (P7127)	Sigma, Steinheim
NADH (N8129)	Sigma, Steinheim
Taxol (A4667)	AppliChem, Darmstadt

2.4.2 Buffers and solution

TAE:
40 mM Tris-acetate
1 mM EDTA
pH 8

Native lysis buffer (NPI-10):
50 mM NaH_2PO_4
300 mM NaCl
10 mM Imidazole
pH 8.0 (NaOH)

Native wash buffer (NPI-20):
50 mM NaH_2PO_4
300 mM NaCl
20 mM Imidazole
pH 8.0 (NaOH)

Native elution buffer (NPI-250):
50 mM NaH_2PO_4
300 mM NaCl
250 mM Imidazole
pH 8.0 (NaOH)

Laemmli running buffer:
0.125 mM Tris
1.25 mM Glycine
0.5% SDS

Laemmli loading buffer 4x:
0,2 M Tris-HCl pH 6,8
8% SDS
40% (w/v) Glycerol
0,004% Bromophenol blue
5% β-Mercaptoethanol

20 x MES running buffer:
1 M MES
1 M Tris-base
69,3 mM SDS
20,5 mM EDTA

Coomassie-stain:
1,25 g Coomassie Brilliant Blue R- 250
225 ml Ethanol (mixed with methanol)
225 ml H_2O
50 ml Acetic acid

Destaining solution:
10% Acetic acid
20% Ethanol (mixed with methanol)
in H_2O

Blotting buffer:
3 g/L Tris-base
14 g/L Glycine

PTM:
1x PBS
2% (w/v) Blotting grade non-fat dry milk
1% Tween® 20

TES buffer:
0.2 M Tris-HCl pH 8.0
0.5 mM EDTA
0.5 Sucrose
sterile-filtrated

PE buffer:
0.5 M Sucrose
0.1 M Tris-HCl pH 8.0
1 mM EDTA

Phage precipitation buffer:
20% PEG 6000
2,5 M NaCl
autoclaved

10x PBS:
2.5 g/l KCl
80 g/l NaCl
14.3 g/l Na_2HPO_4
2.5 g/l KH_2PO_4

PBS-T:
1x PBS
0.1% Tween® 20

All of the salts and chemicals were per analysis grade and purchased from: Merck (Darmstadt), Sigma (Steinheim), BioRad (Munich) or Invitrogen (Carlsbad, USA)

2.5 Laboratory equipment

Product	Manufacturer
Pipettes, PIPETMAN® 1000, 200, 20, 2 µL	Gilson, Middelton (WI)
Multichannel pipettes 5-50 µl, 20-200 µl	Abimed, Langenfeld
PIPETBOY accu	INTEGRA Biosciences, Zizers
Centrifuge 5810R	eppendorf, Hamburg
Centrifuge 5424	eppendorf, Hamburg
Incubator shaker innova ™ 4430	New Brunswick Scientific, New Jersey
Incubator	memmert, Schwabach
PTC 200 Thermo Cycler	MJ Research, Waltham (MA)
NanoDrop 2000	Thermo scientific, Wilmington (DE)
MicroPulser Electroporator	Bio-Rad, Hercules (CA)
SE 215 Mighty Small Multiple Gel Caster	Hoefer, Holliston (MA)

Product	Manufacturer
SE 250 Mighty Small II	Hoefer, Holliston (MA)
XCell SureLock™ Electrophoresis Mini-Cell	Invitrogen, Carlsbad
XCell 4 SureLock™ Electrophoresis Midi-Cell	Invitrogen, Carlsbad
Electrophoresis Power Supply EPS 200, 300, 301, 600	Pharmacia Biotech, Freiburg
Gel documentation GelDoc 2000	BioRad, Munich
UV-Lamp Model UVL 21	Ultra-Violet Products, San Gabriel, USA
Linear shaker	Gerhardt, Königswinter
22 Mighty Small™ Transphor tank transfer unit	Hoefer, Holliston (MA)
Image analyser LAS 1000	Fujifillm, Düsseldorf/ raytest, Straubenhardt
Digital pH-/ mV-/ Thermometer	Greisinger, Regenstauf
AF 20 Flake Ice Machine	Scotsman, Vernon Hills, USA
Vortexer Vortex-Genie	Scientific Industries, New York, USA
weighing scale Adventurer™ Pro AV812	Ohaus, Pine Brook, USA
Biophotometer	Eppendorf, Hamburg
Magnetic stirrer MR3001	Heidolph, Schwabach
Roller TRM-V	IDL, Nidderau
Thermomixer comfort 5355	Eppendorf, Hamburg
Microflow Laminar Flow Workstation	Kendro, Langenselbold
Axioimager.Z1	Zeiss, Göttingen
LSM 700	Zeiss, Göttingen
SpectraMax, Microplate reader	Molecular devices, Sunnyvale (CA)
ÄKTApurifier	GE Helthcare, Munich
LTQ-Orbitrap	Thermo Scientific, Wilmington (DE)

2.6 Laboratory consumables

Product	Manufacturer
Polypropylene tubes 15, 50 mL	Greiner Bio-one, Frickenhausen
Disposable tubes 0.5, 1.5, 2 mL	Eppendorf, Hamburg
Disposable flasks 250, 500 mL	Corning, New York, USA
Polypropylene tubes 14 ml	Greiner Bio-One, Frickenhausen

Product	Manufacturer
Disposable sterile pipettes (5, 10, 25 mL)	Corning, New York, USA
Disposable pipette tips (10, 200, 1000 μL)	Gilson, Middleton, USA; Greiner Bio-One, Frickenhausen, Eppendorf, Hamburg
Disposable stuffed pipette tips (10, 200, 1000 μL)	Biozym, Oldendorf
Inoculation loops	Nunc, Roskilde, Denmark
96-well Flexible PVC Microplates, flat-bottom	Becton, Dickinson and Company, Franklin Lakes, USA
Microtiter plate NUNC-Immuno Plate F96 Maxisorp	Nunc, Roskilde, Danmark
PCR-8 tube stripes	Greiner Bio-One, Frickenhausen
Petri dishes	Greiner Bio-One, Frickenhausen
Electroporation cuvettes (0,1 cm gap)	Bio-Rad, Hercules (CA)
Disposable cuvettes (P948)	Carl Roth, Karlsruhe
Amersham Hybond™ ECL™	GE Healthcare, Freiburg
Whatman Paper 3 mm	Whatman, Maldstone, USA
Graduated cylinder 100-1000 ml	Fortuna, Brilon
Erlenmeyer flasks 250 mL, .05 L, 1L	Schott, Mainz
Glass bottles 100 ml, 250 ml, 0.5 L, 1 L	Schott, Mainz
Spectra/Por dialysis membrane tubing MWCO: 3500 (132 720)	Spectrum Laboratories, CA, USA
Cover slips	Menzel-Gläser, Braunschweig
Microscope slides	Carl Roth, Karlsruhe

2.7 DNA preparation and analysis

2.7.1 Plasmid preparation

Glycerol stocks of the *E. coli* DH10B clones carrying sequence-confirmed mTKIN constructs were used for inoculation of 2xYT medium supplemented with ampicillin. For preparation of smaller plasmid amounts (miniprep) the peqGOLD Plasmid Miniprep Kit I from peqlab was used. The preparation was performed in accordance with the manufacturer's protocol found in the kit's handbook from 4 mL cultures. For production of larger plasmid amounts (maxiprep)

the Plasmid Maxi Kit from Qiagen was used. The pIT2/mTKIN construct was prepared from 100 mL culture in accordance with the standard protocol found in the manufacturer's handbook. For the maxiprep of the pQDKG2/mTKIN the protocol for low-copy plasmids was used and the plasmid was prepared from a 500 mL culture. This was necessary since the pQDKG2 is a derivative of a low-copy plasmid. Irrespective of the manufacturer, both plasmid preparation kits are based on purifying DNA from a soluble cell lysate over a disposable ion-exchange chromatography column.

2.7.2 Analysis of plasmid preparations using DNA restriction digest

The presence of the mTKIN gene in the vector was analyzed by restriction digest of plasmid DNA from the maxiprep of pQDKG2/mTKIN. Digest was carried out with single cutter restriction enzymes. The pQDKG2/mTKIN was digested with an aliquot of EcoRI and HindIII restriction enzymes (Table 2-1). The *in silico* digest with these enzymes should produce a 1522 bp and a 2506 bp long DNA fragment. For a better analysis, an aliquot of a non-digested pQDKG2/mTKIN was loaded on a gel next to the digested sample to rule out additional bands corresponding to non-digested plasmid DNA. The relative size of the bands was determined by comparison with a DNA ladder (GeneRuler™ 1 kb DNA Ladder, Fermentas).

Table 2-1: Reaction mixture for a analytical Plasmid DNA restriction digestion

Plasmid pQDKG2/mTKIN	~380 ng (0,5 µL)
10X NEB buffer EcoRI	2 µL
Eco RI	5 U (0,25 µL)
Hind III	5 U (0,25 µL)
H2O	ad 20 µL
37° C, 1 hour	

2.7.3 DNA gel electrophoresis

For analysis, DNA fragments were chromatographically separated according to their size in an agarose gel using an electric field. The gel consists of a 1% agarose solution in TAE

buffer which was subsequently heated in a microwave oven in order to dissolve the agarose. After the gel cooled down to ~60°C, 1 µL ethidium bromide stock (stock conc. 10 mg/mL) – a DNA intercalating fluorescent compound – was added to each 50 mL agarose solution and was gently mixed. The liquid gel was than poured into a electrophoresis chamber containing a comb to produce sample pockets and let to solidify. Once hardened, the comb was removed from the gel and the chamber was filled with TAE buffer. The samples were mixed with 6x loading dye before loading onto the gel and the gel was run at 80 V for 40 minutes. After gel electrophoresis the position of the DNA fragment was detected by UV light at 254 nm.

2.7.4 mTKIN ORF amplification by polymerase-chain reaction

As a prerequisite for high efficiency of the *in vitro* transcription step within the *in vitro* expression procedure of mTKIN (2.11) a concentrated linear form of the mTKIN ORF was produced. For this purpose the mTKIN ORF was PCR-amplified from the pQDKG2/mTKIN construct using the primers pQE276 and JD 5'. This primer pair was chosen after determining *in silico* that it bind in the flanking regions of the mTKIN ORF and include all necessary promoter regions needed for transcription and translation (Figure 2-1). The PCR was performed in 50 µL reaction volume (Table 2-2).

Table 2-2: Reaction mixture for PCR amplification of the mTKIN ORF, used for *in vitro* expression

10x HF PCR buffer	5 µL
dNTP's	0,2 mM each (4 µL)
JD 5'	10 pmol (1 µL)
pQE276	10 pmol (1 µL)
pQDKG/mTKIN	~90 ng (0,5 µL)
HF PCR Enzyme Mix	2,5 U (0,5 µL)
H_2O	ad 50 µL
Total reaction volume 50 µL	

The PCR cycler program was set as in Table 2-3

Table 2-3: PCR cycler program for the amplification of the mTKIN ORF

Step	Temperature	Time	Cycles
Initial denaturation	95° C	5 min	1x
Denaturation	95° C	20 sec	
Annealing	60° C	30 sec	35x
Elongation	72° C	2 min	
Final elongation	72° C	10 min	1x
End	4° C	∞	

2.7.5 Gel purification of the PCR-amplified mTKIN ORF

For the isolation of the PCR amplified mTKIN ORF the whole 50 µL of the PCR reaction was loaded on a 1% agarose gel. A small aliquot was loaded in a small pocket beside the large pocket where the remaining of the PCR reaction was loaded. The lane with the small aliquot was separated from the gel and used for better orientation of the PCR product position on the gel. The PCR-product band from the larger lane was cut out of the gel as fast as possible while illuminating it with UV light with longer wavelength (365 nm), hence minimizing the chance of introducing DNA damage. The DNA from the gel piece was isolated using the peqGOLD Gel Extraction Kit from peqlab. The isolation was performed in accordance with the manufacturer's protocol. The kit's procedure basically contains a step where the DNA containing gel piece is dissolved in a special buffer and then the DNA fragment is batch purified using a ion exchange chromatography column. Since the purified fragment in this investigation was going to be used for *in vitro* transcription, the DNA was eluted in RNase-free water.

2.7.6 DNA concentration

The concentration of all plasmid DNA or PCR products was determined using a Nanodrop instrument blanked with the buffer in which the DNA was eluted or diluted. The DNA concentration was being quantified relative to the UV absorption of the pyrimidine bases, under the assumption of a 1:1 ratio between the pyrimidine and the purine bases as well as with the respect of measuring double stranded DNA. Additionally, the 260/280nm ration determines the purity of the DNA from proteins.

2.8 Protein expression

2.8.1 Preparation of electrocompetent *E. coli* cells

For the preparation of *E. coli* cells suitable to be transformed with a plasmid using electroporation (2.8.2), a 50 ml of 2xYT medium containing the appropriate antibiotics were inoculated with cells from a glycerol stock of the wanted *E. coli* strain. This starting culture was incubated in an Erlenmeyer flask at 37° C and 180 rpm shaking speed. On the following day the starting culture was used for inoculation of 500 ml of prewarmed (37° C) 2xYT medium containing the appropriate antibiotics to a OD_{600} ~0.05-0.10. The new culture was grown at 37° C and 180 rpm shaking speed until the optical density at 600nm wavelength (OD_{600}) reached a value between 0.3 and 0.5. At this point the culture was placed on ice for 30 minutes, transferred to two pre-chilled 250 ml centrifugation bottles and cells were harvested by centrifugation at 4°C and 3220g for 15 minutes. The supernatant was discarded, the cells were re-suspended in 250 ml ice-cold Millipore-purified water and left on ice for 15 minutes. Next, the cells were once more harvested by centrifugation as described before. The supernatant was discarded, the cells were re-suspended in 100 mL cold Millipore-purified water per bottle, transferred to 50 mL Falcon tubes and incubated on ice for further 15 minutes. After a repeated cell harvesting, cells from two 50 mL tubes were re-suspended in 25 mL ice-cold 10% glycerol (Millipore purified water) solution, transferred to a fresh 50 mL tube, incubated for 15 minutes on ice and harvested again as before. Finally, the cells from each 50 mL tube were re-suspended in 2 mL ice-cold 10% glycerol (Millipore purified water) and aliquoted in 50 µL portions in 0.5 mL Eppendorf cups. The samples were immediately snap-frozen in liquid nitrogen and stored at -80° C until further use.
The quality of the competent cells was tested by determining the colony forming units (cfu) after transformation of a single 50 µL aliquot with 1 ng of pUC18 plasmid carrying an ampicillin resistance cassette (see 1.8.2). A serial dilution of the transformed culture was prepared and 50µl fractions of each dilution step were plated on agar plates with containing the corresponding antibiotic and incubated top-down over night at 37°C. Next day, the colonies were counted and from these counts the transformation efficiency was calculated corresponding to 1µg input DNA.

2.8.2 Transformation of DNA in electrocompetent *E. coli* cells

In order to express the proteins of interest *in vivo*, the expression plasmid contain the sequence of the protein of interest was transformed in *E. coli* cells. For this purpose a 50 µL aliquot of electrocompetent *E. coli* cells was taken from the -80°C storage and transferred

on ice. After the cells thawed on ice, 1 µL of plamid DNA, irrespective whether from a mini or maxi was added to the cells, gently mixed, transferred to an electroporation cuvette (0.1 cm gap). Transfer of the DNA into the cells was caddied out using a Bio-Rad MicroPulser electroporator set for electroporation of *E. coli*. Once the pulse time was between 4 and 5.5 ms, the cells were resuspended in 1 mL of 2xYT medium, transferred to a 1.5 mL Eppendorf cup and incubated at 37°C shaking at 180 rpm for 30-45 minutes. The transformed cells were harvested by centrifugation at 1500 g for 2 minutes in a benchtop centrifuge. 800 µL of the supernatant was discarded, the cells were re-suspended in the remaining supernatant and plated on a 2xYT agarose-plate containing 2% glucose and the appropriate antibiotics, in order to retain transformed plasmid as well as the helper plasmid of the given *E. coli* strain. The plates were incubated top-down overnight at 37° C.

2.8.3 Expression of protein

For production of the protein of interest all freshly transformed cells from a 2xYT agarose plate were scraped off in 3 mL LB medium and used to inoculate prewarmed 50 – 200 mL LB medium containing 2% glucose and the antibiotic needed for retaining the expression plasmid. The presence of the 2% glucose additional represses the expression of the plasmid encoded protein through the *lac*-operon. The expression culture was then grown to an OD_{600} of 0.7 shaking at 37°C and 180rpm and protein expression was induced by addition of IPTG to a final concentration of 1 mM. After induction, the expression cultures were incubated at different conditions: a) 37° C, 180 rpm for 3 hours; b) 30° C, 180 rpm for 4 hours; c) 22° C, 180 rpm for 5 hours; d) 18° C, 160 rpm overnight (16-20 h). For protein purification, cells were finally harvested by centrifugation at 4°C and 3220 g for 20 minutes in 50 mL Falcon tubes. The supernatant was discarded and cells were either used immediately for protein extraction or were stored at -20° C until further use.

2.9 Protein purification

2.9.1 Protein extraction from *E. coli* cells

For extraction of the cytosolic proteins from *E. coli* cells under native conditions the cell pellet from a 50 mL expression culture (2.8.3) was re-suspended in 3 mL native lysis buffer. The cells were lysed by adding 30 µL lysozyme (20 mg/mL) per 50 mL tube and incubating them on ice for 30 minutes. Additionally, cells were sonicated on ice by three 20-second intervals with 20-second pauses in-between. Finally a protein inhibitor cocktail (1 tablet per 1 mL H_2O) and PMSF (serine protease inhibitor) were added to the lysate to a final concentration of

1:100 dilution and 1 mM, respectively. The soluble proteins were separated from the cell debris by a 15-minute centrifugation at 15300 g and 4°C. The supernatant containing the soluble protein was transferred in a 15 mL tube. The insoluble fraction in the pellet was re-suspended in 0.5 or 1 mL 8M urea and used for analytical purposes. All samples were stored at 4° C.

2.9.2 Immobilized metal-ion chromatography (IMAC) purification of recombinant protein using Ni-NTA agarose at gravity flow

The His_6-tagged mTKIN was routinely purified by gravity-flow Ni-NTA affinity chromatography. For each purification, a fresh 500 µL aliquot of re-suspended Ni-NTA agarose (50 % suspension) were added to the soluble protein fraction derived from the lysis (2.9.1) of each 50 mL expression culture. Before adding the Ni-NTA agarose to the soluble protein fraction, an aliquot was taken aside for later analytical purposes. The mixture of the soluble proteins and the Ni-NTA agarose was incubated for an hour on a roller at low speed and 6-8°C. The mixture was than transferred to a 5 mL polypropylene column and the flow though was collected. The Ni-NTA agarose was washed twice with 4 mL washing buffer. Aliquots from the washing steps were collected for analytical purposes. Finally, 1 mL of elution buffer was added to the Ni-NTA agarose and the column flow was stopped. After one hour incubation of the Ni-NTA agarose with the elution buffer in the column, the first elution fraction was collected. The elution step was repeated two to three more times subsequently without performing one hour incubations, thus producing three to four separate 1 mL elution fractions. All elution fractions, as well as the flow-through and other aliquots from the purification procedure were stored at 4°C until further use.

2.9.3 IMAC purification of recombinant protein using Ni-NTA magnetic beads

For Ni-NTA affinity purification of smaller amounts of His_6-tagged protein (<1ml), such as derived from in vitro expression, Ni-NTA functionalized magnetic beads were used as chromatography matrix. Handling of the beads was carried out using a magnetic stand holding the beads in place while the supernatant is taken off carefully with a pipette. First, 100 µL of re-suspended Ni-NTA magnetic beads were added to the protein containing solution and incubated for 1 hour on a roller at low speed and 6°C. Eppendorf cup was placed in the magnetic stand, beads were collected and supernatant was removed. After collecting the supernatant, the beads were washed twice with 500 µL NPI-20 with short re-suspension of the beads in the buffer between the steps by removing the tube from the magnetic stand. The protein was finally eluted twice with 50 µL NPI-250 and once with 100

µL with 5-10 minute incubation time in-between.

2.9.4 IMAC purification of recombinant protein using a Ni-NTA Superflow cartridge on an FPLC system

In order to optimize the purification procedure of the His_6-tagged mTKIN, a 1 mL Ni-NTA Superflow cartridge was used in combination with a ÄKTApurifier FPLC system. The cartridge was washed with 15 column volume (CV) of 0.5 M NaOH at a flow rate of 0.5 mL/min before each purification run and equilibrated with 10 CV NPI-10. The extracted soluble protein fraction from a mTKIN expressing culture was centrifuged two times instead of just once (2.9.1) to remove any remaining larger particles potentially clogging the FPLC system. The soluble protein fraction was loaded in a 10 mL loop connected on the FPLC system. If the volume of the sample was less than 10 mL, the volume was adjusted with NPI-10. After injection, the cartridge was first washed with 2 CV NPI-10 followed by a wash with 10 CV of 96% NPI-10 and 4% NPI-250 simulating a wash with NPI-20. The bound protein was then eluted with different gradients starting with 4% and ending with 100% NPI-250. The presence of proteins was monitored online by light absorption at 280 nm. The flow-through fraction (10 mL), the wash fractions (2 mL) and the elution fractions (1-2 mL) were collected and stored at 4° C. The flow-through and peak fractions were used for further analysis by SDS-PAGE (2.10.1)

2.9.5 ATP-agarose affinity chromatography batch purification

To increase the purity of the recombinantly expressed mTKIN, Ni-NTA purified sample was further purified relying on the ATP-binding property of mTKIN. Four commercially available matrices (ATP Affinity Test Kit, JenaBioscience) differening by the way of ATP-immobilization on agarose were tested: aminophenyl-ATP-agarose, C10-spacer (AP-ATP-agarose), 8-[(6-amino)hexyl]-amino-ATP-agarose (8AH-ATP-agarose), N^6-(6-amino)hexyl-ATP-agarose (6AH-ATP-agarose) and 2'/3'-EDA-ATP-Agarose (EDA-ATP-Agarose). The chemical structures of all four molecules are presented in Figure 2-3.

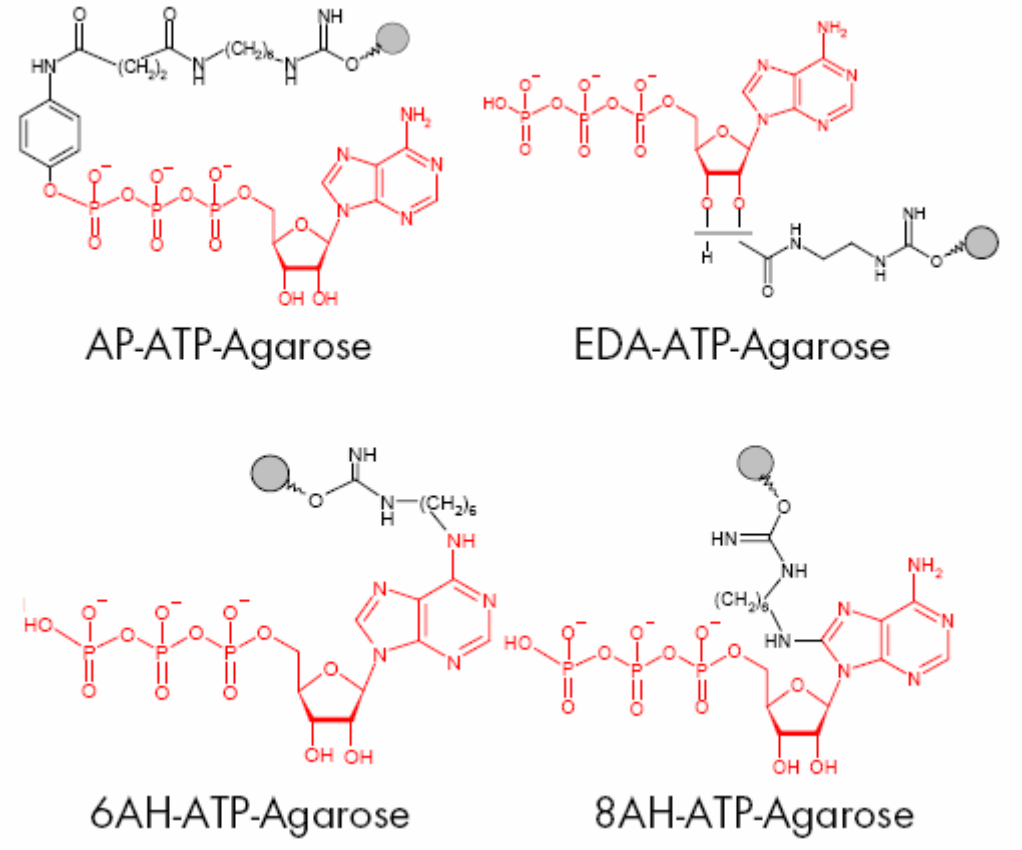

Figure 2-3: Chemical models of the four differently functionalized ATP-agaroses batches with ATP (models adopted from: http://www.jenabioscience.com/images/ab4587dada /AK-102.pdf). In the 6AH and 8-AH-agarose the ATP is immobilized over two different connection points of the adenine base. In the AP-ATP-agarose the ATP is immobilized through the γ phosphate and in the EDA-ATP-agarose through the two OH groups of the ribose.

All washing and elution buffers were prepared as described in the kit's manual with the exception that sodium-orthovanadate and DTT were excluded from the binding, wash and elution buffer. Sodium-orthovanadate is an ATPase inhibitor, which would hamper our goal to yield functionally active kinesin. Further, DTT was not added as our engineered mTKIN contains no cystine residues in its structure. 50 µL of each ATP-agarose was transferred to a 1,5 mL Eppendorf cup and equilibrated three times with 330 µL of washing buffer. In order to separate the agarose from the buffer, the tubes containing an agarose were centrifuged at 1000 g for one minute, as suggested by the manufacturer. After centrifugation, the supernatant was carefully removed from the tube. For the affinity screening with each of the four ATP-agaroses, 1 mL elution of the Ni-NTA purified mTKIN (2.9.3) was mixed with 250 µL binding buffer supplied with the kit and 310 µL of the given mixture were added to each ATP-agarose. The agarose-sample mixtures were incubated on a roller for 2 hours at 6°C. The flow-through fractions were collected. And the ATP-agarose batches were washed three times with 500 µL washing buffer. All wash fractions were collected. Finally, 120 µL elution buffer was added to each ATP-agarose and incubated on a roller at 6°C for 20 minutes. The

elution fractions were collected and the elution step was repeated to evaluate the efficiency of the elution.. After elution ATP-agarose batches were preserved in 500 µL 20% ethanol. The samples, ATP-agaroses and the fractions were kept on ice during the whole process.

2.9.6 FPLC using the EDA-ATP-agarose

To optimize the purification conditions using EDA-ATP-agarose, The batch purification protocol was transferd to the FPLC system. For that, a 1 mL Pharmacia cartridge was packed with ~250 µL bed volume of the previously used an the remaining unused EDA-ATP-agarose and equilibrated with 10 CV of ATP-agarose wash buffer before use. For the test purification, Ni-NTA FPLC elution fractions contain the mTKIN were pooled and diluted 1:5 with ATP-agarose binding buffer. The samples were loaded in a 10 mL loop. Prior injection of the sample, the column was additionally equilibrated with 5 CV wash buffer at 1 mL/min and the sample was injected at 0.5-0.2 mL/min. Unbound proteins were washed away with 7 CV of wash buffer and finally bound proteins were eluted with wash buffer containing 1mM ATP at 0.5 mL/min either in continuous flow or with a 20-minute pause after first detection of ATP. ATP was monitored by light absorption at 254 nm and protein at 290 nm. All fractions were collected an stored at 4°C and the first elution fraction was further analyzed.

2.9.7 Concentrating of proteins

For producing a sample with higher protein and thus mTKIN concentrations the Ni-NTA FPLC purified fraction which contained mTKIN were pooled and loaded in a molecularporous membrane tubing with cut-off size of 3500 kDa. The sample-filled tubing was sealed on one end with a knot and with a clamp and placed in flakes of solid PEG 6000. After achieving the wanted volume reduction the fluid in the tubing was collected at one end and the tubing was cut on the other end. The sample was collected from the dialysis tubing with a pipett.

2.10 Sample protein composition analysis

2.10.1 SDS-PAGE

SDS-PAGE analysis of protein extracts was performed using two different gels, depending on the quality requirements. For broader screenings the SDS-PAA gels were prepared using a multiple gel caster. For casting the gels a 5 cm long 15% polyacrylamid separation gel was poured in the gel caster and overlaid with isopropanol. After polymerization, the isopropanol was removed from the gel caster, which was subsequently filled with 4% polyacrylamid

stacking gel. A comb was placed per one gel section. The distance between the bottom of the comb formed pockets and the front of the separation gel was ~1 cm. For electrophoretic separation of proteins, samples are mixed with 4x Laemmli sample buffer and boiled for 5 minutes. Meanwhile, a gel is placed into the electrophoresis chamber. The comb is removed and the chamber is filled with Laemmli running buffer. After loading the gels with sample material, they were first run at 80 V until the Bromophenol blue front entered the separating gel (~15 min), before the currency was elevated to 200 V for the remaining time. For a more precise separation of the proteins originating from more specific experiments ready made NuPAGE® Bis-Tris gels from Invitrogen were used. With these gels, SDS-PAGE was performed using 1x MES as running buffer. Sample preparation before loading onto gels comprises mixing the sample with 4x Laemmli loading buffer. Equivalent of 1 µL of the original sample were loaded per pocket, where high concentration of mTKIN were expected, whereas 3-6 µL of the original sample were loaded per pocket if the concentration of mTKIN were expected to be relatively low. A prestained protein ladder (5 µL per lane, precision plus protein standard, BioRad) was used for relative comparison of the size of the proteins in the other lanes. For visualization of the separated proteins the gels were stained with Coomassie brilliant blue R-250 (see 2.10.2) or used for western blotting (see 2.10.3).

2.10.2 Coomassie staining

Coomassie brilliant blue R-250 is a dye usually used to uniformly stain all of proteins contained on a gel. The dye binds unspecifically to arginines and aromatic amino acids. For staining the gels were first incubated in a solution with Coomassie dye for 20 to 30 minutes under a continuous linear shaking motion. The dye containing solution was exchanged with a destaining solution and a rolled up cellulose tissue (Kleenex) was placed in the vessel to absorb the Coomassie dye released from the gels. The gels were destained on a linear shaker for half an hour after which the destaining solution was exchanged with deionized water and the tissue was replaced with a new one. The gels were left overnight on the bench to further destain and finally documented using a CCD camera and a white backlight.

2.10.3 Western blot

Proteins separated by SDS-PAGE were transferred from the gel onto a nitrocellulose membrane by a wet blotting method. The transfer was performed in a TE 22 Mighty Small™ Transphor tank transfer unit containing blotting buffer at 400 mA for one hour. After transfer, the membranes were blocked by incubation in PTM for 1 hour of overnight at 6°C under a slow continuous motion of the vessel with the blocking buffer. Next, the blocking buffer was

exchanged with blocking buffer containing a specific detector of choice. Streptavidin-HRP conjugate (1:2500 in PTM) for biotin detection and anti-His-mouse antibody (1:2000 in PTM) for 6xHis detection were used, since the expressed mTKIN carries a 6xHis-tag and biotin (Avi-tag). For the detection of mTKIN presented on M13 bacteriophages an anti-PIII-mouse antibody (1:1000 in PTM) was used. After one hour incubation at room temperature and continuous motion with the first detector the membranes were washed 2-3 times in PBS-T for 5 minutes. The membranes hybridized with anti-His (mouse) and anti-PIII (mouse) antibodies were then further incubated with an anti-mouse-HRP antibody (1:5000 in PTM) for a further hour. After washing away the excess antibodies 2-3 times with PBS-T for 5 minutes each, CN/DAB was given to the membrane as a HRP substrate. The product of the reaction precipitates on the position where the detected protein is. Since the precipitate has a dark brown to black colour, the position of the protein on the membrane can easily be seen. The colouring reaction was stopped with de-ionized water and the blots were dried between two pieces of whatman-paper. For documentation, blots were scanned with a regular office color scanner.

2.10.4 Mass spectrometric identification

Mass spectrometric analyses were performed in order to further verify the integrity of mTKIN as well as to identify the co-purified proteins. For this purpose 6 µL of a Ni-NTA affinity purified mTKIN (FPLC) was run on a SDS-PAGE (15% PAA). Gel was stained with Coomassie in order to detect the proteins present in the sample. Five detected bands (Figure 3-9) were cut out of the gel in duplicate. One of the samples was digested with Trypsin (serine protease) and the other with Asp N endoproteinase according to an adapted protocol from Kaiser et al. (Kaiser et al. 2008). The masses of the produced peptides were analyzed on a HPLC coupled ESI-Orbitrap mass spectrometer. Recorded masses of the peptides were used to identify the corresponding proteins using the Mascot search algorithm using the Proteome Discovery 1.1 software. Protein digest, mass spectrometry and mass spectra analysis was performed by Dr. David Meierhofer (MPI for Molecular Genentics).

2.11 *in vitro* protein expression

A test was conducted to express mTKIN using the EasyXpress Insect Kit II from Qiagen. This expression system is based on cell lysate from a *Spodoptera frugiperda* cell line. In contrast to the prokaryotic in vitro expression systems, where template DNA is given directly to the lysate, for the eukaryotic expression system RNA template had to be produced first.. The *in vitro* transcription of the template DNA was performed using the kit supplied polymerase,

NTP´s and buffer. From the five available reactions, one was performed with RNase-free water (negative control), one with the kit´s control DNA (positive control). The remaining 3 *in vitro* transcription reactions were pooled and the reaction was performed with 3 µg purified (2.7.5) mTKIN PCR product (2.7.4) as template. 51 µL of the mTKIN *in vitro* transcription reaction was purified with the RNeasy MinElute clean up kit and purified RNA was eluted in 12 µL of RNase-free water. All RNA was used as template in a single in vitro expression reaction. The remaining 24 µL of unpurified mTKIN-RNA were used for an *in vitro* expression of mTKIN in a double reaction volume. This was done under the assumption that the produced mRNA was more concentrated in the purified sample than in the unpurified one. The RNA produced in the negative and positive control reactions were not purified and used for a single *in vitro* expression reaction as they were. The translation reactions were mixed and carried out according to the manufacturers protocol by incubating for 90 minutes in a thermomixer at 27°C and 500 rpm. After incubation the reactions were stored at 4°C.

2.12 Periplasmic expression of protein

Apart from the classic cytoplasmic expression of proteins, *E. coli* offers the possibility to express proteins in a secretopry fashion. The expressed protein is translocated to the periplasm of the cells from where it can by easily extracted by hypotonic shock. However, for the transport of the protein into the periplasm the expressed protein has to carry a N-terminal leader sequence. For this purpose mTKIN was cloned in the pIT2 phagemid vector which possesses a pelB leader sequence allowing translocation of the protein to the periplasm via the Sec pathway and an amber stop behind the mTKIN sequence. Expression of mTKIN in pIT vector was carried out in the HB2151 *E. coli* strain. The extraction of periplasmic proteins was performed by subjecting the cells to a mild hypotonic shock. Since the inner cell membrane is structurally stronger as the outer membrane, it will not break under the effect of sudden pressure change by hypotonic shock, while the outer membrane will loose its integrity and break up. This results in the release of periplasmic proteins into the solution while the cytoplasmic proteins are being confined in the spheroplasts by the inner cell membrane. For the periplasmic expression and extraction two different protocols were applied. In both cases, the starting material was a 100 mL expression culture whereby LB or 2xYT medium was inoculated with HB2151 *E. coli* cells of a previous overnight culture (1:100 dilution.)

2.12.1 Protocol I

The culture in LB medium (100 µg/mL Amp) was grown to an OD_{600} of 0,5-0,7 at 37° C

shaking at 180 rpm. At this point the expression of mTKIN was induced by the addition of IPTG to a final concentration of 0,02 mM and further incubated for 16 hours (overnight) at 16°C and 160 rpm. The cells were harvested on the following day by 30 minute-centrifugation at 3220 g.. Cell pellet was re-suspended in 30 mL cold PE buffer and incubated on ice for 30 minutes. At this point the periplasmic membrane is being destroyed by the hypotonic shock achieved through the high sucrose concentration of the buffer. The spheroplasts were separated from the periplasm by centrifugation at 3220 g and 4°C for 30 minutes. The periplasmic proteins containing supernatant was carefully removed and stored at 4°C, while the spheroplasts-containing pellet was stored at -20°C until further use.

2.12.2 Protocol II

The culture in 2xYT medium (100 µg/mL Amp, 0.1% Glucose) was grown to an OD_{600} of 0,5 at 37° C shaking at 180 rpm. At this point the expression of mTKIN was induced by the addition of IPTG to a final concentration of 1 mM and further incubated for 16 hours (overnight) at 30°C and 180 rpm. The cells were harvested on the following day by 30 minute-centrifugation at 3220 g. The cells were re-suspended in 2 mL TES buffer for each 50 mL culture fraction and the hypotonic shock was performed by adding 3 mL 1:5 diluted TES buffer to each 50 mL culture fraction. The cells were incubated on ice for further 30 minutes. The spheroplasts were separated from the periplasm by centrifugation at 20000 g and 4°C for 20 minutes. The periplasmic proteins containing supernatant was carefully removed and stored at 4°C, while the spheroplasts-containing pellet was stored at -20°C.

2.13 mTKIN presentation on phages

For presentation of mTKIN on a M13 bacteriophage, mTKIN was expressed as a pIII-fusion in the pIT2 vector. This is the same vector used for the periplasmic expression of mTKIN, In contrast to the expression in HB2151, a non-suppressor strain for amber stops, expression in a suppressor strain will lead to a direct fusion of mTKIN-pIII, which are separated on the vector only by an amber stop.

2.13.1 mTKIN presenting phage production and preparation

Both of the two commonly used suppressor strains for phage presentation, TG 1 and XL-1 Blue, were used to present mTKIN on the phage surface. For this purpose electrocompetent cells of the two strains were transformed with the pIT2/mTKIN construct as in 2.8.2 and grown on ampicillin containing 2xYT agar-medium. Single colonies were picked and used for

inoculation of 4 mL of 2xYT medium (100 µg/mL Amp and 2% glucose). The starting cultures were grown overnight at 37°C and 180 rpm. The starting cultures were used on the following day for inoculation of 100-200 mL of 2xYT medium (100 µg/mL Amp and 2% glucose). The cultures were grown to OD_{600} ≈0,5 and divided in two halves. One half was infected with 10^{10} cfu M13K07 helperphage, the other with 10^{10} cfu of Hyperphage helperphage. The infected cultures were incubated at 37° C in a stationary incubator for 30 minutes before the cells were collected by a 10 minute-centrifugation at 3220 g and 20°C. After re-suspending the cells in the original culture volume of 2xYT medium (0.1% glucose, 100 µg/mL Amp and 60 µg/mL kanamycin), the cultures were incubated overnight at 30° C and 180 rpm. The handling of the cultures as of the moment of infection were performed in disposable vessels. On the following day the phages were prepared by separating the cells from the phage enriched medium by a 10 minute-centrifugation at 3220 g and 4°C in 50 mL tubes. 42,5 mL supernatant of each tube was mixed with 7,5 mL of phage precipitation buffer containing PEG, which allows the phage to precipitate. Precipitation was performed by two and a half hour incubation on ice and a subsequent centrifugation at 3220 g and 4° C for 30 minutes. The pellets in each 50 mL tube were shortly air-dried and re-suspended in 500 µL PBS or other buffer suitable for downstream experiments. After transferring the re-suspended phages into 2 mL Eppendorf cups, a 10 minute centrifugation at top speed using bench centrifuge was performed to remove remaining cells or cell debris and the phage containing supernatant was transferred to a fresh vessel.

2.13.2 M13KO7 helperphage preparation

Large quantities of M13KO7 helperphages were needed for superinfection of E. coli cells bearing pIT2/mTKIN phagemids as well as for comparative analytical purposes. For this a single helperhpage plaque was needed as a starting point. Hence, a serial dilution of M13KO7 (10^{-1}-10^{-12}) in 90 µL PBS was prepared from a phage stock. The dilutions 10^{-7}-10^{-11} were mixed with 100 µL of TG-1 culture grown to an OD_{600} of 0.5 and incubated for 30 minutes at 37°C. Meanwhile 2xYT TOP-agar was dissolved in a microwave and kept in a liquid state at 43° C. Next, the phage-TG 1 mixtures were added to 4 mL aliquots of the TOP-agar, gently mixed and immediately poured onto a 2xYT agar plate. After solidifying the plates were incubated top down at 37° C overnight. Next day, several 4 mL 2xYT medium aliquots were inoculated with single plaques from the plates containing M13KO7 infected TG 1 cells. The starting cultures were grown at 37°C and 180 rpm for three to four hours and used to inoculate 500 mL 2xYT medium filled flasks. The cultures were grown overnight at 37° C and 180rpm shaking. Harvesting of phage particles was performed as in 2.13.1.

2.13.3 Phage titration

The concentration of prepared phages can be determined relative to their ability to infect *E. coli* cells by monitoring the amount of infectious phages carrying the recombinant phagemid vector after plating infected cultures onto agar plates containing the appropriate antibiotics. All phage titrations were carried out using the *E. coli* strain TG1. First a starting culture was grown overnight at 37°C and 180 rpm in 2xYT medium. The next day, this was used to inoculate 50 mL of 2xYT medium and the culture was incubated at 37°C and 180 rpm until OD_{600} =0,5. Meanwhile, of each phage preparation a 10-times dilution series (factor 10^1-10^{12}) in 90 µL PBS was prepared in a 96-well plate. Next, phage infection was carried out by mixing 100 µL of TG 1 cells with each of the 90 µL phage dilutions on the 96-well plate. The plate with the samples was incubated for half an hour at room temperature. After infection, 10 µL of each dilution was carefully spotted on a single 2xYT agar medium so that it occupied only a distinct area . In addition, control aliquots of the TG 1 culture, PBS, phage preparation and a mix of the used PBS with TG 1 cells were also spotted on each agar-plate. The 2xYT agar medium used for titration contained 2 % glucose and 60 µg/mL kanamycin for helper phages titration or 2 % glucose and 100 µg/mL ampicillin for titration of phagemid carrying phages. The agar-pates were left to dry at room temperature until the aliquots were absorbed in the agar medium and incubated top down at 37° C overnight. The concentration was determined by multiplying the number of observed colonies with the corresponding dilution factor and 211, which allows to express the phage concentration in colony forming units per mL phage suspension (cfu/mL).

2.14 Production of microtubules

Microtubules (MTs) are necessary for the biochemical and mechanochemical characterization of kinesins, as kinesins bind and move on MTs. Microtubules were were polymerized from lyophilized bovine tubulin and X-rhodamine labeled tubulin. First, tubulin was dissolved to a concentration of 4 µg/µL in BRB 80 buffer supplemented with 1 mM GTP and incubated at 37° C for at least 20 minutes to polymerize. The polymerized MTs were then stabilized by adding BRB 80 supplemented with 1 mM GTP and 200 µM taxol until an end-concentration of 20 µM taxol was reached. Finally, MTs, were further diluted 1:200 in BRB 80 supplemented with 1 mM GTP and 20 µM taxol, separated in 100-200 µL aliquots, snap-frozen in liquid nitrogen and stored at -80° C. Before use the MTs were thawed at 37°C and incubated for at least 10 minute at the same temperature. The procedure to assemble microtubules using mixture of tubulin and X-rhodamine labeled tubulin (ROX-MTs) was the same as for unlabeled MTs, except that the buffers contained 10% glycerol. All vessels used

for ROX-MT production were wrapped in aluminum foil for protection from light.

2.15 Determination of ATP hydrolysis kinetics of mTKIN using a coupled NADH oxidation enzyme assay

The coupled NADH oxidation assay was used to observe the steady-state kinetics of ATP hydrolysis by mTKIN (Gilbert and Mackey 2000). There are two key features of the assay (Figure 2-4).

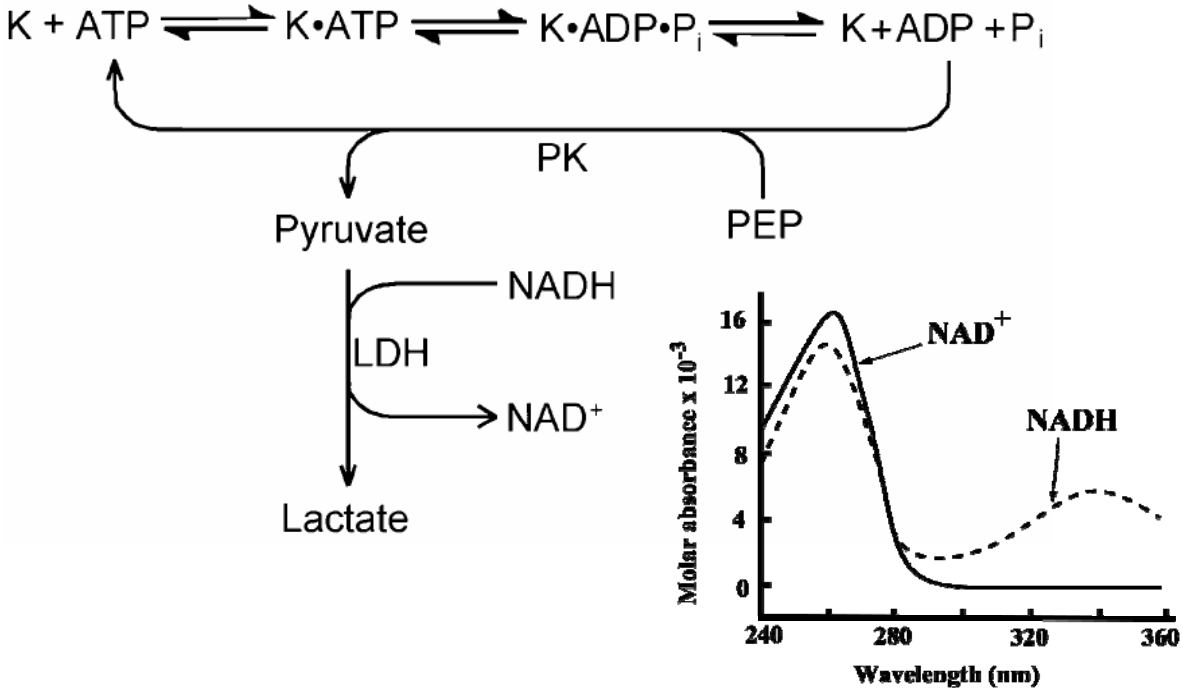

Figure 2-4: Reaction scheme of the NADH oxidation coupled observation of a kinesin (K) ATPase activity. Figure taken from Gilbert and Mackey 2000; and the NAD^+ and NADH ultraviolet light absorption spectra adopted from http://en.wikipedia.org/wiki/File:NADNADH.svg

First, it replenishes the hydrolyzed ATP form ADP thus simulating a constant ATP concentration. Second, the reaction stoichiometry between the oxidation of one NADH is equivalent to the hydrolysis of one ATP. The kinesin mediated ATP hydrolysis reaction was performed in a buffer containing 2 mM $MgCl_2$, 1 mM DTT, 3 mM phosphoenol pyruvate (PEP), 0.2 mM NADH, 50 mM Tris-acetate pH 7.5, 1.75% (v/v) pyruvate kinease/lactose dehydrogenase solution and 2-0.1 mM ATP (Matsushita et al. 2009). The reactions were carried out in 200 µL reaction volumes on a 96-well microtiter-plate. The oxidation of NADH was observed by the loss of light absorption at 340 nm in a microtiter-plate reader. A reaction containing no NADH was used as a blank, since microtubules absorb light at 340 nm.

2.16 *in vitro* motility assay

To investigate the mechanochemical property of mTKIN to transport microtubule an *in vitro* motility assay was performed. The experiment is based on the mode of transport. Kinesin molecules are fixed onto a surface and added polymerized MTs are being moved in a seemingly gliding manner (Figure 1-8, B). First, a flow cell was build from a microscope slide, double sided adhesive tape and a cover slip. The flow cell was then loaded with kinesin in a buffer containing 1 mM ATP and incubated for 5 minutes. The buffer was than exchanged against ROX-MTs (20 ng/µL) supplemented with 1 mM ATP by extracting the buffer from one side of the chamber with a kimwipe and adding the ROX-MTs from the other side of the flow cell. The flow cell was than immediately used for microscopy. The microtubules were observed using x63 objective. Using normal fluorescence microscopy the plane was found where the microtubules were being bound to the kinesin coated surface. A time series of 60 images within 3:42 minutes where taken from a chosen area using laser scanning of the kinesin coated plane. This way a more precise images could be taken in comparison of standard fluorescence microscopy since all of the ROX-MTs which are bound to kinesin lie in the same plane along all their length. The movement was then observed by assembling a film from the taken images.

3 Results

The goal of this investigation was to express and characterize a cystein-free engineered form of the thermostable kinesin mTKIN. First, optimal expression conditions for mTKIN regarding temperature, incubation time and host strain usage were determined to obtain soluble protein. Additionally, alternative strategies for the expression of mTKIN were assessed. Next, chromatography procedures for the isolation of potentially active mTKIN were developed for batch purification as well as on an FPLC-system. Furthermore, the presentation of the mTKIN on M13 bacteriophage surface was assessed in combination with different host strains and helperphage systems. Finally, the activity of the mTKIN was investigated by measuring its ATPase activity and its ability to move along microtubules in an *in vitro* motility assay.

3.1 Optimization of growth conditions for soluble expression of the mTKIN in the vector pQDKG2

The aim of these studies was to obtain an optimized protocol for the expression of mTKIN in order to yield mainly soluble protein in the cytoplasm. First parameters under investigation were the influence of temperature and induction time. This analysis was carried out in an *E. coli* strain regularly used to obtain in vivo biotinylated proteins in our laboratory (AG Konthur), namely BL21 (DE3) STAR pRARE3. *E. coli* cells were transformed with the pQDKG2/mTKIN followed by expression of the construct at varying temperatures and induction times. For this, initial starting cultures were split at OD_{600} ≈0.7 , induced with IPTG and placed at differerent temperatures for further growth, 37°C, 22°C and 18°C. The induction times were accordingly modified to 3h, 5h and 18h respectively. Cells were harvested and soluble and insoluble protein fractions of the total cell lysates were used for analysis. Triplicate SDS-PAGEs were performed with 1 µL of each fractions from the different expression condition. One of the gels was used for visualisation of the proteins by Coomassie staining, while the other two gels were used to transfer the proteins to membranes by Western blotting. Streptavidin-HRP conjugate was used for detection of all biotinylated proteins on one of the blots. On the other blot, a mouse α-His antibody was used in combination with a HRP-coupled rabbit α-mouse antibody for detecting all His_6-tagged recombinant proteins. Comparing the three detection strategies a strong band at ~60 kDa can be seen in both blots which does not stand out in the Coomassie stained gel (Figure 3-1). The observed size of ~60kDa corresponds well with the *in silico* calculated size of recombinant biotinylated mTKIN which is ~56 kDa. The

Immunoblots also demonstrate that mTKIN is *in vivo* biotinylated and possesses the hexahistidine expression-tag. The expression of mTKIN at 18°C and induction time of 18 hours yielded larger amounts of mTKIN and smaller amounts of N-terminal degradation products in the soluble protein fraction than under the other expression conditions.

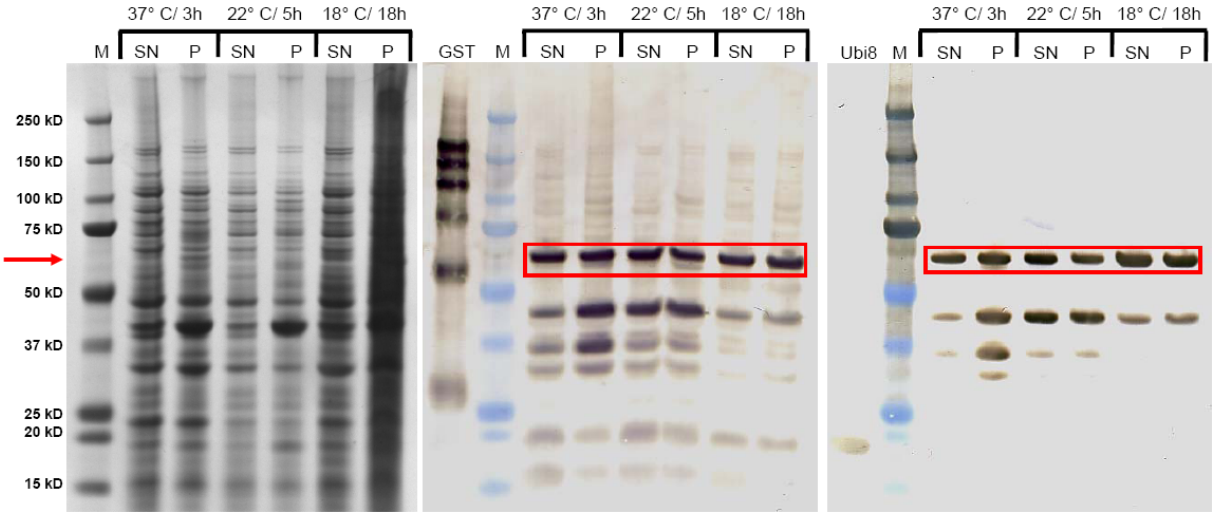

Figure 3-1: Comparison of mTKIN expression in BL21 (DE3) Star pRARE3 at different temperatures and induction times. 1 µL of the soluble protein fraction (SN) and insoluble protein fraction (P) from a 50 mL expression culture were distributed on gradient SDS-PAA gels in triplicate. The first gel (right) was stained with Coomassie, the second gel (middle) was blotted and hybridized with streptavidin-HRP and the third (left) was blotted and hybridized with mouse α-His and rabbit α-mouse-HRP antibodies. Biotin-labeled GST and His6-tagged ubiquitin (Ubi8) were used as positive control for the hybridization. M is a pre-stained protein ladder. The red pointer and boxes highlight the position of the Avi-His_6-tagged mTKIN.

In the next step four different *E. coli* host strains were asses for their ability to produce more full-length mTKIN and less N-terminal degradation products. The strains under investigation were: BL21 (DE3) Star pRARE3, BL21 (DE3) pLysS, BL21 CodonPlus (DE3)-RIL and Origami B (DE3) pLacI. Again, mTKIN was expressed in all of the strains and under all of the tested conditions. The different pattern of the detected bands in the blots demonstrated that mTKIN is being expressed differently in each *E. coli* strain and the different expression conditions applied. The expression of the mTKIN in the four different strains showed also some differences in the soluble protein fraction. Figure 3-2 shows the expression of mTKIN at 18°C as an example. Strains BL21 CodonPlus (DE3)-RIL and Origami B (DE3) pLacI gave the best results. The BL21 CodonPlus (DE3)-RIL cells grew faster and more reproducible than that the Origami B (DE3) pLacI which were more difficult to cultivate.

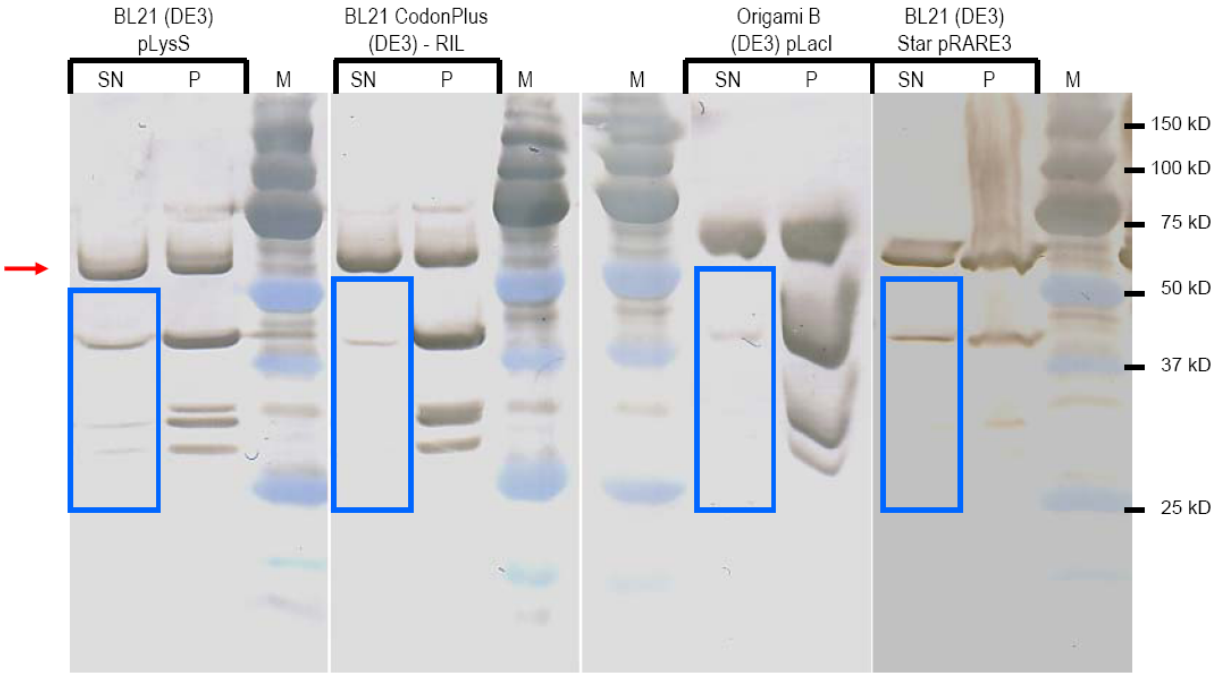

Figure 3-2: Comparison of mTKIN expression in different *E. coli* strains by induction for ~18 hours at a temperature of 18°C. 1 µL of the soluble protein fraction (SN) and insoluble protein fraction (P) from a 50 mL expression cultures were distributed on 15% SDS-PAA gels. After the electrophoresis the gels were blotted and hybridized with mouse α-His (mouse) and rabbit-α-mouse-HRP antibodies. M is a pre-stained protein ladder. The red pointer highlight the position of the Avi-His-tagged mTKIN and the blue boxes highlight the mTKIN degradation products.

3.2 *In vitro* expression of mTKIN

This experiment was conducted to asses the possibility to obtain soluble mTKIN using a eukaryotic *in vitro* expression system. The reactions were assembled as described in 2.11, with purified and unpurified mTKIN template RNA and a positive control reaction contained in the kit (His-tagged luciferase). After expression, the recombinant proteins were harvested with Ni-NTA magnetic beads, run on an SDS-PAA gel and transferred to a membrane. Immunostaining with α-His antibody revealed a faint signal for the positive control at ~60 kD and a visible signal at ~55 kDa corresponding to the mTKIN elution fractions of the reaction with unpurified mRNA (Figure 3-3).

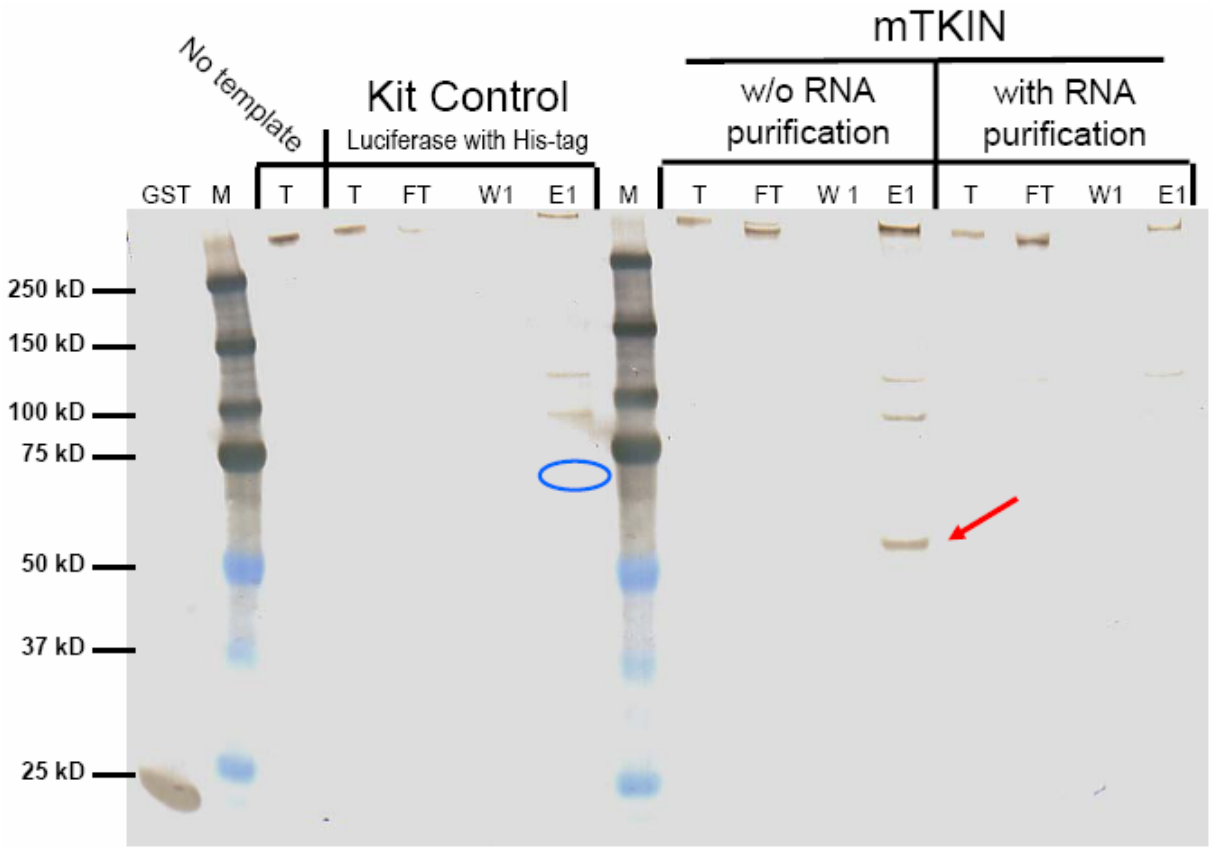

Figure 3-3: Analysis of the *in vitro* translation reactions after Ni-NTA purification of His_6-tagged proteins. 6 µL of the reaction mix (T) the flow-through (FT), first wash (W1) and first elution (E1) fractions from the not purified transcription fractions were loaded on gradient gel. The gel was blotted and hybridized with a-His (mouse) and a-mouse-HRP antibodies. M is a pre-stained protein ladder. The red pointer highlight the position of the Avi-His-tagged mTKIN and the blue circle highlights the position of a faint band from the His-tagged luciferase, which is hardly visible after digitalization of the blot.

The attempt to further purify the *in vitro* expressed mTKIN with ATP-agarose resulted in no detectable mTKIN, neither on Coomassie stained SDS-PAA gels nor by detection with an anti-His antibody on a western blot.

3.3 Periplasmic expression of mTKIN

Alternatively, targeted expression of mTKIN to the periplams of E. coli host cells was assessed for yielding larger amounts of soluble protein. Expression was conducted using the pIT2/mTKIN construct in *E. coli* strain HB2151. Two different protocols were applied with slightly different media components and IPTG concentration. Western blot examination of the periplasmic fractions loaded beside lysed spheroblasts of the same sample showed that

His_6-tagged protein was only present in the spheroblasts (Figure 3-4). After a native lysis of the spheroblasts and separation of the soluble from the insoluble proteins, the detection with an α-His antibody on a western blot showed that the His_6-tagged mTKIN was present in both fractions at similar concentration.

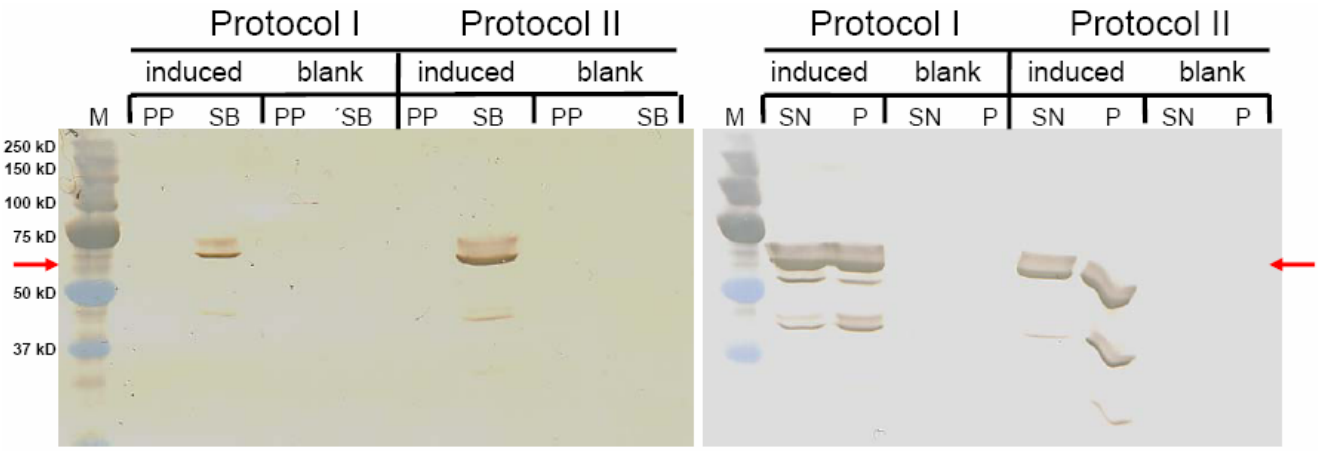

Figure 3-4: Analysis of the periplasmic expression of mTKIN applying two different protocols. On the left blot, 6 µL of the periplasmic preparations (PP) and aliquot of the spheroblasts (SB) were loaded on a 15% SDS-PAA gel, blotted and hybridized with mouse α-His and rabbit α-mouse-HRP antibodies. A pre-stained protein ladder (M) was used for size orientation. The position of the His_6-tagged mTKIN is highlighted by the red box. On the right blot, 1 µl of the soluble (SN) and insoluble (P) fractions of the lysed spheroblasts were loaded on a 15% SDS-PAA gel, blotted and hybridized with mouse α-His and rabbit α-mouse-HRP antibodies.

3.4 Purification screening using Ni-NTA agarose by gravity-flow

A simple procedure to isolate mTKIN from cell lysate applying Ni-NTA agarose batch purification by gravity-flow was assessed. Following the standard purification protocol recommended by the manufacturer resulted in co-purification of many other proteins together with the mTKIN, as can be seen on a Coomassie stained gel after SDS-PAGE (Figure 3-5). From western blots of such purification it was observed that the Avi-His_6-tagged mTKIN is depleted from the flow-through fraction and enriched in the elution fractions. A 4-fold enrichment factor is achieved through volume difference between the cell lysate from a 50 mL culture and a single elution fraction. When larger expression cultures are used for purification this enrichment factor is higher since that elution volume is held constant.

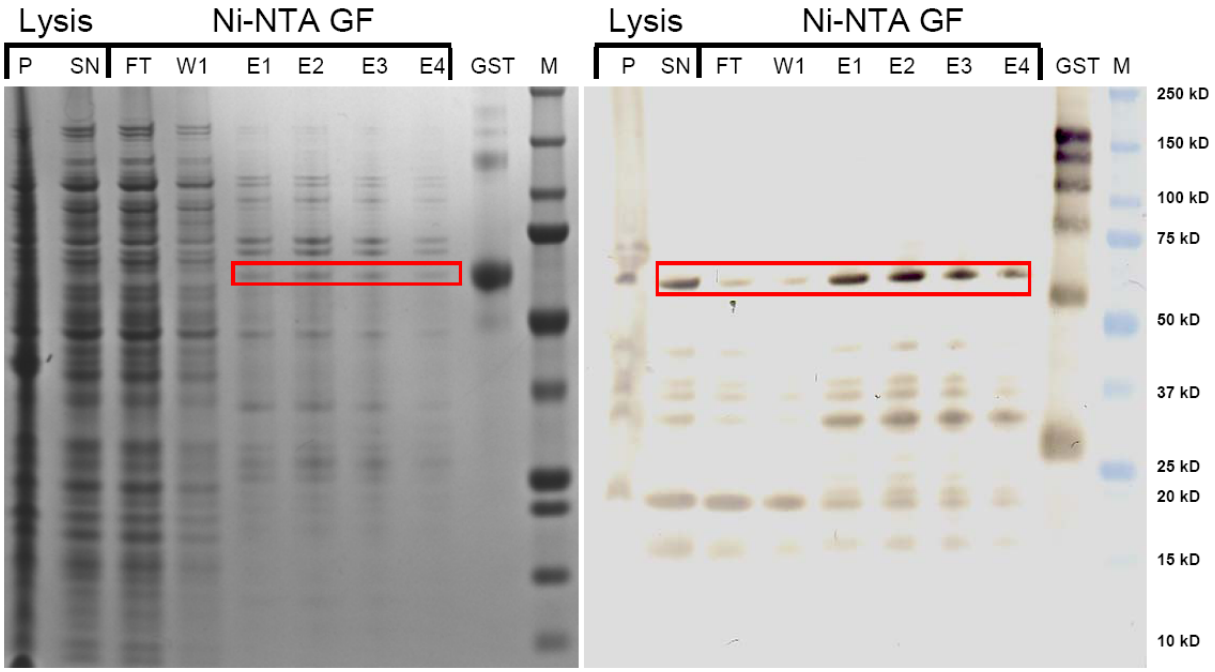

Figure 3-5: **Analysis of the Ni-NTA gravity flow purification fractions from a 200 mL mTKIN expression culture in BL21 CodonPlus (DE3)-RIL. 1 µL of the insoluble (P) and soluble (SN) protein fraction collected after cell lysis as well as of the flow-through (FT), first wash (W1) and all four elution fractions (E1-4) were separated on gradient SDS-PAA gels in duplicate. One gel was stained with Coomassie (right), the other was blotted and subsequently hybridized with streptavidin-HRP (left). Biotinylated GST was used as control for the hybridization and the prestained protein ladder (M) was used for size orientation. Red boxes highlight expressed mTKIN.**

3.5 Purification of mTKIN using immobilised ATP affinity chromatography

To further increase the purity of mTKIN after Ni-NTA agarose batch purification by gravity flow, the ATP-binding property of kinesins was used. Four available matrices differing in the way the ATP is linked to the agarose were tested: aminophenyl-ATP-agarose, C10-spacer (AP-ATP-agarose), 8-[(6-amino)hexyl]-amino-ATP-agarose (8AH-ATP-agarose), N^6-(6-amino)hexyl-ATP-agarose (6AH-ATP-agarose) and 2'/3'-EDA-ATP-Agarose (EDA-ATP-Agarose). In the first instance, all ATP-agaroses were incubated with Ni-NTA purified mTKIN (B/GF procedure) from a 50 mL Origami B (DE3) pLacI culture. Western blot analysis using streptavidin-HRP as a detector, small amounts of mTKIN were found only in the elution fraction of EDA-ATP-agarose (data not shown). The repetition of the whole affinity chromatography procedure including Western blot analysis with Ni-NTA elution fractions originating from 100 mL BL21 (DE3) pLysS and later from 200 mL BL21 CodonPlus (DE3)-RIL. expression cultures a stronger enrichment of the mTKIN with the EDA ATP-agarose was observed. Figure 3-6 shows a Coomassie stained SDS-PAA gel and a corresponding

Western blot analysis with streptavidin-HRP. Considerable enrichment and decrease of mTKIN can be observed in the elution and the flow-through fractions of EDA-ATP-agarose, respectively. In contrast, the other three ATP-agaroses did not show to specific retain mTKIN as most of the mTKIN was found in the flow-through fractions. from the other three types of ATP-agarose batches. The batch purification method applying ATP-affinity chromatography still results in some unspecific proteins in the elution fractions that can be detected on Coomassie stained SDS-PAA gels as well as in Western blots hybridized with streptavidin-HRP.

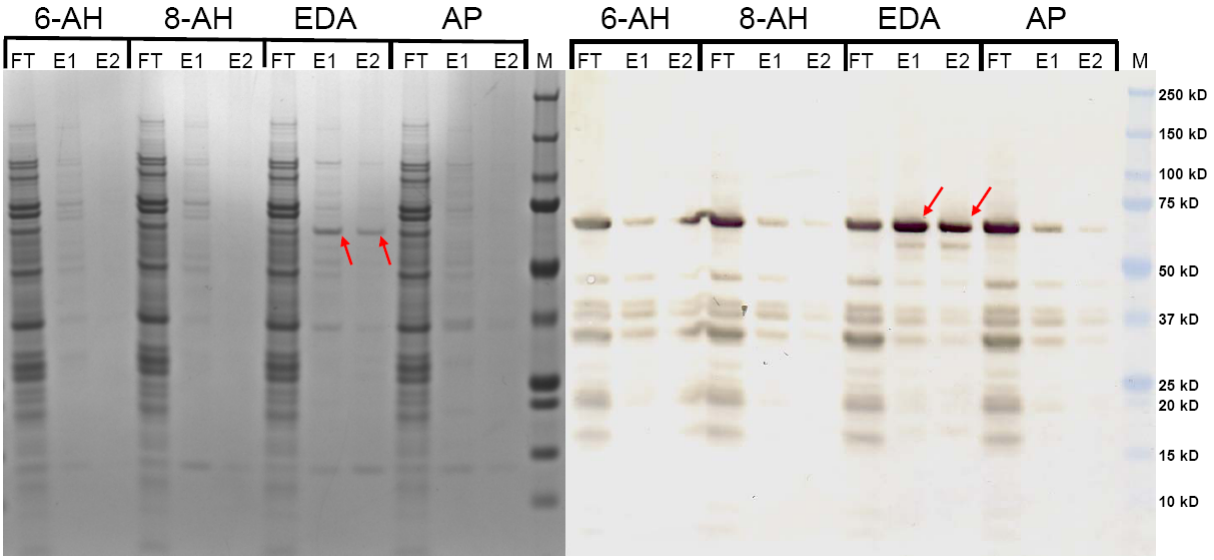

Figure 3-6: **Batch purification of Ni-NTA (B/GF) pre-purified mTKIN from a 200 mL BL21 CodonPlus (DE3)-RIL culture applying four different types of ATP-agaroses (Jena Bioscience). 4 µL of sample of the flow-through (FT) and elution fractions (E1, E2) from each ATP-agarose purification, were separated on a gradient SDS-PAA gel in duplicate. One gel was stained with Coomassie (right), the other was blotted and hybridized with streptavidin HRP (left). A pre-stained protein ladder was used for size orientation. The red pointers highlight the ATP-agarose enriched mTKIN.**

3.6 FPLC purification with Ni-NTA superflow cartridge

Aim of this study was to determine the optimal imidazole concentration for mTKIN elution and to reduce the background of co-purified protein at the same time. In the first attempt, a soluble protein fraction extracted from a 100 mL expression culture was loaded on a FPLC-system equipped with a 1 mL Ni-NTA superflow cartridge. Elution was carried out applying a linear gradient from 19.6 mM to 250 mM imidazole concentration, which resulted in a single peak at 70 mM imidazole. SDS-PAGE and Western blot analysis discovered that the peak contained five proteins in total, two larger and two smaller proteins than mTKIN. At the same time, mTKIN seemed to be eluted in higher concentration at slightly elevated imidazole concentrations compared to the other proteins. For comparison, recombinant Avi-His_6-tagged

ubiquitin precursor protein (Ubi8) was purified with the same column and gradient. This resulted in a peak at 96.7 mM imidazole concentration, which corresponds with the shifted elution of the mTKIN relative to the other detected proteins (Figure 3-7).

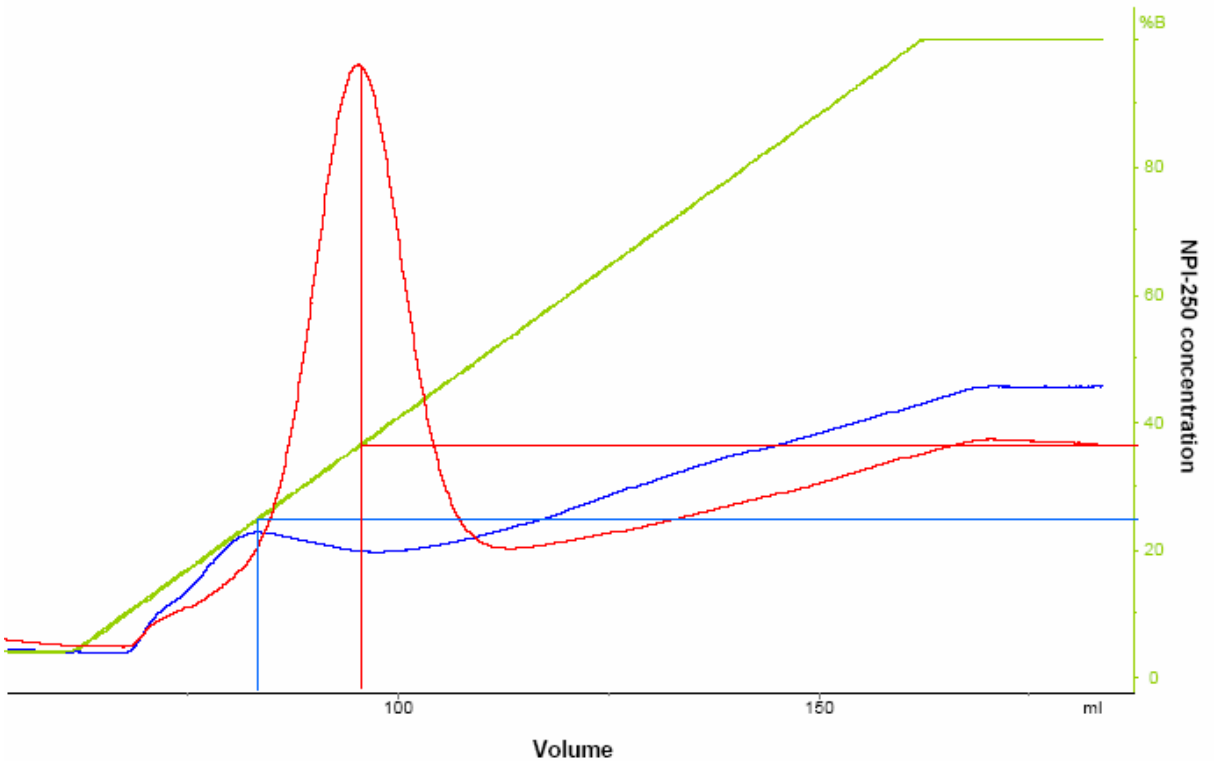

Figure 3-7: Overlay of the 280 nm UV-light absorption curves from a Ni-NTA affinity FPLC of Avi-His_6-tagged mTKIN (blue) and Ubi8 (red) from a protein extract. mTKIN sample originated from 100 mL expression culture of BL21 CodonPlus (DE3)-RIL and Ubi8 from 50 mL expression culture of BL21 (DE3) Star pRARE3. In both cases, elution was performed applying a linear gradient (green), starting from 4% NPI-250/96% NPI-10 and ending at 100% NPI-250 in a total volume of 100 mL.

To specifically deplete the unspecific proteins, a complex gradient was applied starting with a linear gradient from 19.6 mM up to 58 mM imidazole concentration, followed by a first isocratic elution step with 130 mM imidazole and a final isocratic elution step with 250 mM imidazole (Figure 3-8). This modification to the protocol resulted in a further shift of the mTKIN elution relative to the other two larger proteins (Figure 3-10, Figure 3-9)

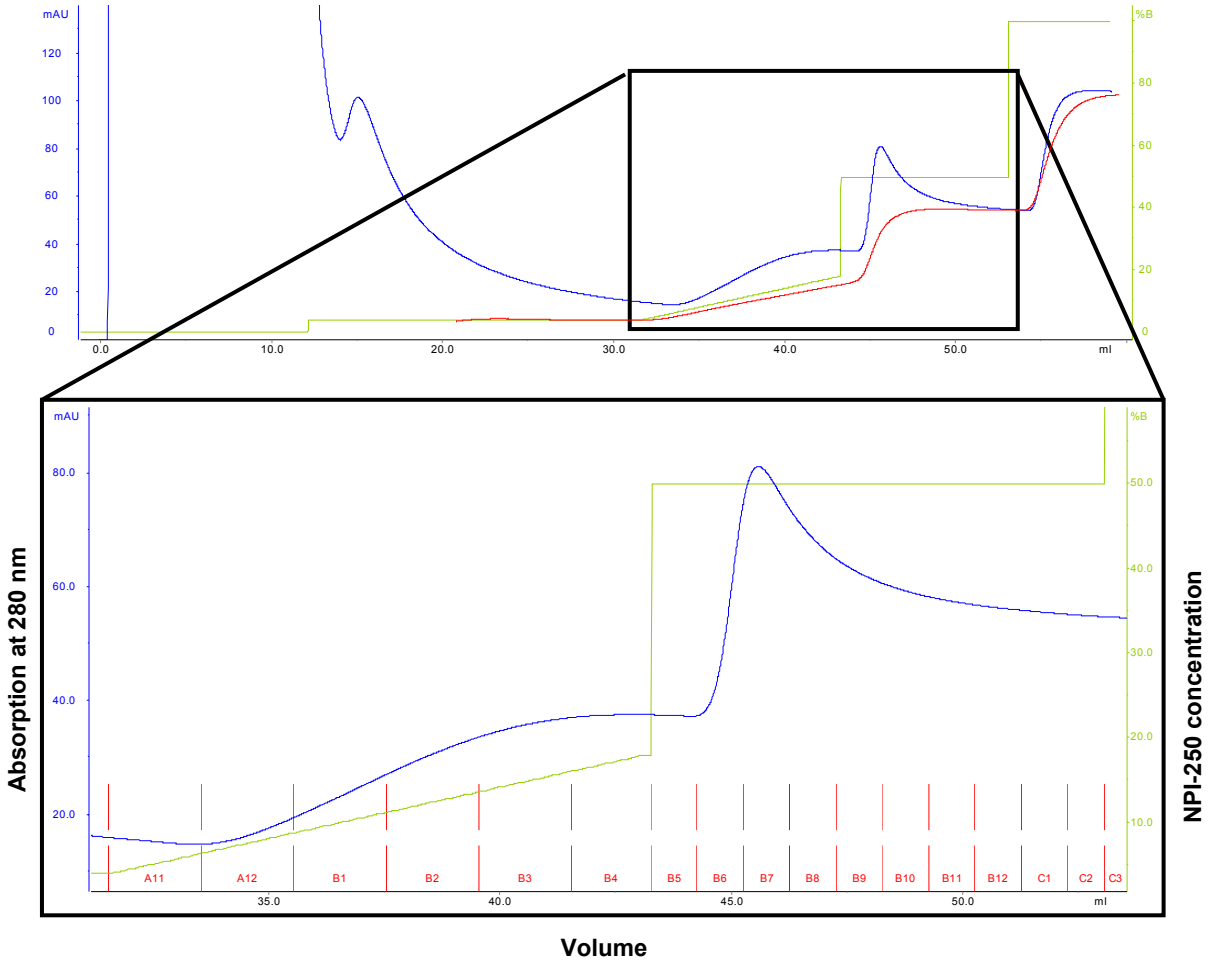

Figure 3-8: **Ni-NTA FPLC purification of mTKIN from a 200 mL BL21 CodonPlus (DE3)-RIL culture with a complex gradient (green curve). Proteins were observed through absorption at 280 nm (blue curve). The collected fractions are designated with red colour. The presented fractions in the zoomed window were used for protein composition analysis as well as for functional characterization. The red curve is produced by a FPLC run over a Ni-NTA column without protein to represent the light absorption at 280 nm of imidazole relative to its concentration defined by the gradient.**

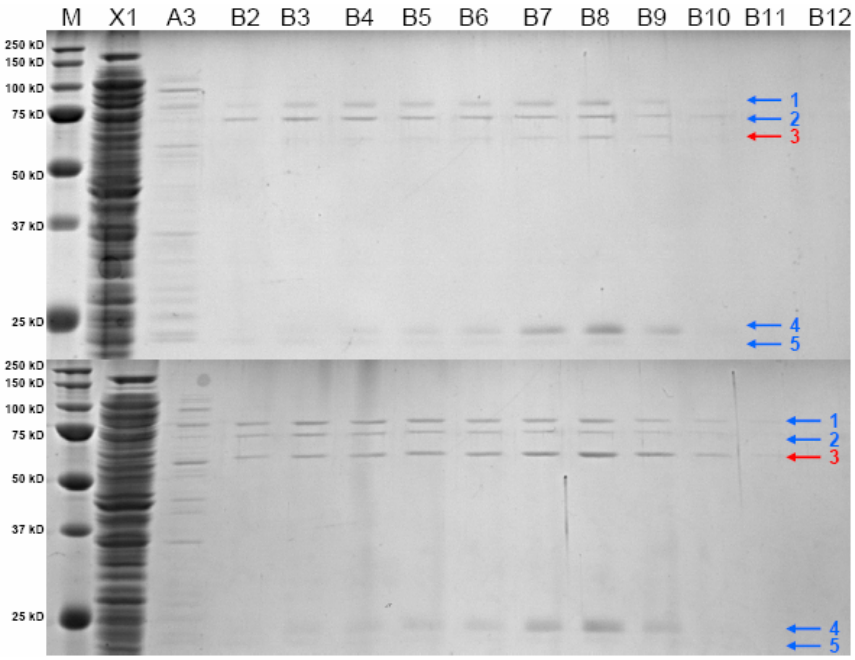

Figure 3-9: **Coomassie stained 15% SDS-PAA gels loaded with fractions of a Ni-NTA FPLC purification of soluble protein extracts from 200 mL BL21 CodonPlus (DE3)-RIL (upper gel) and Origami B (DE3) pLacI (lower gel) mTKIN expression cultures using the same elution gradient. 6 µL of flow-through (X1), wash (A3) and a series of elution fractions (B2-B12) were loaded. The third band from the top in the elution fractions is mTKIN (red pointer), the other four bands (blue pointers:1, 2, 4 and 5) correspond to proteins being co-purified with mTKIN.**

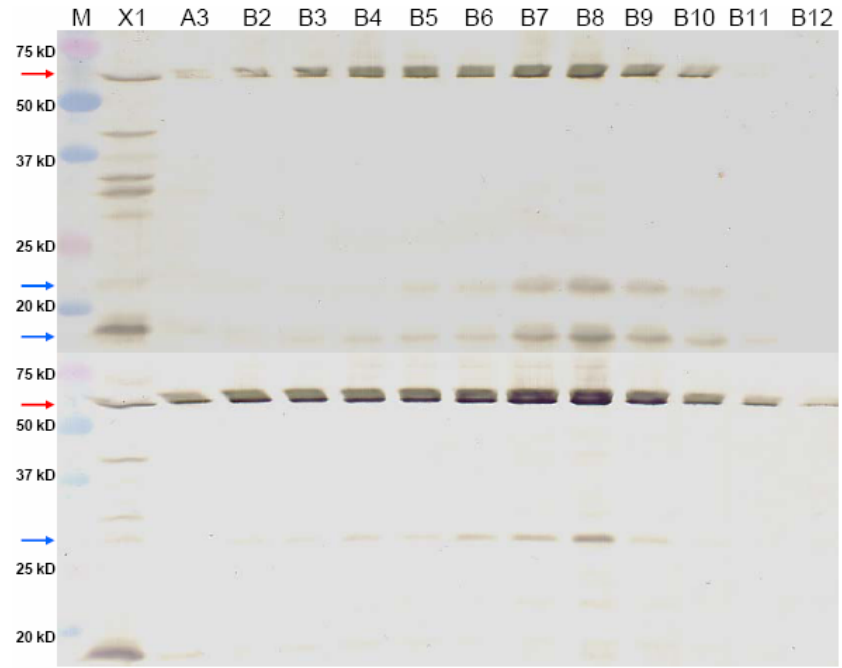

Figure 3-10: **Western blot analysis of the Ni-NTA FPLC fractions. Identical gels to those from Figure 3-9 were blotted and hybridized with streptavidin-HRP. The samples originate from a BL21 CodonPlus (DE3)-RIL (upper blot) and from a Origami B (DE3) pLacI (lower blot) expression culture. Red and blue pointers show biotinylated mTKIN and probably N-terminal degradation products of mTKIN, respectively.**

Repeating this purification strategy with pooled mTKIN containing fractions from the previous run resulted in a separation of the two larger proteins from the mTKIN. The two larger proteins remained in the flow-though fraction, while mTKIN and one of the smaller proteins were eluted with the 130 mM imidazole concentration step of the complex gradient. The amount of the smaller protein was significantly higher than that of mTKIN (Figure 3-11)

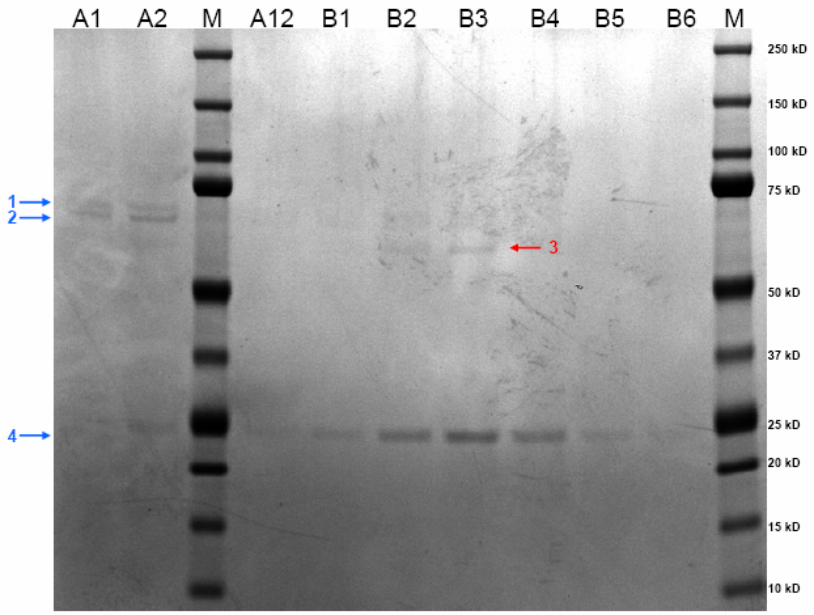

Figure 3-11: Coomasie stained gradient SDS-PAA gel loaded with the flow-though (A1 and A2) and series of elution fractions with the 50% NPI-250 (A12-B6) produced by a repeated Ni-NTA affinity FPLC purification with pooled mTKIN containing fractions as starting sample. The bands highlighted with a blue pointer are the unspecific co-purified proteins and the band highlighted with the red pointer is the mTKIN. The numbers of the pointers show the corresponding bands from Figure 3-9

3.7 Testing if the ATP-agarose is suitable for FPLC purification of mTKIN

Next, a self assembled EDA-ATP-Agarose column was applied using the FPLC to further purify potentially active mTKIN from the Ni-NTA purified fractions. Column was loaded with pooled mTKIN-containing fractions and bound mTKIN was eluted with an ATP-rich buffer. No characteristic peak, but rather a plateau was observed. Western blot examination showed that the majority of mTKIN did not bind to the column and was located in the flow-through fraction. Elution fractions contained only tiny amounts of pure mTKIN evenly distributed throughout all fractions (data not shown). To test the time dependence of mTKIN elution, the purification was repeated introducing two 20-minute pauses. One at the initial detection of ATP at 254 nm, and a second pause 4 mL after the first. This strategy lead to the elution of mTKIN in the fraction directly collected after the first pause, as demonstrated with a visible

band in a Coomassie stained SDS-PAGE. An additional second band was detected with streptavidin-HRP on a Western blot in the fraction just collected after the second pause (Figure 3-12).

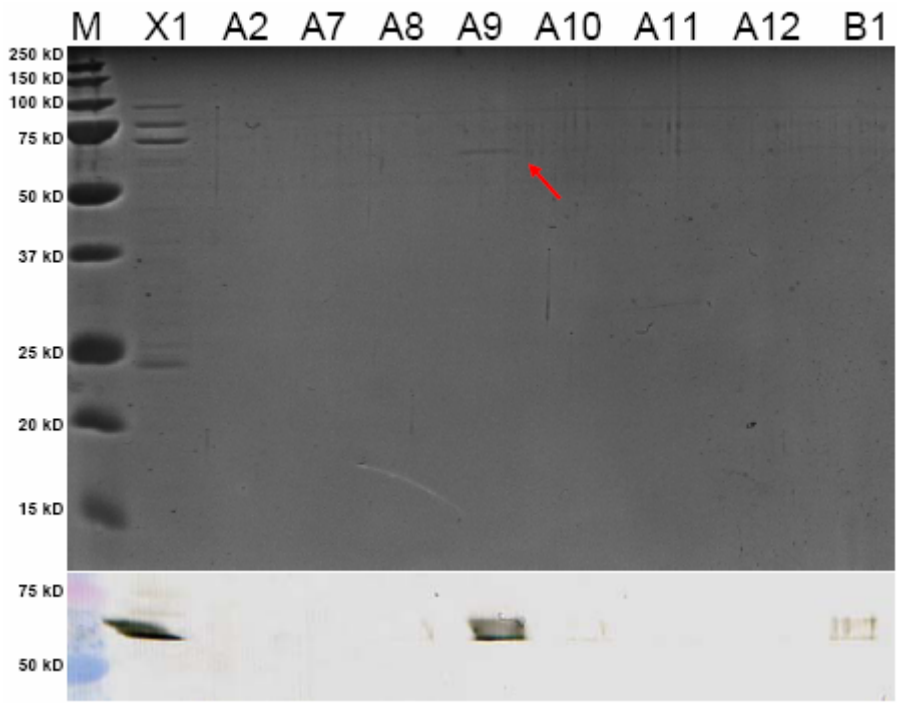

Figure 3-12: Coomassie stain and western blot analysis of a flow-through (X1) a wash (A2) and a series of elution fractions from the FPLC purification with introduced pauses using an EDA-ATP-agarose loaded column. The sample of pooled mTKIN containing fractions from a Ni-NTA FPLC was injected at 0.2 mL/min and the run was paused for 20 minutes right after ATP was first recorded at the detector (before fraction A9). This resulted in a visible band of specifically eluted mTKIN in fraction A9 on the Coomassie stained gel (upper image, red pointer). The second pause before the B1 fraction resulted in a second band detectable only by streptavidin-HRP on a western blot (lower image). 15% SDS-PAA gels were used for the SDS-PAGE.

3.8 Mass spectrometric identification of mTKIN and co-purified proteins

To find out whether all proteins in the elution fractions of a Ni-NTA purification correspond to mTKIN, a mass spectrometry analysis was performed. Five samples corresponding to the bands shown in Figure 3-9 , were excised from a Coomassie stained SDS-PAA gel. Samples were individually digested with two different proteases and analysed on a HPLC-coupled

ESI-Orbitrap mass spectrometer. This analysis confirmed that protein 3 was indeed mTKIN (52.41% sequence coverage). Analysis of the spectra from both digests (trypsin and AspN) revealed in each case five mTKIN-matching peptides with low false discovery rate (1%) when compared with a computationally generated peptide database (Figure 3-13). Additionally the two different digest produced together another seven peptides which were identified to be characteristic for mTKIN as well as KIF1A, B, and C from *Homo sapiens*, *Mus musculus* and *Rattus norvegicus*, as well as Unc-104 from *Aedes aegypti*, *Anopheles gambiae*, *Drosophila melanogaster* and *Drosophila pseudoobscura pseudoobscura*. The other four detectable proteins by Coomassie staining (Figure 3-9) were identified as *E. coli* originating proteins. Protein 1 was identified as bifunctional polymyxin resistance protein arnA (48.48% sequence coverage), protein 2 was identified as glucosamine-fructose-6-phosphate aminotransferase (56.49% sequence coverage), protein 4 was identified as FKBP-type peptidyl-prolyl cis-trans isomerase slyD (47.45% sequence coverage) and protein 5 was identified as catabolite gene activator (66.67% sequence coverage).

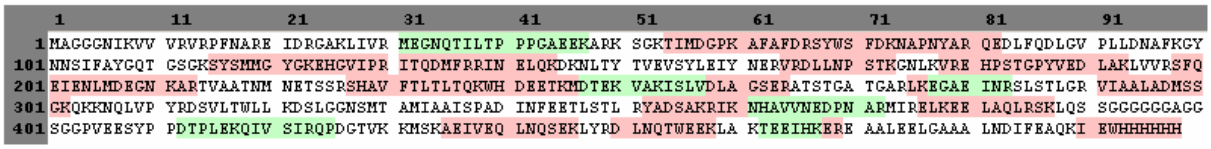

Figure 3-13: Sequence coverage of the mTKIN mass spectrometry analysis. The green highlighted peptides are detected peptides with false discovery rate of less than 1%, the red highlighted peptides with false discovery rate of more than 5%

3.9 Phage display

Here, the possibility to present mTKIN on the surface of M13 bacteriophages was assessed. For this purpose, pIT2/mTKIN was expressed in combination with two different helperphages in two commonly used *E. coli* strains for phage display, namely TG1 and XL1-blue. The two different helperphages M13KO7 and Hyperphage allow either monovalent or multivalent display of mTKIN on the bacteriophage surface, respectively. Western blot analysis using a mouse anti-pIII monoclonal antibody identified mTKIN-pIII fusion in all types of prepared phages, except for the phages produced with hyperphage in *E. coli* TG1 (Figure 3-14). In XL1-blue, phages produced with Hyperphage show more mTKIN-pIII fusion than those produced with M13KO7. The expected size of the mTKIN-pIII fusion protein without the pelB leader sequence is ~98 kD, where as the size of the pIII is ~53 kD.

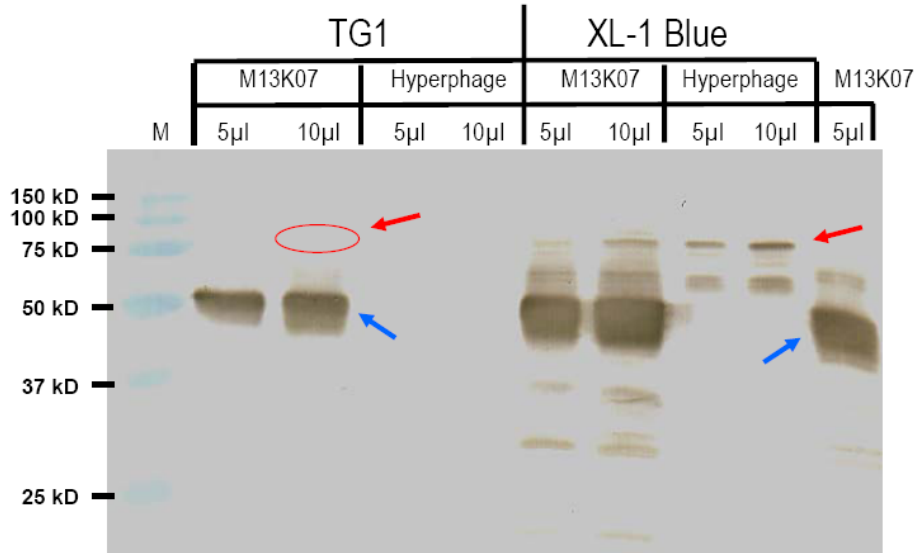

Figure 3-14: Western blot analysis of the four different mTKIN presenting phage populations resulting from the combinatorial application of two helperphages and two *E.coli* host strains. Additionally, the M13KO7 helperphage is loaded as a control and for comparison. Respective volumes of a phage preparation were loaded on a 15% SDS-PAA gel, and blotted. Wild-type pIII and mTKIN-pIII fusion were detected by hybridization with mouse a-pIII monoclonal and rabbit α-mouse-HRP antibodies. The blue and red arrows point to wild-type pIII and mTKIN-pIII fusion proteins, respectively. The red circle highlights the position of a faint band of mTKIN-pIII, which is hardly visible after digitalization of the blot.

Next to Western blot analysis, the amount of infective phage particles from 50 mL culture volumes was assessed by titration. The results showed that the majority of all four types of phages were carrying the mTKIN phagemid (Table 3-1) Generally the infection with M13KO7 yielded more phages than the infection with hyperphage as shown by the combination of XL-1 host strain with M13KO7 helperphage. In all cases, the ratio between packaged helper phage genomes and pIT2/mTKIN phagemids is in the order of 2-3-magnitudes.

Table 3-1: Titre of infectious phage particles of all four phage populations. Phages produced from the four possible combinations of the two *E. coli* host strains TG 1 and XL1-blue and the two helper phages M13KO7 and Hyperphage were titrated for helperphage genome and for mTKIN-phagemid carrying phages. The number of helperphage genome containing and pIT2/mTKIN phagemid containing particles was determined by plating on kanamycin or ampicilin containing agar-plates.

Host	Helper phage	Kanamycin (Helper)	Ampicilin (mTKIN phagemid)
TG 1	M13K07	$2{,}1 \cdot 10^{10}$ cfu/mL	$3{,}6 \cdot 10^{12}$ cfu/mL
	Hyper-phage	$1{,}0 \cdot 10^{7}$ cfu/mL	$2{,}1 \cdot 10^{9}$ cfu/mL
XL-1 Blue	M13K07	$1{,}0 \cdot 10^{11}$ cfu/mL	$1{,}5 \cdot 10^{14}$ cfu/mL
	Hyper-phage	$8{,}0 \cdot 10^{8}$ cfu/mL	$2{,}5 \cdot 10^{11}$ cfu/mL

3.10 Determining the ATPase activity of mTKIN using the NADH oxidation coupled double enzyme ATPase assay

Measurement of ATP hydrolysis rate allows to determine the activity of kinesins, as they require ATP to move along MTs. First, the coupled NADH oxidation assay was successfully established using standard 1 cm photometric cuvettes as well as using a microtiterplate by directly adding ADP as a substrate. The reduction of light absorption at 340 nm by excess ATP in combination with small amounts of ADP as substrate proved that the enzymatic system was not inhibited by an ATP to ADP ratio similar to the situation in which a kinesin starts producing ADP through ATP-hydrolysis. The kinetic properties of the EDA-ATP-agarose purified mTKIN expressed in BL21 CodonPlus (DE3)-RIL was assessed by performing this assay on a microtiterplate at eight different ATP concentrations and in presence or absence of MTs (0.1 µg/mL or ~ 1 mM αβ-tubulin). The same was repeated with a 1:2 dilution of a KIF1A-GFP stock solution, a recombinant full-length kinesin-3 from *R. norvegicus* C-terminally fused with His_6-tagged GFP, as a control (courtesy of Prof. Lipowsky, MPI for Colloids and Interfaces). The total concentrations of the kinesins in the reactions were roughly estimated to be ~66 nM for the KIF1A-GFP and ~5 nM for the EDA-ATP-agarose FPLC-purified mTKIN (Figure 3-15)

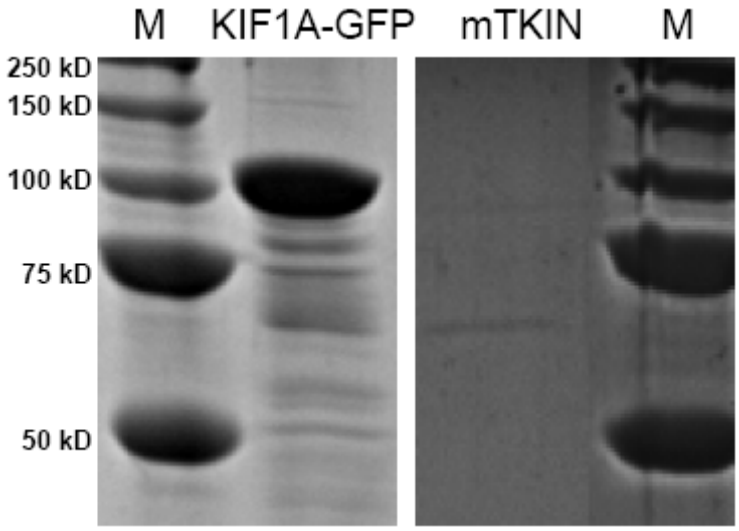

Figure 3-15: Comparison between the concentration of KIF1A-GFP stock solution and EDA-ATP-agarose FPLC-purified mTKIN by SDS-PAGE analysis. Coomassie stained 15% SDS-PAA loaded with 6 µl of each sample and a prestained protein ladder (M) for protein size comparison.

The NADH oxidation coupled assay showed an intrinsic ATPase activity for both kinesins, i.e. in the absence of MTs. However, the rates of ATP hydrolysis in presence of MTs were considerably higher (Figure 3-16).

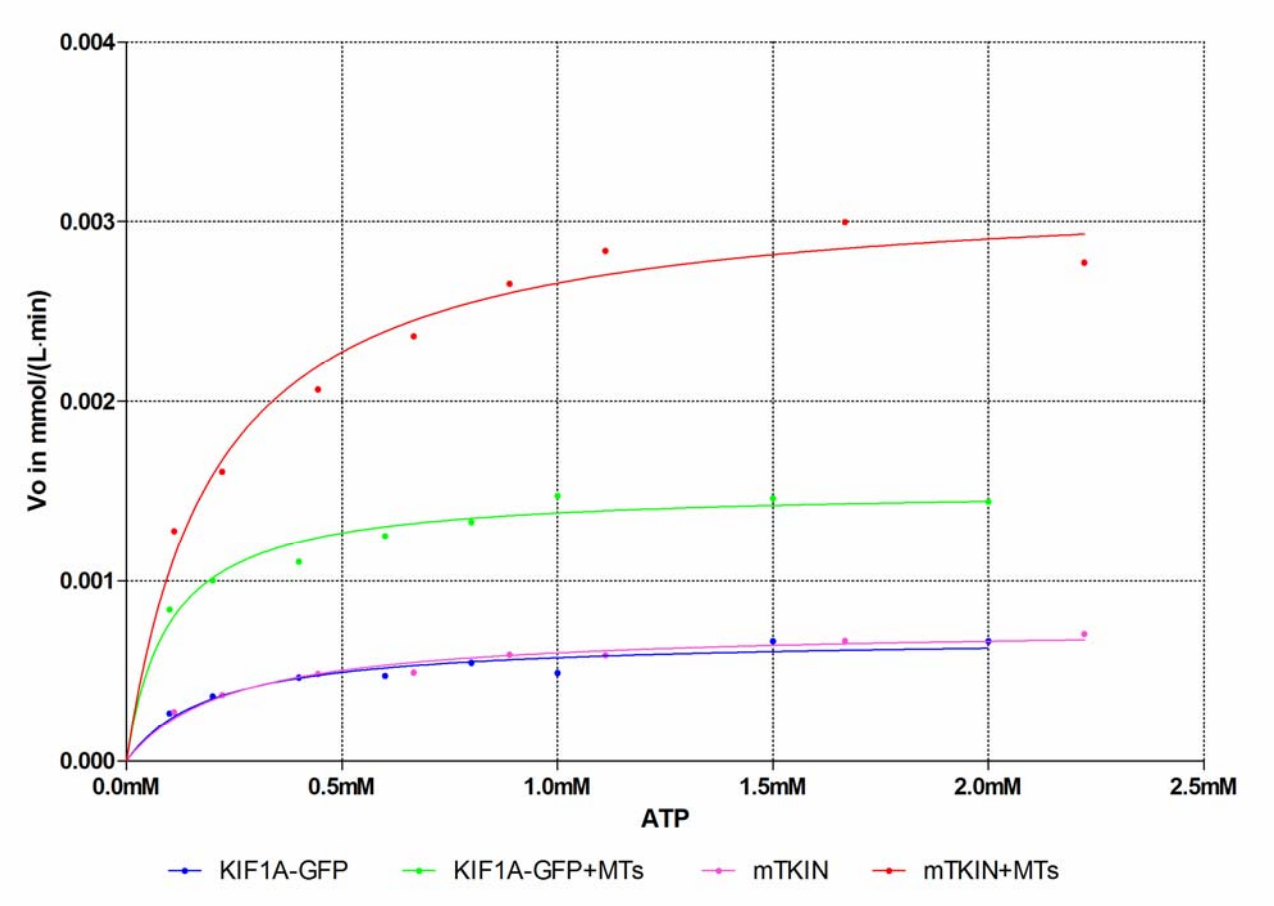

Figure 3-16: Michaelis-Menten curves for the ATPase activity of mTKIN and the positive control (KIF1A-GFP) in the presence or absence of microtubules. The V0 values were calculated using the Lambert-Beer's law from the measured ΔE/dt of a microtiterplate-format NADH oxidation coupled assays and plotted against the different ATP concentrations.

The V_{max} and the K_m values of the mTKIN and the KIF1A-GFP were similar when no MTs were present in the reactions (Table 3-2). The presence of MTs raised the k_{cat} of KIF1A-GFP around 2.2-fold while the K_m was lowered 0.5-fold. The K_m of mTKIN was also lowered under the same conditions, but less (0.85-fold), while the k_{cat} of mTKIN had increased considerably (4.3-fold) in presence of microtubules.

Table 3-2: Evaluation of the Michaelis-Menten curves obtained by the ATPase assay measurement of mTKIN and KIF1A-GFP using GraphPad Prism software. The k_{cat} values have error around 25%, as they are calculated using only roughly estimated protein concentrations.

Reaction	V_{max} (mmol/L·min)	K_m (µM)	k_{cat}	R^2 of curve fit
KIF1A-GFP	$0.69 \cdot 10^{-3}$ ± 6.74%	197.6 ± 54.64	~0.175 s^{-1}	0.8843
KIF1A-GFP+MTs	$1.51 \cdot 10^{-3}$ ± 3.29%	97.9 ± 18.21	~0.378 s^{-1}	0.9181
mTKIN	$0.74 \cdot 10^{-3}$ ± 4.16%	238.3 ± 39.19	~2.46 s^{-1}	0.9586
mTKIN+MTs	$3.2 \cdot 10^{-3}$ ± 3.80%	202.5 ± 32.67	~10.66 s^{-1}	0.9573

3.11 Microtubule gliding assay

Finally the ability of immobilized mTKIN to move microtubules was assessed in a motility assay. The assay was successfully established with KIF1A-GFP fusion protein, as directed gliding movement of the ROX-MTs was observed in a distinct plane scanned by a LSCM (Figure 3-17). The plane corresponded to KIF1A-GFP coated surface. Next, this experiment was repeated with diluted stocks KIF1A-GFP 1:2 in NPI-250, the elution buffer of mTKIN purification on the FPLC-system. The observed gliding motion of ROX-MTs confirmed that presence of 125 mM imidazole is not hampering the glide assay mechanics. The glide assay performed with a Ni-NTA FPLC-purified mTKIN from 200 mL BL21 CodonPlus (DE3)-RIL using a streptavidin-coated slide resulted just in a very low rate of binding of ROX-MTs onto the plane where the biotinylated mTKIN was previously enriched and no gliding was detected. A 20-times more concentrated Ni-NTA FPLC-purified mTKIN from 400 mL OrigamiB (DE3) pLacI expression culture was used in motility assays with standard glass slide and streptavidin coated slides. Again only very rare binding events of ROX-MTs onto the mTKIN functionalized surface seen and no gliding was recorded. However, the ROX-MTs were occasionally truncated in shorter segments disassociating from the surface during the scanning procedure.

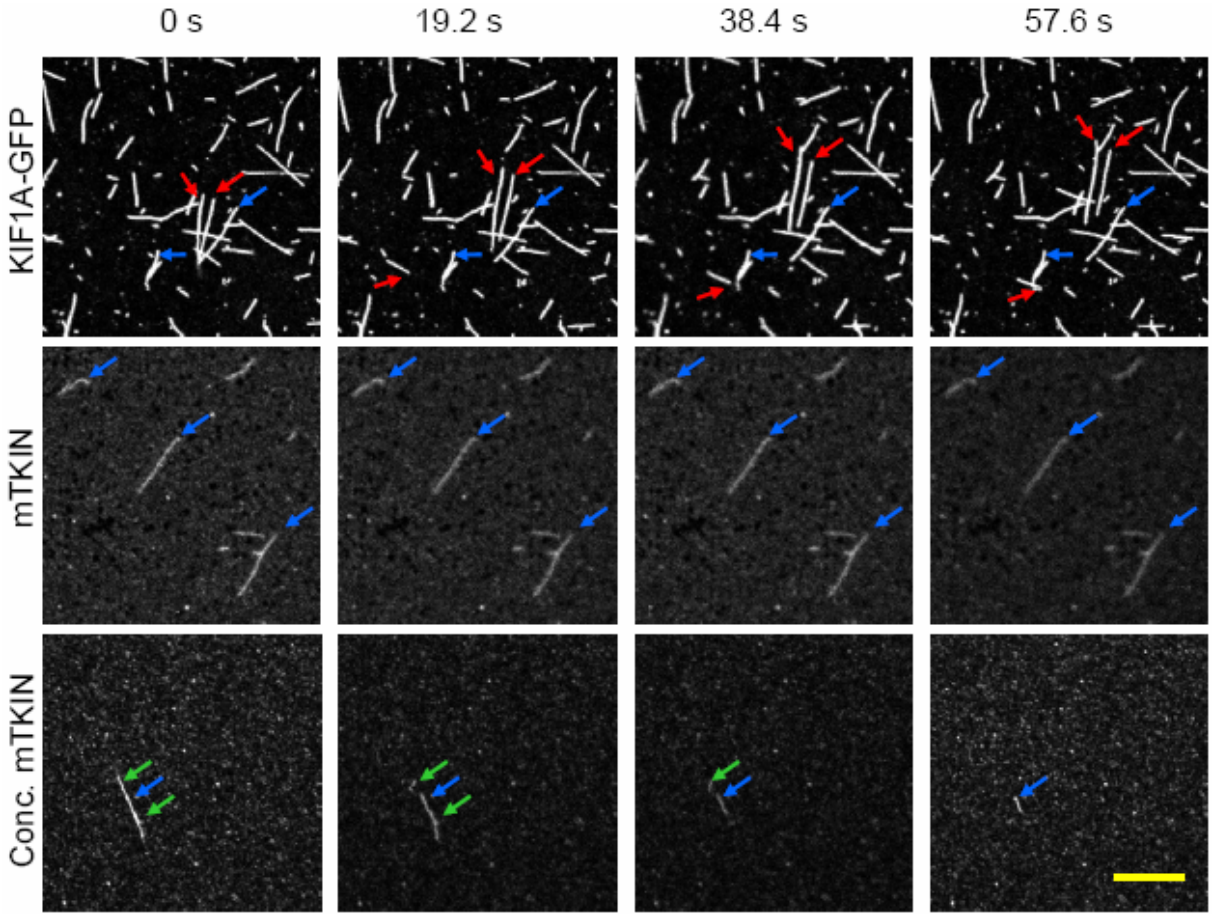

Figure 3-17: Snapshots taken in same time intervals of three glide assays done with KIF1A-GFP (positive control), mTKIN (on streptavidin slide) and concentrated mTKIN (standard glass slide). The red pointers highlight kinesin driven gliding of ROX-MTs, the blue pointers highlight immobile ROX-MTs bound to the kinesin coated surface and the green pointer highlight the truncation of ROX-microtubule segments over time. Yellow magnification bar = 10 µm.

The full movies of the individual gliding assays presented in Figure 3-17 can be found on the CD in the appendix of the thesis, on the back cover.

4 Discussion

The kinesin-microtubules transportation system has been evolved and optimized in nature over millions of years and therefore represents an excellent basis for future lab-on-a-chip applications. Since it is an active transporting system it can be used for movement of macromolecules from one chamber to another. In principle, this could be done selectively over channels which the macromolecules can not passage without active transport. The possibility to use a kinesin molecule which shows superior stable at higher temperatures and possesses a longer half live without loosing its activity and property for nanotechnological applications has not yet been described and investigated. Additionally, no attempts to present kinesins or mutated kinesin libraries on bacteriophage surfaces for purposes of protein engineering has been published. Inevitably, production of specifically tuned kinesin in respect of temperature, motility velocity or even substrate specificity by phage display selection techniques would allow a much greater flexibility in the construction of future lab-on-chip or other nanotechnological applications.

4.1 Expression screening of modified TKIN (mTKIN)

The modified kinesin (mTKIN) is derived from kinesin-3 (TKIN) from *T. lanuginosus* (Rivera et al. 2007) The major differences are the lack of cysteines and that it is a truncated version of the protein (aa1-498). The initial expression attempts in the BL21 (DE3) Star pRARE3 strain showed that mTKIN can be expressed as a soluble protein in sufficient quantities (Figure 3-1). This means that there is no need to use insoluble mTKIN, which then has to be solubilised under denaturing conditions and refolded into functional conformation before use. The feature of soluble expression becomes especially important in nanotechnology. The easier and less time-consuming the production process of a kinesin is, the more useful its application possibility in nanotechnological applications will be. All downstream processes under investigation in this study were conducted bearing this in mind. The purification and characterization studies were initially designed as simple as possible and the produced and purified mTKIN was simply stored at 4°C. Hence, the major focus of this study was directed towards isolation of mTKIN from the soluble protein fraction of E. coli cell lysates, and the insoluble fraction was rather used for comparative reasons, as the insoluble fraction contained similar amounts of soluble mTKIN. The expression levels of mTKIN were however low in contrast to previously expressed kinesin-3 isoforms (Rivera et al. 2007; Sakowicz et al. 1999). Because of the low expression levels of mTKIN the corresponding band in the soluble protein fraction cannot be easily identified on a Coomassie-stained SDS-PAGE. To be able to monitor the difference in mTKIN yield during the expression screening phase all

evaluations were carried out by Western blot analysis. Therefore the detection of Avi-His_6-tagged mTKIN with streptavidin on one Western blot and with anti-His antibody on another enabled a far better identification of the mTKIN and were mainly used for orientation and comparison of the expression patterns under different conditions and *E.coli* strains of interest. The reasons for the low expression of the mTKIN can be explained through the introduced modifications. Most probably the chosen length of the mTKIN stalk domain is the reason for the poor expression. A similar finding based on a fungus-deriving kinesin-3 with shorter stalk region, without the FHA and PH domains, was reported (Adio et al. 2006). Kinesins could possess potentially toxic properties in prokaryotic organisms. For sure, the lack of suitable tRNA can not be the reason for low yield of mTKIN, since its sequence has been codon-optimized. Further, successful expression of multiple Avi-His-tagged proteins points out that the Avi-His tag is most likely not hampering the expression yield of mTKIN (Z. Konthur, pers. communication) Finally, a rather remote reason for low expression levels could be the choice of vector for the expression of mTKIN. Although pQDKG2 is a derivative of a standard protein expression vector from Qiagen (pQE30), it might not be suitable for yielding larger amounts of the mTKIN. To my knowledge, no other kinesin has been ever reported to be expressed in a pQE- or pQE-derived vector. When comparing the expression patterns of mTKIN after varying induction time periods and expression temperatures, several differences were observed. Firstly, the induced expression of mTKIN at lower temperatures over a longer period of time changed the ratio between soluble and the insoluble mTKIN. Expression of mTKIN at 37°C for 3 hours produced more insoluble than soluble mTKIN, whereas expression at 22° C for 5 hours or 18°C for 18 hours yielded almost the same amounts of both soluble and insoluble mTKIN. Over all, larger amounts of mTKIN were produced at lower temperatures and longer time periods. It might be possible that certain kinesins are more toxic for *E. coli* cells than others due to a higher intrinsic ATPase activity. In such a case, expression of large amounts of mTKIN could lead to accumulation of larger quantities of mTKIN within single cells. This in turn might lead to recruitment of a defense mechanism which keeps the soluble mTKIN below a certain concentration by depositing the excess quantities in inclusion bodies. During a prolonged period of induction under lower temperature the expression of mTKIN within individual cells might be low. Furthermore this might not lead to overloading of the host cell folding machinery. Culturing at these conditions (18° C for 18 h) produce more biomass and overall similar amounts of mTKIN are expressed as other expression conditions (37° C for 3h), while keeping the ratio in favor of the soluble mTKIN. Next to higher yield of soluble protein, another positive aspect was observed in respect of degradation products. Since the Avi-His_6-tag is positioned on the C-terminus of mTKIN, only N-terminal degradation products can be detected on Western blots. In this respect, the lowered temperature and prolonged induction time gave again better results, as

reduced numbers and amounts of N-terminal degradation products relative to the other expression conditions were produced. The reduction of degradation product can be observed more clearly form the anti-His detection where 2-3 degradation products are found when expressing at 37°C for 3 hours and just one detectable degradation product is seen from the expression of mTKIN at 18°C and 18 hours. The reasons for this are most probably the same as for the ratio shift between soluble and insoluble mTKIN. So it might be possible that larger quantities of mTKIN per cell are being degraded more excessively. This concludes that optimal mTKIN expression can be achieved by induction at 18° C for 18 hours.
In order to investigate if mTKIN expression can be further improved in regard to larger quantities of soluble protein and reduced production of degradation product, the expression of mTKIN was tested using in total four different *E. coli* expression strains. BL21 (DE3) Star pRARE3 was used as it is the strain established in the laboratory of Dr. Zoltán Konthur for the production of biotinylated recombinant proteins. Two other strains were chosen because their use to express kinesins successfully has been reported. BL21 CodonPlus (DE3)-RIL has been used to express kinesin-3 from *Neurospora crassa* and BL21 (DE3) pLysS has been used to express recombinant kinesin of *Drosophila melanogaster* (Berliner et al. 1994). The last strain used for the expression screening was Origami B (DE3) pLacI, which possesses the properties of the Tuner (DE3) pLacI strain that has been used for the recombinant expression of the wild-type TKIN from *Themomyces lanuginosus* (Rivera et al. 2007). The results of the screen showed that all four strains are expressing similar amounts of soluble mTKIN, however, different amounts of d3egradation products were observed. Strain BL21 (DE3) pLysS, produced three N-terminal degradation products whereas the other three strains produced only one (Figure 3-2). The BL21 (DE3) Star pRARE3 produced only one detectable degradation product of mTKIN, however the amounts of the mTKIN degradation product produced by this strain were larger than those produced by BL21 CodonPlus (DE3)-RIL and Origami B (DE3) pLacI. Strains BL21 CodonPlus (DE3)-RIL and Origami B (DE3) pLacI gave the best results. Notably, strain BL21 CodonPlus (DE3)-RIL grew faster and showed less batch to batch variation than Origami B (DE3) pLacI strain which was more difficult to cultivate. The mTKIN used for purification and further characterization in this investigation was produced using either the BL21 CodonPlus (DE3)-RIL or the Origami B (DE3) pLacI strain. The presence of mTKIN C-terminal degradation products is not relevant, since mTKIN was subsequently purified using Ni-NTA affinity chromatography. All C-terminal degradation products should not bind the matrix as they are missing the C-terminal Avi-His_6-tag and thus are being washed away. Another important feature of mTKIN expression is its potential of being biotinylated. Since biotin forms a strong interaction with streptavidin, biotinylation of mTKIN enables it directly to interact either with streptavidin-functionalized surface or streptavidin conjugated proteins. From the Western blot

analyses it becomes evident (Figure 3-1) that mTKIN was very efficiently biotinylated in all of *E. coli* strains under investigation, even though an earlier investigation on the production of a biotinylated kinesin (Berliner et al. 1994). However, in that report not the AVI-tag was used, but a larger biotinylation acceptor site derived from the biotin carrier complex protein (BCCP).

4.2 *In vitro* expression of mTKIN

As an alternative to *in vivo* expression in *E. coli*, the possibility to express mTKIN *in vitro* was investigated using a commercially available in vitro expression kit. From the Western blot analysis (Figure 3-3) of the *in vitro* expressed mTKIN purified with Ni-NTA magnetic beads purified, we can see that mTKIN was successfully produced using not unpurified mRNA template in the reaction. The absence of an expression product in the *in vitro* translation reaction after mRNA purification could be due to a massive RNA loss during the purification step, or a RNase contamination. The unsuccessful attempt to further purify the *in vitro* produced mTKIN with on ATP-agarose can be interpreted in multiple directions. One is that the *in vitro* produced mTKIN failed to fold properly and, hence, did not bind to the EDA-ATP-agarose. Another possibility is that only a small proportion of the produced mTKIN folded properly and since the initial concentration of mTKIN in the translation reaction was already very low, the concentration of ,mTKIN in the elution fractions after EDA-ATP-agarose purification was simply below the detection limit. Because of time and financial restrictions, the expression of mTKIN was not further investigated using *in vitro* expression systems. In principle, if any in vitro expression system would succeed to produce larger quantities of functional mTKIN, its application in nanobiotechnology and nanotechnology could be of high interest.

4.3 Developing a two-stage purification procedure for kinesins

Following the logic of using easy, fast and cost-effective means of producing purified mTKIN a novel Ni-NTA agarose and subsequent ATP-agarose affinity purification procedure was established. The first part of this two step purification procedure included a standard and routinely applied Ni-NTA affinity purification procedure of His_6-tagged proteins. This purification procedure is fast, inexpensive and in its simplest form it is composed of batch hybridization of the target protein followed by washing and elution applying gravity flow using a polypropylene column. As a direct consequence, only small amounts of reagents and buffers are consumed per run and, if stored properly, the Ni-NTA agarose can be reused several times. However, this procedure is principally suited for one step purification only when the recombinant protein is being expressed in large quantities. This was not the case

for mTKIN as many other proteins were co-eluted from the matrix (Figure 3-5). Although a range of unspecific proteins were co-purified with mTKIN, a depletion of the mTKIN in the flow-through fraction was demonstrated. This was concluded from Western blot analyses of the purification fractions (Figure 3-5). Since mTKIN possesses a AVI and a His_6-tag, all following Western blot analyses were performed with streptavidin-HRP so that the biotin-tagged mTKIN could be identified among the other Ni-NTA-co-purified proteins. The number of proteins which can be purified with Ni-NTA agarose and that can be detected with an anti-His6 antibody differ substantially. This is due to the difference in the interaction mechanism of the hexahistidine polypeptide. The anti-His_6 antibody is very specific for His_6-tagged proteins. However, if a protein has less than six histidines at any terminal, the antibody will most probably not bind or – in best case – just weakly bind to the protein. On the other hand Ni-NTA will undergo an interaction with two closely positioned histidines (Figure 4-1) and theoretically a His_6-tagged protein can be immobilized by three Ni-NTA complexes. However, if other proteins have two neighboring histidines spatially accessible for the Ni-NTA ,or two histidines which are positioned in a very close proximity through structural conformation and are spatially accessible for the Ni-NTA at the same time, they will most probably also be bound. Hence other unspecific proteins can be co-purified with the His_6-tagged protein if its concentration is low and many free valences of the Ni^{2+} ions remain available. Furthermore, in cases where not all six histidines are accessible, the His6-tagged protein could be partially or completely eluted while trying to wash away unspecific proteins with higher imidazole concentrations.

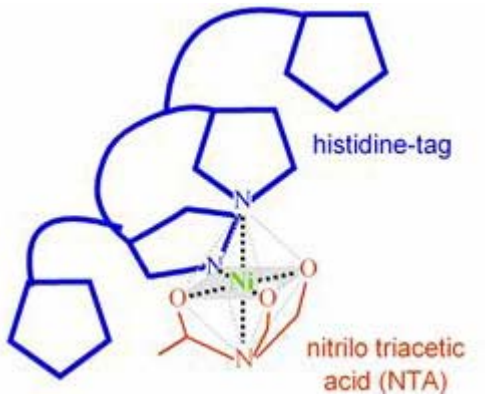

Figure 4-1: Schematic representation of how two histidines from a poly-histidine-tag interact with Ni-NTA taken from :http://www.biologie.uni-osnabrueck.de/Biophysik/Piehler/grafik/research_figure4new.jpg

Like all other kinesins, mTKIN possess an ATP binding pocket and ATPase activity. This characteristics was exploited in a second chromatography step to purify mTKIN on ATP-functionalized agarose. To my knowledge the purification of kinesin on ATP-agarose has not been shown previously. ATP-affinity chromatography was used to further purify mTKIN from the unspecific Ni-NTA co-purified proteins. Since it is expected that only properly folded

mTKIN to possess a functionally folded ATP-binding pocket capable of binding to ATP-agarose, all misfolded mTKIN would be removed in the flow-through or washing fractions together with the unspecific proteins. Additionally, the N-terminal proximity of the ATP-binding pocket prevents most N-terminal degradation products to bind ATP. Thus, these proteins will also be removed efficiently. Hence, with this two-stage protocol it should be generally possible to specifically purify only functional kinesin. The results observed from the Coomassie stained SDS-PAGE demonstrated this nicely as only full-length mTKIN was enriched in the elution fraction and depleted in the flow-through fraction (Figure 3-6). Furthermore, from Western blot analyses it could be observed that N-terminal degradation products were detected primarily in the flow-through are were hardly present in the elution fractions. The only N-terminal degradation product which was detectable in the elution fraction after purification was a product right below the full length mTKIN which otherwise were not detectable, possibly because it is normally present only in quantities below the detection level of Streptavidin-HRP. It can be argued, that this fragment is probably a N-terminal degradation fragment only missing a few N-terminal residues, thus neither compromising the ATP-binding pocket, nor hampering ATP binding activity. Thus, it might well be fully functional. Another important feature in establishing an ATP-agarose mediated mTKIN purification procedure is the possibility to determine the way ATP is being bound by mTKIN. This is possible because there are four different ways ATP can be coupled onto the agarose (Figure 2-3). As no prior information was available, a purification screening was set up to test all four types of ATP-agarose and by analyzing the flow-through and elution fractions by SDS-PAGE and Western blot, the screen could identify which of the ATP-agaroses is most suitable for purification (Figure 3-6). EDA-ATP agarose suites best to purify mTKIN efficiently. The failure to enrich mTKIN with AP-ATP-agarose indicates that the γ-phosphate is most probably being held by a residue positioned inside the ATP pocket where it can be hydrolytically separated from the ATP. Furthermore, mTKIN was neither enriched with 6AH-ATP agarose nor 8AH-ATP-agarose (Figure 2-3). This implies that adenine is very specifically recognized by the ATP-binding pocket, suggesting that other purine nucleotides like GTP can not be used as substrate by mTKIN. Bearing in mind that the purpose of ATP-affinity-chromatography was to obtain functionally active kinesin molecules, the manufacturers recommendations for buffer supplements was significantly amended. Firstly, DTT was omitted from the wash and elution buffers, since mTKIN is cysteine-free and hence can not build disulfide bonds, which could lead to missfolding of a protein in absence of DTT. Moreover, the successful purification of mTKIN with EDA-ATP-agarose demonstrates that folding of mTKIN was most probably not affected by the exchange of cysteine residues present in the wildtype TKIN. Secondly, sodium-orthovanadate was also omitted from the binding, wash and elution buffer. The intended function of sodium-orthovanadate is to protect

the hydrolysis of the functionalized ATP on the agarose by ATPases found in a crude protein extract, as it is an ATPase-inhibitor. In this case mTKIN was previously Ni-NTA-purified so it was unlikely that other ATPases were present in the used mTKIN containing sample. A more important reason of avoiding sodium-orthovanadate has been previously reported. Orthovanadate occupies the γ-phosphate position in the ATP binding pocket of myosin, another motor protein, and impairs the release of ADP, thus stalling the function of myosin (Rayment 1996). This would have meant that mTKIN would have been rendered inactive by sodium-orthovanadate during the purification process if added. Third and final remark on the purification procedure is the inefficiency of the batch purification method in itself. The fact that the ATP-affinity chromatography was carried out in batch where the ATP-agarose is collected by centrifugation and the supernatant collected by a pipette, makes it possible for other proteins to remain in the elution. The proteins can be either held by the ATP-agarose or are simply not being diluted sufficiently during the washing, as the wash buffer of the ATP-agarose void volume can not be collected by a pipette. This is reflected in the Coomassie stain and Western blot analyses of the fractions, where small amounts of unspecific proteins detectable in the flow-through are being carried on in the elution fraction in all four types of ATP-agaroses. Adapting the approach to gravity-flow column was unfortunately not possible due to the small amounts of ATP-agarose used in this purification screening. In order to avoid this contamination larger amounts of ATP-agarose should be used, which after the batch hybridization can be washed and eluted in a column by gravity-flow. Nevertheless the results show that this novel two-stage approach for purification of mTKIN was successful. Apart from the almost exclusive purification of full-length, properly folded mTKIN it also provides information if some of the performed sequence modifications effect the folding and function of the mTKIN. In conclusion, this two step purification method should be with no doubt applicable for other His_6-tagged kinesins. It would be, however, interesting to investigate whether other kinesins will also only bind to the EDA-ATP-agarose. This way it could be determined how conserved the functional structure of the kinesin ATP-binding pocket is.

4.4 Adapting the two-staged purification procedure to FPLC-systems

Binding of unspecific proteins to Ni-NTA-agarose demonstrated that mTKIN can not be purified sufficiently using the batch/gravity-flow procedure. An alternative to increase the efficiency of Ni-NTA affinity purification is the use of a FPLC system. The initial Ni-NTA affinity FPLC run was performed with a long linear gradient and resulted in a peak fraction containing five proteins detectable by Coomassie stain after SDS-PAGE. A Western blot

analysis hybridizing streptavidin-HRP confirmed that the ~60 kD protein band corresponds to biotinylated mTKIN. However, the peak in the chromatogram was rather formed by two larger proteins. From the analyses by Western blot and Coomassie stained SDS-PAGE (data not shown) it became evident that mTKIN was eluted almost in the same range as the two proteins larger in size, but its peak elution fraction was at higher imidazole concentration. To assess, whether this shifted elution peak on the chromatogram generally apply to Avi-His_6-tagged proteins, another Ni-NTA FPLC chromatography run of an Avi-His_6-tagged ubiquitin precursor protein (Ubi8) was performed using the same gradient. The elution peak of Ubi8 matched the expectation, that Avi-His_6-tagged proteins produce a peak at a slightly higher imidazole concentrations than the other unspecific proteins (Figure 3-7). For this reason a custom gradient for the purification of the relatively small amounts of mTKIN was produced. This included a linear gradient starting from the wash buffer imidazole concentration up to the imidazole concentration where the Avi-His_6-tagged proteins were starting to be eluted in order to deplete unspecific proteins as much as possible without loosing the mTKIN. This was followed by an isocratic step of imidazole concentration where the elution peak of mTKIN was expected. Finally another isocratic step was added at maximum imidazole concentration to elute any remaining proteins (Figure 3-8). This method resulted in earlier depletion of unspecific proteins and hence improved the protein composition of the elution containing fractions just a little in favor of mTKIN. The Ni-NTA FPLC run with the same custom gradient using soluble protein extract from 200 mL cultures of mTKIN expressed in BL 21 CodonPlus (DE3)-RIL and Origami B (DE3) pLacI surprisingly discovered further differences between the expression pattern of these two strains. The Coomassie stained SDS-PAGE analysis of the elution fractions from the two purifications pointed out that although the same five proteins were observed in both sets of elution fractions, the sample derived from the Origami B (DE3) pLacI strain produced smaller amounts of the two larger proteins. At the same time larger amounts of mTKIN relative to the amounts purified from the BL 21 CodonPlus (DE3)-RIL strain was produced (Figure 3-9). The two significantly smaller proteins which were shown to be consistently co-purified, were found in roughly the same concentrations in both strains. Western blot analysis of the same fractions revealed that none of the four observed unspecific proteins is an Avi-His_6-tagged protein or a mTKIN N-terminal degradation product. Nevertheless the Western blot surprisingly discovered that the two strains were producing different N-terminal degradation products (Figure 3-10). This can be explained through the difference in the culture volume and the buffer changes during the purification procedure. BL 21 CodonPlus (DE3)-RIL produced two N-terminal degradation products smaller in size, but in larger quantities than the single degradation product produced by Origami B (DE3) pLacI. This results pointed out that the Origami B (DE3) pLacI was the best strain for mTKIN expression, although it needs more time to grow to the optimal

cell density for expression and is generally more difficult to cultivate in comparison to the BL21 CodonPlus (DE3)-RIL. To further increase the effect of the shifted elution peak the mTKIN containing fractions from a Ni-NTA FPLC run were pooled, diluted 1:2 with NPI-10 in order to lower the imidazole concentration and used this as a loading sample in a second identical Ni-NTA affinity FPLC run. This was expected to further deplete the unspecific proteins and resulted in the removal of the two larger proteins from the mTKIN elution-fractions, while one of the smaller unspecific proteins still co-purified with mTKIN (Figure 3-11). To better understand this situation, mTKIN and the four unspecific proteins detected on the SDS-PAA gel were analyzed using mass spectrometry in order to investigate if the other four proteins (1, 2, 4 and 5 form Figure 3-9) are in any way linked with mTKIN (band 3 from Figure 3-9). The results discovered that all four unspecific proteins were actually endogenous proteins from *E. coli*. However, the protein corresponding to band 4 is a chaperone (PPI) and was eluted at the same imidazole concentrations as mTKIN. This suggests that PPI might be bound to mTKIN and not to the Ni-NTA agarose. However, this protein can not be detected by Coomassie stain in the elution fractions obtained from EDA-ATP-agarose purification (Figure 3-6). If the assumption is correct that PPI binds mTKIN, a possible explanation for this might be that PPI disassociates from mTKIN in presence of ATP, This would also mean that ATP stabilizes the correct mTKIN conformation. To test this hypothesis a Ni-NTA FPLC should be performed using buffers which contain 1 mM ATP. If under these conditions PPI is not detectable any more by Coomassie stain in the mTKIN-containing elution fractions, this hypothesis will be proved. Another important aspect of the mass spectrometric data is the identification of 7 peptides from the mTKIN which share characteristics for 12 other KIF1/Unc104 kinesins. This confirms the high degree of homology between mTKIN and the kinesin-3 family. In the course of adapting the two-stage purification for FPLC systems a cartridge was assembled by loading with 250-300 µL bed volume of EDA-ATP agarose that has been already used in batch purification. In a first attempt, the cartridge was loaded with mTKIN-containing sample. The isocratic elution with 1 mM ATP resulted in steady elution of equal mTKIN amounts throughout the elution fractions (data not shown). These amounts of mTKIN produced only faint signals on a Western blot. One possible reason for continuous mTKIN elution over time could be that 1mM ATP elutes only small amounts of mTKIN, as it might correspond to a start of a elution peak. This could be tested by repeating the purification run under the same conditions with 2-3 fold higher ATP concentration during elution. The second reason for this elution behaviour could be the fact that in contrast to Ni-NTA, where the binding of the His_6 tag is being competed by the imidazole which has a higher affinity for the Ni-NTA, the ATP-agarose purification follows a different mechanism. In this case the binding of the protein to the ATP-agarose is not being competed away by the ATP in the elution, but rather lies on the continuous association and

disassociation of the ATP from the mTKIN's ATP-binding pocket. Higher concentrations of ATP during elution would then not effect the dissociation, but rather circumvent re-association of released mTKIN. So the elution of the mTKIN would be a function of time rather than ATP concentration. To test the time dependent manner of mTKIN elution from the ATP-agarose, the FPLC purification was repeated including two 20-minute pauses after the column was flooded with elution buffer. The fraction containing the elution directly after the first pause contained enough mTKIN to be detectable by Coomassie stain after SDS-PAGE. The fraction containing the elution after the second pause contained less mTKIN, which was only detectable using Western blot (Figure 3-12). This confirmed that larger amounts of mTKIN can be eluted as a function of time. Due to time restrains the elution with higher ATP concentrations was not performed, so it is still not clear if mTKIN can form a peak by elution with higher ATP-concentrations. For the optimal investigation of this open question, the FPLC purification should be performed using the 1 mL EDA-ATP-toyoperl column offered from the same manufacturer as the ATP-agarose. This column has a tightly packed matrix making it is suitable for experimenting with different gradients. As of now, the optimal purification of large amounts pure, properly folded and functional mTKIN would contain two stages. First, a Ni-NTA affinity purification on a FPLC systems using the customized gradient would be performed. In a second step, pooled mTKIN containing elution fractions of the first purification step would be used for batch/gravity flow purification with the EDA-ATP-agarose.

4.5 Periplasmic expression and phage display of mTKIN

For all experiment described in this section the pIT2/mTKIN construct was used. This construct allows either the expressed mTKIN to be translocated to the periplasm, or the presentation of mTKIN as a pIII-fusion on the surface of M13 bacteriophage. Depending whether mTKIN is targeted to the periplasm or to the phage surface, either the non-suppressor *E. coli* strain HB2151, or the suppressor strains TG1 and XL1-blue were used for expression. Switching between these two types of expression is possible because the vector construct is generated in such a way that an amber stop is encoded between the mTKIN and pIII molecule. Furthermore, mTKIN is expressed together with the pelB leader sequence at its N-terminus. First periplasmic expression of mTKIN was investigated. One reason for this was to assess whether mTKIN could be produced in the periplasm in larger amounts than in the cytoplasm. This might be advantageous, as the presence of the pelB leader sequence would cause the mTKIN to be translocated to the periplasm in an unfolded state over the Sec pathway where it could then refold in its functional state (Nilsson et al. 1991). mTKIN was expressed according to two different protocols in *E. coli* strain HB2151. Next, protein samples from periplasmic preparation and spheroblasts were analyzed for mTKIN

expression in a Western blot by detection with an anti-His-antibody (Figure 3-4) The results suggest, that mTKIN is only expressed in the spheroblasts irrespective of the preparation protocol and translocation of the mTKIN to the periplasm does not occur. However, this can not be interpreted as a proof that there is no mTKIN in the periplasm, because it could be highly diluted by the relatively large volume of the periplasm preparation. The fact that mTKIN was detectable in the spheroblast confirms that mTKIN is overall expressible in *E. coli* HB2151 cells. To present mTKIN on the surface of phage particles, mTKIN-pIII fusion was expressed in TG1 and XL1-blue cells. Phage production in these cells is possible after superinfection with helper phages, M13KO7 and Hyperphage. Former allows monovalent display and latter allows multivalent display of mTKIN on the phage particle. First, all four combinations of host and helper phages were used to prepare phage particles. From the western blot analysis of the four different types of phages (Figure 3-14) it was seen that mTKIN was successfully displayed as a pIII fusion protein on phages produced in both strains. Notably,this also confirms the ability to translocate mTKIN to the periplasm, as this is a prerequisite for presentation of mTKIN on the phage surface. As expected, the amount of mTKIN-pIII fusion detected on the Western blot was higher when superinfection was done with hyperphage allowing for multivalent display The absence of detectable mTKIN-pIII fusion on the phage particles prepared with hyperphages produced in TG 1 host strain is explainable through the titration values (Table 3-1). These phage suspensions is 100-times less concentrated than the ones produced in XL-1 Blue host strain with the same helper phage. From the western blot analysis also the phenotypical difference between the phage populations generated by M13KO7 or hyperphage superinfection can be seen. The phage particles made with M13KO7 usually carry only one pIII fusion protein and the remaining four are wild-type pIII proteins. This is reflected on the western blot, as large amounts of pIII are detected in the corresponding phage populations and just a small portion of mTKIN-pIII fusion protein is available. On the other hand the phage particles generated with hyperphage are constructed in such way that only the pIII fusion protein, in this case the mTKIN-pIII, is being expressed. So all five copies of pIII needed for the phage assembly are fusion proteins (Rondot et al. 2001). This superior presentation efficiency of mTKIN-pIII fusion protein comes with a prize on the overall yield of phage particles. From the titration it can be seen that irrespective of the host strain around 10^2-10^3 times less phage particles are generated by hyperphage superinfection in comparison to the M13KO7 superinfection. The presentation efficiency of M13KO7 helper phage derived phage population is known to be around 1-10% (Rhyner et al. 2003), hat is 1-10% of phage particles carry a mTKIN-pIII fusion protein on its surface. Bearing this and the reduced yield of phage particles produced with hyperphages in mind, the overall number of presenting phage particle in both populations is more comparable. The difference is primarily found in the number of mTKIN molecules fusion

presented on an individual phage. This can be of interes in future applications, as kinesin molecules are homodimers and dimerisation is a prerequisite of efficient transport. These correlations are important for a later study and attempts to use the phages for selection. Also from the titration values we can observe that irrespective of the helper phage the XL-1 Blue host strain produces 10^2 times more phages than the TG 1 host strain. This points out that the XL-1 Blue host strain will be most probably used for production of mTKIN presenting phages in the future. The ability of mTKIN presenting phages to bind to MTs was tested by a phage ELISA. However, coating of the microtiterplate wells with MTs failed and no signals could be recorded. Immobilistion of MTs, for instance indirectly with anti-tubulin antibody studies should be optimized in the future, before this ELISA can be repeated.

4.6 NADH oxidation coupled double enzyme ATPase assay

For transporting microtubules kinesins require energy which they obtain from consumption of ATP. Hence measurement of ATPase activity with and without the addition of MTs is a clear indicator for the functionality of kinesins. For this purpose, a NADH oxidation coupled double enzyme ATPase assay in microtitre plate format was established. It allows to determine kinetic data of ATPase activity by measuring the change of light absorption at 340nm using a microtitre plate reader. The produced data for mTKIN as well as a positive control kinesin construct (KIF1A-GFP) was very precise and the need of less amounts of reagent meant that larger number of measurements could be performed. The advantage of this ATPase assay is that the double enzymatic system quickly replenishes the hydrolyzed ATP, thus simulating a reaction at constant substrate concentration. This is important for the evaluation, because the rate of the reaction is not being affected by the usually changing substrate concentration and is therefore held at the starting rate of ATP hydrolysis. The second advantage of this system is the 1:1 stoichiometry of the hydrolyzed ATP to oxidized NADH. With help of the specific extinction coefficient for NADH at 340 nm and the length of the light path through the solution the concentration of NADH, or in this case the change in NADH concentration, can be calculated in accordance with the Lambert-Beer law. With this, the initial rate of ATP hydrolysis at a given concentration can be observed. These features made it possible to measure a steady rate of hydrolysis over longer periods of times. In most cases the fit of the linear regression (R^2) of the measured absorption values was between 0.99 and 0.98 (Figure 4-2).

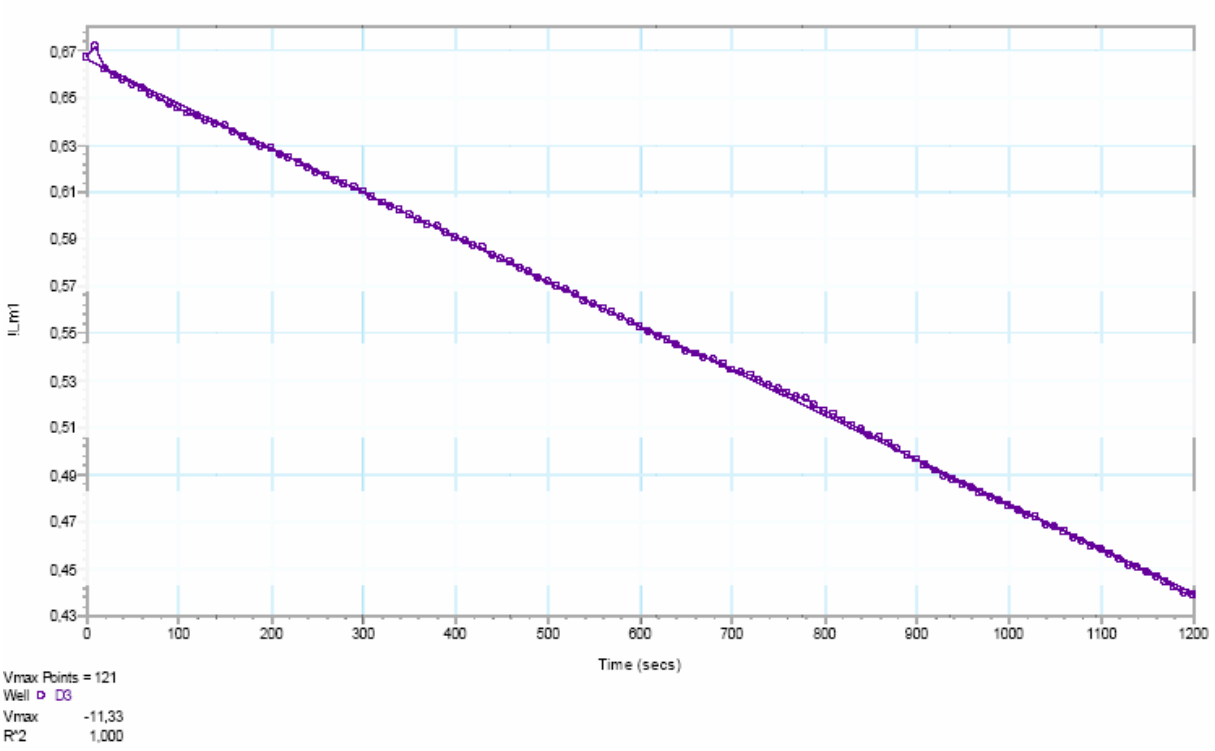

Figure 4-2: A representative series of absorption measurements at 340 nm from a single well containing mTKIN, MTs and 2 mM ATP with a fitted linear regression. Generated using SoftMax Pro software.

The measured changes of the ATP hydrolysis rates by different ATP concentrations for KIF1A-GFP and mTKIN displayed typical Michaelis–Menten kinetics (Figure 3-16). The evaluated V_{max} and K_m values for the intrinsic ATPase activity of the KIF1A-GFP and mTKIN were very similar. However in presence of 1 mM MTs, which is well over the reported MT concentration required for half-maximal velocity measured for wild-type TKIN (Rivera et al. 2007), the ATP hydrolysis rates increased for both kinesins under evaluation. Regarding the maximal ATP hydrolysis rate, this was more dramatic for the mTKIN (4.3-fold) than for the KIF1A-GFP (2.2-fold). This is a clear biochemical evidence that mTKIN interacts with MTs, which causes a strong increase of its ATPase activity. This feature is characteristic for kinesins as it can also be observed in the case of the positive control (KIF1A-GFP). The K_m values for the ATPase activity of the mTKIN in presence 202.5 ± 32.67 µM and absence of MTs 238.3 ± 39.19 µM are overlapping when observed within their statistical error. Also these K_m values which were calculated from measurements taken at ~30° C fit between the two K_m values 42 ± 6.8 µM and 1600 ± 300 µM for the ATPase activity of the wild-type TKIN measured at 25° C and 50° C, respectively (Rivera et al. 2007). Hence confirming the rise of the TKIN's K_m value with rising temperatures. The ATP turnover of mTKIN in presence of MTs (~10,6 s^{-1}) is very similar to the one reported for TLKIF1 (~8 s^{-1}), another isoform of the *T. lanuginosus* kinesin-3 (Sakowicz et al. 1999) Unfortunately the basal ATP turnover rate of TLKIF1 and the ATP turnover rates in presence and absence of MTs for the wild-type TKIN

have not been reported. So the rise of the ATP turnover by mTKIN (4.3-fold) upon addition of MTs can not be properly compared. Also, these results are not comparable with other kinesins. For example the ATP turnover of *D. melanogaster*-derived kinesin increases 3000-fold (Huang and Hackney 1994) and in the case of kinesin-3 from *N. crassa*, which is very closely related to mTKIN, the ATP turnover increases around 100-fold upon addition of MTs (Adio et al. 2006) Therefore, MTs-mediated rise of ATP turnover is rather variable among kinesins and the relatively small increase observed for mTKIN can not be interpreted as an effect produced by the introduced modifications. In summary, these results show that the conservative substitution of the cysteine residues do not affect the normal biochemical properties of mTKIN. This is very important since these modifications play a key role in the folding of mTKIN in a functionally active form. This raises the chances that phage-displayed mTKIN should also be biochemicaly active. However within the given timeframe of this study the ATPase activity of phage displayed kinesisn couldnot be determined using the NADH oxidation coupled double enzyme ATPase. So it is of high interest to biochemical characterize mTKIN presenting phages with this ATPase assay once new phages will be prepared.

4.7 *In vitro* motility assay

The best way to observe and prove the mechanochemical property of kinesins is to moitor their movement along microtubules by an *in vitro* motility assay. One way of performing this assay is to coat a microscope slide surface with kinesin and to add fluorescently labeled MTs. The fluorescently labeled MTs are well observable under a microscope and directed movement (gliding) of MTs above a kinesin coated surface can be observed in presence of ATP. This kind of assay was successfully established and movement of ROX-MTs could be observed in a simple build flow cell previously incubated with stock solution of KIF1A-GFP. This confirmed that the applied procedure for the motility assay is successful. However, when mTKIN was used to coat the flow cell and ROX-MTs was added, no movement could be observed. More importantly, ROX-MTs did not adhere to the surface which should have been coated with the mTKIN as was the case with the positive control (Figure 3-17). This could be explained through the low mTKIN stock concentration at hand. The concentration of the KIF1A-GFP stock solution was ~10 times higher than the total protein concentration of the Ni-NTA affinity FPLC purified mTKIN (around 170 µg/mL). The use of ATP-agarose purified mTKIN was not considered, since its concentration was *per se* lower than that of the previously used mTKIN fraction. The use of such low protein concentrations (under 100 µg/mL) have been also reported for the wild-type TKIN as marginal for observing kinesin driven MTs movement was 100 µg/mL (Rivera et al. 2007). However the actual surface

density of kinesin can not be determined from the solution concentration of the protein. For this reason several mTKIN fractions were pooled and concentrated to a total protein concentration of around 300 µg/mL of mixed protein population. The adherence of the ROX-MTs to the supposedly mTKIN coated surface was still very weak. Interestingly, truncating of the ROX-MTs was observed in this attempt. This can be interpreted as a result of a functional interaction with mTKIN, but as it was rarely reproducible it might well be a technical artifact. The failure to observe a mTKIN-driven ROX-MT-movement are most probably caused by the relatively low partial concentration of mTKIN in the used fractions. Another potential problem could be that unspecific proteins resulting from the purification process might populate the surface. The coating of the surface with other proteins could lead to an even lower surface density of mTKIN or even preventing it to adhere to the surface completely as the other proteins might possess more “sticky” properties towards the glass surface. Also the attempt to observe MTs movement by enriched mTKIN onto a streptavidin coated surface was unfruitful. In this case the mTKIN might have been spread evenly all over the surface without the possibility for eventual clustering which would improve the adherence and movement of the MTs. However the few observed ROX-MTs which adhered to the surface were immobile. Hence it is still not proven that mTKIN is mechanochemicaly inactive. The observed MTs might have simply stalled similarly to the many stalled ROX-MTs in the positive control assay after being directionally moved by the KIF1A-GFP. There are two ways to overcome this problem. Either much larger quantities and more concentrated samples of pure mTKIN need to be produced, or an alternative approach of the motility assay need to be performed. This could be for instance done by inverting the transportation mode. In this case, the fluorescently labeled MTs would be first functionalized onto a slide surface, most probably by using anti-tubulin antibodies. Then, in order to overcome the molecule density problem, small (< 2 µm Ø) streptavidin-coated fluorescent beads or quantum dots would be functionalized with biotin tagged mTKIN (Shishido et al. 2010) Finally, the mTKIN loaded beads would be added to the MT-coated flow cell and their movement along the MTs would be observed. Due to temporal restrains the inverted motility assay could not be performed. . Similarly this approach might be applicable for the investigation of the mechanochemical properties of phage-displayed mTKIN. As multiple kinesins are presented at one end of the phage particle, the local concentration of kinesins could be strong enough to drag the whole phage particle along microtubule tracks. So it might be possible to observe phages moving along MTs, if the phage capsid would be decorated with fluorescently-labeled antibodies.

4.8 Future prospects

Within this study mTKIN expression and purification schemes were established. Furthermore,

the ATPase activity of mTKIN was successfully determined and an in vitro motility assay was set up. The next steps to be conducted would be to express larger quantities of mTKIN and to repeat the motility assay with higher concentrations of mTKIN. In parallel, it should determined whether mTKIN produces dimers. This can be tested in two ways, either by native PAA gel electrophoresis or by size exclusion chromatography using a column, such as a Superdex 200. The second approach would be more precise and the collected fractions could be further analysed using SDS-PAGE and Western blot. In case mTKIN dimerises, a protein peak at around 110 kD should be detected, which should result in single band on an SDA-PAA gel corresponding to 55 kD in size. Size exclusion chromatographic investigation of wild-type full-length TKIN showed no presence of dimers (Rivera et al. 2007). However, since mTKIN contains only the first CC1 domain, the situation might be different and might lead to dimerization. This is plausible since it has been reported that NcKin3, which possesses a short stalk without the FHA and PH domains, does form dimers (Adio et al. 2006). Another important characteristic of mTKIN to be investigated would be the measurement of the force it produces while gliding along MTs by hybridization onto streptavidin coated beads and using optical tweezers for manipulation as described in Figure 4-3.

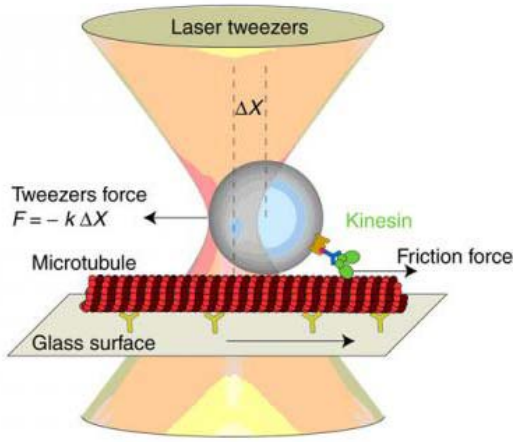

Figure 4-3: Picture of the basic principle how the force of a kinesin is being measured using optical tweezers, picture taken from: http://www.sciencedaily.com/images /2009/08/090814100101-large.jpg

A final investigation would be testing the thermostability of the mTKIN as well as the loss of activity at different storage temperatures and time periods. This would show how robust the mTKIN is and its advantage over other kinesins for its use in nanotechnological applications.

5 Summary

Advancement in technology had made it possible to perform high throughput investigations by processing many samples at the same time. This massive parallelization of experiments and samples was achieved with the use of pipetting robots. Meanwhile, the next step to further increase the number of processed samples is the miniaturization of these processes. Today, there are already commercially available lab-on-chip applications based on microfluidic systems for some simple, routinely used laboratory methods in molecular biology. For future development of the lab-on-chip concept and other nanotechnological application an active transporting system, such as the kinesin-microtubules system available in nature, could offer larger system flexibility. In this study the sequence of kinesin-3 (TKIN), a motor protein from the thermophylic fungi *Thermomyces lanuginosus* (Rivera et al. 2007) was modified in different ways, even amenable to phage display. The goal was to test if this modified kinesin (mTKIN) is more suitable for nanotechnological use than other kinesins due to its thermostability. The possible display of mTKIN on phages in a functional form should open up novel possibilities for the selection and production of custom kinesins. First, an expression screening in different *E. coli* strains applying different conditions was conducted which showed that optimal expression of the mTKIN is possible in the Origami B (DE3) pLacI strain. This strain produces the largest amount of full-length mTKIN and the smallest number and amounts of N-terminal degradation products by induced expression at 18°C for 18 hours. mTKIN was than successfully purified with a novel two stage affinity chromatography protocol, first using Ni-NTA and then EDA-ATP-agarose. The second step enabled purification only of properly folded mTKIN. Furthermore, purification of mTKIN on a FPLC-system showed better results than batch/gravity flow procedure, which however was still not comparable to a purification combined with EDA-ATP-agarose. The presentation of mTKIN as a pIII fusion protein on phages using two different host strains and two different helper phages was successful. The titration values of phages discovered that the obtained presentation rates should be suitable for performing selections. Finally a NADH oxidation coupled enzymatic assay was used to test for ATPase activity. This showed that mTKIN has similar biochemical properties which are comparable with the wild-type TKIN as well as other kinesins. A mechanochemical characterization utilizing a motility assay was unfortunately not possible due to insufficiency of time. Nevertheless this in vitro motility assay was successfully established as directional movement of fluorescent microtubules was observed using another kinesin (KIF1A-GFP) as a reference. Further characterization experiments and alternative approaches for unsuccessful tests need to be performed in order to better characterize soluble and phage-presented mTKIN.

Zusammenfassung

Durch fortlaufende technologische Weiterentwicklungen ist es heut zu Tage möglich, Hochdurchsatz-Untersuchungen durchzuführen, wodurch eine enorm große Probenmenge zeitgleich analysiert werden kann. Die Entwicklung und Nutzung von Pipettier-Robotern hat zudem die massive Parallelisierung von Experimenten zugänglich gemacht. Um in Zukunft die Anzahl an parallel zu verarbeitenden Proben zu erhöhen, ist der nächste logische Schritt die Miniaturisierung des Systems. Einige dieser mikrofluidalen Lab-On-Chip Systeme sind für einfache molekularbiologische Untersuchungen mittlerer Weile auf dem Markt käuflich zu erwerben. Für die Weiterentwicklung der Lab-On-Chip Systeme sowie weiterer nanotechnologischer Anwendungen kann ein aktives Transportsystem, sowie das des in der Natur vorkommenden Kinesin-Mikrotubuli Systems, für eine bessere Systemflexibilität genutzt werden. Innerhalb dieser Studie wurde die Sequenz des Motor-Proteins Kinesin-3 aus dem thermophilen Pilz *Thermomyces lanuginosus* (Rivera et al. 2007) auf verschiedene Art und Weise modifiziert, um es unter anderem für das Phage Display System nutzbar zu machen. Das Ziel lag darin herauszufinden, ob das modifizierte Kinesin (mTKIN) sich aufgrund seiner thermostabilen Eigenschaften für die Verwendung in der Nanotechnologie weitaus besser eignet als andere Kinesine und ob es sich auf Phagen in funktioneller Form präsentieren lässt. Dies würde letztlich die Selektion sowie die Herstellung von spezifischen Kinesinen ermöglichen.Um dies zu erreichen wurde in unterschiedlichen *E.coli* Stämmen sowie unter verschiedenen Bedingungen ein Expressions-Screening durchgeführt. Dabei hat sich herausgestellt, das sich der *E. coli* Stamm Origami B (DE3) pLacI für die Expression von mTKIN am besten eignet. Im Vergleich zu anderen Stämmen produziert dieser Expressionsstamm bei induzierter Expression bei 18°C innerhalb von 18 Stunden die größte Menge an full-length mTKIN und zudem die kleinste Anzahl und geringste Menge an N-terminalen Degradationsprodukten. Das exprimierte mTKIN konnte schließlich durch eine neu entwickelte zweistufige Affinitätschromatographie erfolgreich aufgereinigt werden. Bei der ersten Stufe handelt es sich um Ni-NTA-, die zweite Stufe ist EDA-ATP-Agarose. Die EDA-ATP-Agarose ermöglicht dabei ausschließlich die Aufreinigung des richtig gefalteten mTKIN's. Des Weiteren konnte mit einer Aufreinigung des mTKIN über Ni-NTA Affinitäts-FPLC ein besseres Ergebnis erzielt werden als über die Batch/Gravity Flow Methode, wobei diese im Vergleich zur EDA-ATP-Agarose eher verunreinigtes mTKIN produziert.
Das Motor-Protein mTKIN konnte zudem auf vier Phagen-Typen, bestehend aus der Kombinatorik zweier unterschiedlichen Wirtsstämmen sowie zweier Helferphagen, als pIII Fusionsprotein erfolgreich präsentiert werden. Durch die Phagentitration konnte zudem herausgefunden werden, dass sie sich für ein Selektionsverfahren eignen.
Zu guter Letzt wurde die ATPase Aktivität des mTKIN's durch einen NADH Oxidations-gekoppelten doppel-enzymatischen Assay getestet. Dieser hat gezeigt, dass das exprimierte

mTKIN über die gleichen biochemischen kinesin-charakteristischen Eigenschaften verfügt wie das nicht-modifizierte TKIN. Die mechano-chemische Charakterisierung mittels eines Gleit-Assay konnte aufgrund unzureichender Zeit leider nicht durchgeführt werden. Das Gleit-Assay konnte dennoch erfolgreich etabliert werden, da eine unidirektionale Bewegung von fluoreszenzmarkierten Mikrotubuli beobachtet werden konnte. Diese Bewegung wurde durch ein anderes rekombinantes Kinesin (KIF1A-GFP) als Referenz erreicht.
Um das rekombinante mTKIN sowie das auf den Phagen präsentierte Protein noch besser charakterisieren zu können, müssen weitere Experimente und alternative Ansätze für fehlgeschlagene Experimente durchgeführt werden.

6 Literature

Adio, S., M. Bloemink, M. Hartel, S. Leier, M.A. Geeves, and G. Woehlke. 2006. Kinetic and mechanistic basis of the nonprocessive Kinesin-3 motor NcKin3. *J Biol Chem* **281:** 37782-37793.

Basaveswara Rao, V., N.V. Sastri, and P.V. Subba Rao. 1981. Purification and characterization of a thermostable glucoamylase from the thermophilic fungus Thermomyces lanuginosus. *Biochem J* **193:** 379-387.

Berliner, E., H.K. Mahtani, S. Karki, L.F. Chu, J.E. Cronan, Jr., and J. Gelles. 1994. Microtubule movement by a biotinated kinesin bound to streptavidin-coated surface. *J Biol Chem* **269:** 8610-8615.

Carroll-Portillo, A., M. Bachand, and G.D. Bachand. 2009. Directed attachment of antibodies to kinesin-powered molecular shuttles. *Biotechnol Bioeng* **104:** 1182-1188.

Clackson, T., H.R. Hoogenboom, A.D. Griffiths, and G. Winter. 1991. Making antibody fragments using phage display libraries. *Nature* **352:** 624-628.

Corey, D.R., A.K. Shiau, Q. Yang, B.A. Janowski, and C.S. Craik. 1993. Trypsin display on the surface of bacteriophage. *Gene* **128:** 129-134.

Damaso, M.C., M.S. Almeida, E. Kurtenbach, O.B. Martins, N. Pereira, Jr., C.M. Andrade, and R.M. Albano. 2003. Optimized expression of a thermostable xylanase from Thermomyces lanuginosus in Pichia pastoris. *Appl Environ Microbiol* **69:** 6064-6072.

DeBoer, S.R., Y. You, A. Szodorai, A. Kaminska, G. Pigino, E. Nwabuisi, B. Wang, T. Estrada-Hernandez, S. Kins, S.T. Brady, and G. Morfini. 2008. Conventional kinesin holoenzymes are composed of heavy and light chain homodimers. *Biochemistry* **47:** 4535-4543.

Devlin, J.J., L.C. Panganiban, and P.E. Devlin. 1990. Random peptide libraries: a source of specific protein binding molecules. *Science* **249:** 404-406.

Feilmeier, B.J., G. Iseminger, D. Schroeder, H. Webber, and G.J. Phillips. 2000. Green fluorescent protein functions as a reporter for protein localization in Escherichia coli. *J Bacteriol* **182:** 4068-4076.

Gilbert, S.P. and A.T. Mackey. 2000. Kinetics: a tool to study molecular motors. *Methods* **22:** 337-354.

Guo, R.F., D.C. Li, and R. Wang. 2005. [Purification and properties of a thermostable chitinase from thermophilic fungus Thermomyces lanuginosus]. *Wei Sheng Wu Xue Bao* **45:** 270-274.

Guydosh, N.R. and S.M. Block. 2009. Direct observation of the binding state of the kinesin head to the microtubule. *Nature* **461:** 125-128.

Gyoeva, F.K., E.M. Bybikova, and A.A. Minin. 2000. An isoform of kinesin light chain specific for the Golgi complex. *J Cell Sci* **113 (Pt 11):** 2047-2054.

Hammond, J.W., D. Cai, T.L. Blasius, Z. Li, Y. Jiang, G.T. Jih, E. Meyhofer, and K.J. Verhey. 2009. Mammalian Kinesin-3 motors are dimeric in vivo and move by processive motility upon release of autoinhibition. *PLoS Biol* **7:** e72.

Hess, H., G.D. Bachand, and V. Vogel. 2004. Powering nanodevices with biomolecular motors. *Chemistry* **10:** 2110-2116.

Huang, T.G. and D.D. Hackney. 1994. Drosophila kinesin minimal motor domain expressed in Escherichia coli. Purification and kinetic characterization. *J Biol Chem* **269:** 16493-16501.

Kaiser, P., D. Meierhofer, X. Wang, and L. Huang. 2008. Tandem affinity purification combined with mass spectrometry to identify components of protein complexes. *Methods Mol Biol* **439:** 309-326.

Kashina, A.S., G.C. Rogers, and J.M. Scholey. 1997. The bimC family of kinesins: essential bipolar mitotic motors driving centrosome separation. *Biochim Biophys Acta* **1357:** 257-271.

Khodjakov, A., E.M. Lizunova, A.A. Minin, M.P. Koonce, and F.K. Gyoeva. 1998. A specific light chain of kinesin associates with mitochondria in cultured cells. *Mol Biol Cell* **9:** 333-343.

Lee, Y.C., F.E. Samson, Jr., L.L. Houston, and R.H. Himes. 1974. The in vitro polymerization of tubulin from beef brain. *J Neurobiol* **5:** 317-330.

Li, D.C., J. Gao, Y.L. Li, and J. Lu. 2005. A thermostable manganese-containing superoxide dismutase from the thermophilic fungus Thermomyces lanuginosus. *Extremophiles* **9:** 1-6.

Marx, A., J. Muller, E.M. Mandelkow, G. Woehlke, C. Bouchet-Marquis, A. Hoenger, and E. Mandelkow. 2008. X-ray structure and microtubule interaction of the motor domain of Neurospora crassa NcKin3, a kinesin with unusual processivity. *Biochemistry* **47:** 1848-1861.

Matsushita, M., R. Yamamoto, K. Mitsui, and H. Kanazawa. 2009. Altered motor activity of alternative splice variants of the mammalian kinesin-3 protein KIF1B. *Traffic* **10:** 1647-1654.

McCafferty, J., R.H. Jackson, and D.J. Chiswell. 1991. Phage-enzymes: expression and affinity chromatography of functional alkaline phosphatase on the surface of bacteriophage. *Protein Eng* **4:** 955-961.

Miyazono, Y., M. Hayashi, P. Karagiannis, Y. Harada, and H. Tadakuma. 2009. Strain through the neck linker ensures processive runs: a DNA-kinesin hybrid nanomachine study. *EMBO J* **29:** 93-106.

Nilsson, B., C. Berman-Marks, I.D. Kuntz, and S. Anderson. 1991. Secretion incompetence of bovine pancreatic trypsin inhibitor expressed in Escherichia coli. *J Biol Chem* **266:** 2970-2977.

Nitta, T. and H. Hess. 2005. Dispersion in active transport by kinesin-powered molecular shuttles. *Nano Lett* **5:** 1337-1342.

Rayment, I. 1996. The structural basis of the myosin ATPase activity. *J Biol Chem* **271:** 15850-15853.

Rezessy-Szabo, J.M., Q.D. Nguyen, A. Hoschke, C. Braet, G. Hajos, and M. Claeyssens. 2007. A novel thermostable alpha-galactosidase from the thermophilic fungus Thermomyces lanuginosus CBS 395.62/b: purification and characterization. *Biochim Biophys Acta* **1770:** 55-62.

Rhyner, C., Z. Konthur, K. Blaser, and R. Crameri. 2003. High-throughput isolation of recombinant antibodies against recombinant allergens. *Biotechniques* **35:** 672-674.

Rivera, S.B., S.J. Koch, J.M. Bauer, J.M. Edwards, and G.D. Bachand. 2007. Temperature dependent properties of a kinesin-3 motor protein from Thermomyces lanuginosus. *Fungal Genet Biol* **44:** 1170-1179.

Rondot, S., J. Koch, F. Breitling, and S. Dubel. 2001. A helper phage to improve single-chain antibody presentation in phage display. *Nat Biotechnol* **19:** 75-78.

Sakowicz, R., S. Farlow, and L.S. Goldstein. 1999. Cloning and expression of kinesins from the thermophilic fungus Thermomyces lanuginosus. *Protein Sci* **8:** 2705-2710.

Schnapp, B.J., J. Gelles, and M.P. Sheetz. 1988. Nanometer-scale measurements using video light microscopy. *Cell Motil Cytoskeleton* **10:** 47-53.

Shishido, H., K. Nakazato, E. Katayama, S. Chaen, and S. Maruta. 2010. Kinesin-Calmodulin fusion protein as a molecular shuttle. *J Biochem* **147:** 213-223.

Smith, G.P. 1985. Filamentous fusion phage: novel expression vectors that display cloned antigens on the virion surface. *Science* **228:** 1315-1317.

Thie, H., T. Schirrmann, M. Paschke, S. Dubel, and M. Hust. 2008. SRP and Sec pathway leader peptides for antibody phage display and antibody fragment production in E. coli. *N Biotechnol* **25:** 49-54.

Vale, R.D. 2003. The molecular motor toolbox for intracellular transport. *Cell* **112:** 467-480.

Vale, R.D., T.S. Reese, and M.P. Sheetz. 1985. Identification of a novel force-generating protein, kinesin, involved in microtubule-based motility. *Cell* **42:** 39-50.

Valent, Q.A. 2001. Signal recognition particle mediated protein targeting in Escherichia coli. *Antonie Van Leeuwenhoek* **79:** 17-31.

Verhey, K.J. and J.W. Hammond. 2009. Traffic control: regulation of kinesin motors. *Nat Rev Mol Cell Biol* **10:** 765-777.

Wilson, L., H.P. Miller, K.W. Farrell, K.B. Snyder, W.C. Thompson, and D.L. Purich. 1985. Taxol stabilization of microtubules in vitro: dynamics of tubulin addition and loss at opposite microtubule ends. *Biochemistry* **24:** 5254-5262.

7 Abbreviations

ahpC	Mutated alkyl hydroperoxide reductase for conferring disulfide reductase activity	KM	Michaelis-Constant
Amp^r	Ampicilin resistance	L	Liter
AMPPNP	Non-hydrolysable ATP analog	$lacI^q$	Lac repressor overexpression
BCCP	Acetyl-CoA carboxylase biotin carboxyl carrier proteinsubunit	LDH	Lactic dehydrogenase
bimC	Tetrameric kinesin	LSCM	Laser scanning confocal microscope
bp	Base pairs	M	Molar concentration (mol/ L)
° C	Degrees Celsius	M13	Filamentous bacteriophage
CC	Coiled coil domain	mA	miliAmper
CCD camera	Charge-coupled device camera	MES	2-(N-morpholino) ethanesulfonic acid
CFU	Colony Forming Units	MTs	Microtubules
CV	Column volume	NADH	Nicotinamide adenine dinucleotide
DMSO	Dimethylsulfoxid	Ncd	D. melanogaster kinesin 14
DNA	Desoxyribonucleic acid	Ni-NTA	Nickel nitrilotriacetic acid
dsDNA	Double stranded DNA	ORF	Open reading frame
dNTP	Desoxynucleotides	PAA	Polyacrylamide
DTT	Dithiothreitol	PBS	Phosphate buffered saline
EDTA	Ethylenediaminetetraacetic acid	PCR	Polymerase chain rection
EGTA	Ethylene glycol tetraacetic acid	PEG	Polyethylen glycol
EM	Electron microscopy	PEP	Phosphoenolpyruvic acid

endA	Elimination of endonuclease A	pelB	Leader sequence for the Sec pathway
E/OD	Extinction, Absorption, Optical density	PIPES	Piperazine-N,N′-bis(2-ethanesulfonic acid)
ESI	Electrospray ionization	PK	Pyruvate kinase
FHA	Forkhead-associated domain	PPI	Peptidyl prolyl cis-trans-isomerase
FPLC	Fast protein liquid chromatography	ROX-MTs	X-rhodamine labeled microtubules
g	Gram	SDS	Sodium dodecyl sulfate
GF	Gravity-flow	SDS-PAGE	SDS- Polyacrylamide gel electrohporesis
GFP	Green fluorescent protein	Sec pathway	Secretory pathway
gor522	Mutation in glutathione reductase; enhances disulphide bond formation	SRP	Signal recognition particle
GST	Glutathione S-transferase	ssDNA	Single stranded DNA
H_2O, bidest.	Aqua, water - bidestilated	Tat	Twin-arginine translocation pathway
HEPES	4-(2-hydroxyethyl)-1-piperazineethanesulfonic acid)	TEMED	N,N,N,N-Tetramethyl-ethylenediamine
His_6	Hexahistidine homopolymer	mTKIN	Modified kinesin-3 from T. lanuginosus
HRP	Horse reddish peroxidase	TLKIF1	Another iyoform of Kinesin-3 from T. lanuginosus
HRP	Horse reddish peroxidase	TPR	Tetratico peptide repeats
IMAC	Immobilised metal-ion chromatography	Tris	Tris-(hydroxymethyl)-aminomethane
IPTG	Isopropyl-β-D-thiogalactopyranosid	trxB	Mutation in thioredoxin reductase; enhances disulphide bond formation
KAP	Kinesin associated protein	U	Units (for enzymes)

Abbreviations

k_{cat}	Turnover number	Ubi8	Avi-His_6-tagged ubiquitin precursor protein
kD	kiloDalton (1 kD =1000 g/mol)	Unc104/KIF1	Kinesin-3 family
KHC	Kinesin heavy chain	UV	Ultra-violet light
KIF1A-GFP	Kinesin-3 from R. norvegicus fused with GFP	V	volt
KLC	Kinesin light chain	xg	x-fold of mean earth gravitational acceleration

Eidesstattliche Erklärung

Ich versichere eidesstattlich, dass ich die vorliegende Diplomarbeit selbstständig und ohne Hilfsmittel außer den angegebenen verwendet habe, und dass diese Diplomarbeit an keiner anderen Fakultät eingereicht worden ist.

Berlin den 08.05.2010

Dejan Gagoski